



HAL
open science

Développement et mise en place au BIPM d'un système international de comparaison et d'étalonnage pour la dosimétrie en mammographie

Cecilia Kessler

► **To cite this version:**

Cecilia Kessler. Développement et mise en place au BIPM d'un système international de comparaison et d'étalonnage pour la dosimétrie en mammographie. Médecine humaine et pathologie. Conservatoire national des arts et métiers - CNAM, 2013. Français. NNT : 2013CNAM0864 . tel-00841601

HAL Id: tel-00841601

<https://theses.hal.science/tel-00841601>

Submitted on 5 Jul 2013

HAL is a multi-disciplinary open access archive for the deposit and dissemination of scientific research documents, whether they are published or not. The documents may come from teaching and research institutions in France or abroad, or from public or private research centers.

L'archive ouverte pluridisciplinaire **HAL**, est destinée au dépôt et à la diffusion de documents scientifiques de niveau recherche, publiés ou non, émanant des établissements d'enseignement et de recherche français ou étrangers, des laboratoires publics ou privés.



ÉCOLE DOCTORALE TECHNOLOGIQUE ET PROFESSIONNELLE

Laboratoire commun de métrologie LNE Cnam

THÈSE présentée par :

Cecilia KESSLER

soutenue le : 23 avril 2013

pour obtenir le grade de : **Docteur du Conservatoire National des Arts et Métiers**

Discipline/ Spécialité : Laser, métrologie, communications/Physique

**DÉVELOPPEMENT ET MISE EN PLACE AU BIPM
D'UN SYSTÈME INTERNATIONAL DE
COMPARAISON ET D'ÉTALONNAGE POUR LA
DOSIMÉTRIE EN MAMMOGRAPHIE**

THÈSE dirigée par :

M HIMBERT Marc

Professeur du CNAM, CNAM-Saint-Denis

RAPPORTEURS :

M NÖEL Alain

Physicien médical, HDR, Enseignant-chercheur émérite, Centre de Recherches en Automatique de Nancy

M BORDY Jean-Marc

Chef de laboratoire, Laboratoire National Henri Becquerel (LNE-LNHB)

JURY :

M CHAUDAUDRA Jean

Physicien médical, professeur émérite à l'INSTN

Service de physique médicale, Institut Gustave Roussy

M BORDY Jean-Marc

Chef de laboratoire, HDR, Laboratoire National Henri Becquerel (LNE-LNHB)

M NÖEL Alain

Physicien médical, HDR, Enseignant-chercheur émérite, Centre de Recherches en Automatique de Nancy

Mme LUCCIONI Catherine

Professeure des universités, CNAM, CNAM-Paris

Mme ALLISY-ROBERTS Penelope

Ancienne directrice du Département des rayonnements ionisants, Bureau international des poids et mesures

M LEDU Dominique

Physicien médical, HEGP (Hop Eur G.Pompidou) - Oncologie-Radiothérapie

M HIMBERT Marc

Professeur du CNAM, CNAM-Saint-Denis

Acknowledgments

I wish to express my gratitude to my supervisor Dr Penelope Allisy-Roberts for giving me the opportunity to work on this project and for her valuable support, guidance and encouragement. I also would like to thank Mr Philippe Roger for his precious help and collaboration in this project and Dr David Burns for his guidance, assistance and technical discussions. Also, I would like to show my greatest appreciation to Celine Planche for her help in the translation of the introduction into French and Dr Guy Ratel for his advice on my manuscript. Finally, I would like to thank to Dr. Himbert for accepting being the Director of this thesis.

Résumé

La mammographie est une technique d'imagerie par rayons x, considérée comme la technique actuelle la plus efficace pour dépister le cancer du sein à un stade précoce. A cause des risques de carcinogénèse induite par les rayonnements associés à l'examen par rayons x, il est donc essentiel de réaliser un étalonnage précis du faisceau de rayonnements afin de réduire au maximum la dose de rayonnement délivrée au sein du patient et d'obtenir la meilleure qualité d'image possible. L'étalonnage du faisceau de rayons x est effectué avec des chambres d'ionisation, instruments du commerce qui doivent être préalablement étalonnés dans des laboratoires d'étalonnage de référence, de préférence dans le même type de faisceaux de rayonnements que celui utilisé pour le diagnostic.

Dans un pays donné, les laboratoires d'étalonnage de référence en dosimétrie des rayonnements sont généralement rattachés au laboratoire national de métrologie ; ce sont des laboratoires de référence primaires ou secondaires de dosimétrie. Les laboratoires primaires vérifient l'exactitude de leurs mesures conduites avec des étalons primaires en participant à des comparaisons internationales alors que les laboratoires secondaires, détenteurs d'étalons secondaires, doivent procéder à la caractérisation de leurs instruments de référence.

Afin de répondre aux besoins des laboratoires nationaux de métrologie le Bureau international des poids et mesures (BIPM) maintient des étalons de référence stables pour la dosimétrie des rayonnements ionisants et met à disposition de ses États Membres des équipements internationaux pour la comparaison des étalons primaires et la caractérisation des étalons nationaux secondaires afin d'assurer l'unification mondiale des mesures et leur traçabilité au Système international d'unités (SI).

Le Département des rayonnements ionisants du BIPM a effectué les premières comparaisons internationales dans des faisceaux de rayons x aux basses énergies en 1966 et, en 2001, les Instituts nationaux de métrologie (INM) ont pour la première fois proposé que le BIPM étende ses activités à la mammographie.

Une description du travail que j'ai entrepris au BIPM pour répondre aux besoins des laboratoires nationaux de métrologie en matière de comparaisons et d'étalonnages dans ce domaine est présentée dans cette thèse et distribuée en quatre parties :

- l'établissement de sept faisceaux de rayonnement en utilisant un tube à rayons x à anode en tungstène et filtre en molybdène (faisceau W/Mo);

- l’installation d’un tube à rayons x à anode en molybdène avec filtre en molybdène et l’établissement de quatre faisceaux de rayonnement (faisceau Mo/Mo);
- conception et fabrication d’un nouvel étalon primaire pour la dosimétrie dans les faisceaux mammographiques.
- la création d’une nouvelle série de comparaisons en continu du BIPM, identifiées dans la base de données du BIPM sur les comparaisons clés KCDB sous la référence BIPM.RI(I)-K7 et un programme pour l’étalonnage des étalons nationaux secondaires qui inclut le nouveau dispositif expérimental dans le système managérial de la qualité du département des rayonnements ionisants (RI) du BIPM.

L’expertise acquise lors de ce travail est maintenant transféré aux INM pour les aider dans le développement de leurs propres étalons primaires et à améliorer leurs dispositifs expérimentaux existants.

Jusqu’à aujourd’hui 6 comparaisons ont été menées à bien dans le nouveau dispositif expérimental établi au BIPM ; la participation à la nouvelle comparaison-clé continue permet aux INM de soutenir leurs capacités d’étalonnages et de mesures (CMC). La caractérisation et l’étalonnage des étalons nationaux secondaires ont été réalisés pour l’heure pour 5 INM.

Mots clés: dosimétrie pour la mammographie, comparaisons internationales pour la mammographie

Summary

Mammography is an x-ray examination of the breast, considered to be the most sensitive technique currently available for early detection of breast cancer. Because of risks of radiation-induced carcinogenesis associated with the use of x rays, accurate calibration of the x-ray unit is essential in order to minimize the radiation dose delivered to the patient breast but having a good image quality. The beam calibration is made using ionization chambers, commercial instruments that need to be characterized at standard reference dosimetry laboratories in well-defined x-ray beams similar to those used in the diagnostic institutes.

Standard reference laboratories for radiation dosimetry are usually part of the National Metrology Institute of each country; they can either be Primary or Secondary Standard Dosimetry Laboratories. Primary Laboratories verify the accuracy of their measurements using the primary standards by taking part in international comparisons while the Secondary Laboratories, holding secondary standards, need the characterization of their reference instruments.

In order to fulfil these requirements of the National Metrology Institutes (NMIs), the Bureau International des Poids et Mesures (BIPM) maintains stable reference standards for radiation dosimetry and provides to the its Member States an international facility for comparisons of primary standards and characterization of secondary standards to ensure world-wide uniformity of measurements and their traceability to the International System of Units (SI).

The Ionizing Radiation Department of the BIPM started international comparisons and characterizations in low-energy x-ray beams in 1966 and in 2001, the NMIs required the BIPM to extend these activities to mammography beams.

A description of the work I carried out at the BIPM to provide an international facility for comparisons and calibrations in the mammography field is presented in this thesis, divided into four stages:

- establishment of seven reference radiation beams using the combination tungsten-anode x-ray tube and molybdenum filtration (W/Mo beams);
- installation of a molybdenum-anode x-ray tube with molybdenum filtration and establishment of four reference radiation beams (Mo/Mo beams);
- design and construction of a new primary standard free-air chamber for the dosimetry of the mammography beams;

- establishment of a new ongoing international comparison in the new reference mammography beams, registered in the BIPM key comparison database KCDB as BIPM.RI(I)-K7 and a programme for the calibration of national secondary standards by including the new facility in the quality management system of the Ionizing Radiation (IR) Department of the BIPM.

The experience obtained during this work is now transferred to the NMIs to help them in the development of primary standards and to improve their existing facilities.

To date, six successfully comparisons have been carried out in the new facility established at the BIPM; the participation in the new ongoing key comparison allow the NMIs to support their calibration and measurement capabilities (CMCs). Characterization and calibration of national secondary standards have been done for five NMIs.

Key words: mammography dosimetry, international comparisons in mammography

Table des matières

Acknowledgments	2
Résumé	3
Summary	5
Table des matières	7
Liste des tableaux	10
Liste des figures	12
Liste des figures	12
Introduction	14
Cancer du sein et mammographie : le rôle du BIPM	15
Cancer du sein	15
Mammographie	16
Dosimétrie de référence pour la mammographie	17
Rôle du BIPM.....	19
Chapter 1. Breast cancer and mammography: the role of the BIPM.....	31
Introduction	31
1.1. Breast cancer	31
1.2. Mammography	32
1.3. Reference dosimetry for mammography.....	32
1.4. The role of the BIPM	34
Chapter 2. Establishment of simulated mammography radiation qualities using a tungsten target x-ray tube with molybdenum and rhodium filters.....	44
2.1. Introduction	44
2.2. Establishing new radiation beams: determination of the beam quality and the air kerma rate.....	46
2.2.1. X-ray production	46
2.2.2 X-ray tube.....	50
2.2.3 X-ray characterization	51
2.2.4 X-ray irradiation facility at the BIPM	53
2.2.5 The BIPM standard	54
2.2.6 New radiation qualities.....	54
2.3. Determination of spectra	62
2.3.1 Experimental spectra determination.....	62

2.3.2 Spectra determination by simulation.....	65
2.4. Results	67
2.4.1 Spectral measurements	67
2.4.2 Spectral simulations	67
2.5. Calibration of transfer ionization chambers	69
2.6. Summary	70
2.7. Conclusions	71
Chapter 3. Design and construction of a primary standard for mammography dosimetry	72
3.1. Introduction	72
3.2. Definitions.....	73
3.3. Free air chamber.....	75
3.3.1. Principle of operation	75
3.3.2. Design of a free-air chamber.....	78
3.4. The BIPM free-air chamber design.....	81
3.5. Correction factors.....	84
3.6. Comparison with the existing standard	92
3.7. Conclusions	97
Chapter 4. Establishment of mammography radiation qualities.....	98
4.1. Introduction	98
4.2. Establishing new radiation beams: determination of the beam quality and the air kerma rate.....	99
4.2.1. The BIPM irradiation facility.....	99
4.2.2. Mo-anode x-ray tube and calibration bench.....	100
4.2.3. The BIPM standard for mammography qualities.....	101
4.2.4. Radiation beam.....	102
4.2.5. New radiation qualities.....	103
4.2.6. Measurement and simulation of energy spectra.....	104
4.2.7. Determination of the air-kerma rate	105
4.3. Conclusions	108
Chapter 5. A study of the response of commercial ionization chambers to mammography beams.....	109
5.1. Introduction	109
5.2. Calibration of ionization chambers	111
5.2.1. Ionization chambers	111

5.2.2. Irradiation facilities and radiation qualities.....	113
5.2.3. Positioning of the ionization chambers	114
5.2.4. Charge measurement and leakage	114
5.2.5. Radial non-uniformity correction.....	115
5.2.6. Reproducibility of the ionization chamber measurements.....	115
5.2.7. Additional measurements	116
5.3. Uncertainties.....	116
5.4. Results and discussion.....	117
5.5. Conclusion.....	120
Chapter 6. Implementation of an international comparison and calibration facility for mammography dosimetry at the BIPM	122
6.1. Introduction	122
6.2. An international facility for mammography.....	124
6.2.1. International comparisons	124
6.2.2. Calibration of national secondary standards in mammography beams.....	140
6.2.3. Technical cooperation	142
6.3. Quality system.....	142
6.4. Conclusions	144
Chapter 7. Final conclusions.....	145
General conclusions	145
Résumé.....	151
Summary	151

Liste des tableaux

Table 2.1. Main characteristics of the W-anode x-ray tube	53
Table 2.2. Main characteristics of the standard.....	54
Table 2.3. Characteristics of the simulated mammography radiation qualities	55
Table 2.4. Physical constants used in the determination of the air-kerma rate	57
Table 2.5. Interpolated correction factors for the BIPM standard	57
Table 2.6. Comparison between interpolated and calculated correction factors for the BIPM standard	60
Table 2.7. Relative standard uncertainties in the BIPM determination of air kerma rate for mammography x-ray qualities.....	61
Table 2.8. Characteristics of the radionuclides used for the Ge detector calibration.....	64
Table 3.1. Ion recombination for the FAC-L-02.....	86
Table 3.2. Response of the FAC-L-02	93
Table 3.3. Effect of contact potentials between collector and guard plate.....	94
Table 3.4. Effect of different diaphragms in FAC-L-02	95
Table 3.5. Effect of field size	95
Table 3.6. Effect of different collector sizes	96
Table 3.7. Effect of the non co-planarity between collector and guard plate.....	96
Table 4.1. Main characteristics of the Mo-anode x-ray tube	100
Table 4.2. Main characteristics of the standard.....	101
Table 4.3. Characteristics of the reference radiation beams for mammography.....	103
Table 4.4. Correction factors for the BIPM standard FAC-L-02	106
Table 4.5. Relative standard uncertainties in the BIPM determination of air-kerma rate for mammography x-ray qualities.....	107
Table 5.1. Main characteristics of the ionization chambers.....	111
Table 5.2. Main characteristics of the BIPM primary standards.....	112
Table 5.3. Characteristics of the W/Mo radiation qualities.....	114
Table 5.4. Characteristics of the Mo/Mo radiation qualities.....	114
Table 5.5. Characteristics of the CCRI reference quality	116
Table 5.6. Uncertainties associated with the calibration of the ionization chambers at the BIPM.....	116
Table 5.7. Response of the ionization chambers to the W/Mo and Mo/Mo beams	120
Table 6.1. Comparison results and combined relative standard uncertainty.....	131

Table 6.2. Comparison results and combined relative standard uncertainty.....	132
Table 6.3. Comparison results and combined relative standard uncertainty.....	136
Table 6.4. Comparison results and combined relative standard uncertainty.....	138
Table 6.5. Degrees of equivalence	139

Liste des figures

Figure 1. Degrés d'équivalence D_i et leurs incertitudes U_i ($k = 2$), in mGy/Gy	28
Figure 1.1. Degrees of equivalence D_i and uncertainty U_i ($k = 2$), in mGy/Gy	42
Figure 2.1. Fast electrons in the proximity of a nucleus are deflected and the emission of x-rays is produced in this process.....	46
Figure 2.2. The resulting bremsstrahlung radiant energy spectrum (unfiltered and filtered), generated in a thick target of any atomic number Z by an electron beam of incident energy T_0	47
Figure 2.3. Following the creation of a K-shell vacancy, an electron from another higher shell fills it, and emits a fluorescence photon having a quantum energy equal to the difference in the two energy levels involved.....	47
Figure 2.4. The characteristic lines at these specific energies (difference in the two energy levels involved) and the continuous spectrum.	48
Figure 2.5. BIPM spectra corresponding to a W anode (top) and Mo anode (bottom) x-ray tube operated at 30 kV (spectra measured at the BIPM using the Compton scatter method)..	49
Figure 2.6. Spectra corresponding to a W anode x-ray tube with Mo filtration operated at 30 kV (top) and the mass attenuation coefficient, μ , for molybdenum (bottom).....	50
Figure 2.7. Schema of an x-ray tube	51
Figure 2.8. Half value layer determination	56
Figure 2.9. Simulation of the BIPM standard L-01 using the PENELOPE geometry package ..	59
Figure 2.10. Schematic diagram of the Compton spectrometer	62
Figure 2.11. Energy calibration curve for the multichannel analyzer	64
Figure 2.12. Compton spectrometer, low-energy Ge detector and multichannel analyser	65
Figure 2.13. Model of the x-ray tube, filters and collimators	66
Figure 2.14. Tungsten target spectra measured with the Compton spectrometer	67
Figure 2.15. Comparison of the simulated and measured spectra for the 30 kV, Mo filter quality.....	68
Figure 2.16. Comparison of the simulated and measured spectra for the 30 kV, Rh filter quality.....	68
Figure 2.17. Normalized calibration coefficients for the Radcal chamber RC6M s.n. 9112...	70
Figure 3.1. Schematic diagram of a free-air chamber [26]	76
Figure 3.2. The new free-air chamber, L-02. A schematic representation (not to scale) showing the various components and important dimensions.....	82

Figure 3.3. Linear fit to the measured points to calculate k_{init} and k_{vol}	86
Figure 3.4. Mapping of the field strength (upper graph) and electric field vectors in the air gap between collector and guard plate (lower graph); lines of equal potential are also plotted.	87
Figure 3.5. Schematic representation of the experimental arrangement for air attenuation measurements	88
Figure 3.6. A cut-away of the geometry used for Monte Carlo simulations, created using the PENGEO code of PENELOPE. A 3D representation is shown at the left; the shaded region shown in the 2D representation at the right is identified as the “scoring region” and the blue region at the centre of the air cavity is the “collecting region”, used for the calculation of the correction factors.	90
Figure 4.1. Horizontal and vertical beam profiles.....	103
Figure 4.2. Half value layer determination using BIPM coded filters	104
Figure 4.3. Comparison of the simulated and measured spectra for the Mo30 quality	105
Figure 5.1. Normalized calibration coefficients for the Radcal chamber	117
Figure 5.2. Normalized calibration coefficients for the Exradin A11 TW chamber.....	118
Figure 5.3. Normalized calibration coefficients for the Exradin Magna chamber.....	118
Figure 5.4. Normalized calibration coefficients for the PTW TM34069 chamber	119
Figure 6.1. Normalized N_K for the Radcal RC6M-9646. The dotted line represents a quadratic fit to the NRC data.	129
Figure 6.2. Normalized calibration coefficients N_K for the PTW23344-0948. The dotted line represents a quadratic fit to the NRC data.....	130
Figure 6.3. Normalized results for the transfer chamber calibration coefficients at the NIST and the BIPM. The dashed blue line through the NIST data represents a linear fit to the NIST data points, including the CCRI 25 kV quality but excluding the Mo-23 quality (see explanation in text).	134
Figure 6.4. Normalized air kerma rate at the BIPM corresponding to the Mo/Mo 25 and Mo/Mo 30 radiation qualities	144

Introduction

Cancer du sein et mammographie : le rôle du BIPM

Cancer du sein

Le cancer du sein est une pathologie maligne qui atteint les tissus mammaires dont les cellules se développent de façon anormale jusqu'à créer une tumeur. Une tumeur maligne est un groupe de cellules cancéreuses capables d'envahir les tissus adjacents ou de s'étendre à d'autres zones du corps en formant des métastases. Le cancer du sein est une maladie qui touche presque uniquement les femmes, mais les hommes peuvent également en être atteints.

Le cancer du sein est de loin le cancer le plus fréquent chez la femme avec 1,38 million de nouveaux cas diagnostiqués dans le monde entier en 2008 (soit 23 % des cancers) et se situe, tous sexes confondus, au deuxième rang de l'ensemble des cancers (10,9 % des cancers). C'est désormais le cancer le plus courant, à la fois dans les pays développés et dans ceux en voie de développement, avec environ 690 000 nouveaux cas estimés dans chacune de ces deux catégories de pays.

Les taux d'incidence varient de 19,3 pour 100 000 femmes en Afrique de l'est à 89,7 pour 100 000 femmes en Europe de l'ouest ; ils sont élevés (plus de 80 pour 100 000) dans les pays développés (à l'exception du Japon) et faibles (moins de 40 pour 100 000) dans la plupart des pays en voie de développement.

La variation des taux de mortalité est beaucoup plus faible (de 6 à 19 pour 100 000 environ) : cela s'explique par le taux de survie au cancer du sein plus favorable dans les pays développés (au taux d'incidence élevé) en raison d'un diagnostic et d'un traitement précoces. Ainsi, le cancer du sein est, dans le monde entier, la cinquième cause de mortalité par cancer (458 000 décès), mais c'est encore la cause de mortalité par cancer la plus fréquente chez les femmes, à la fois dans les pays en voie de développement (269 000 décès, 12,7 % des cancers) et dans les pays développés où le nombre de décès par cancer du sein (189 000 décès) est équivalent à celui des décès par cancer du poumon (188 000 décès) en ce qui concerne la population féminine [1].

Étant donné que les facteurs responsables de l'apparition du cancer du sein sont mal déterminés, la prévention reste problématique. Bien que divers facteurs de risque, tels que l'héritage génétique, aient été mis en évidence par des recherches, il est impossible d'identifier ceux propres à la majorité des femmes atteintes d'un cancer du sein. C'est pourquoi le dépistage précoce de la maladie est le seul moyen de contrôler l'existence d'un cancer du sein chez une femme et de réduire la mortalité.

Mammographie

La mammographie est considérée comme la technique actuelle la plus efficace pour dépister le cancer du sein à un stade précoce. La mammographie est une technique d'imagerie par rayons x qui permet d'obtenir une radiographie de la structure interne du sein. Les rayons x permettent de déceler des grosseurs anormales ou des anomalies de la structure mammaire avant qu'elles ne puissent être identifiées par quelque autre méthode, y compris l'autopalpation. C'est la meilleure technique pour révéler des cancers non palpables ou faiblement détectables. Elle permet également d'effectuer une localisation de la zone atteinte afin de pouvoir effectuer une biopsie ou administrer un traitement.

L'usage de la mammographie débuta en 1960, mais la mammographie moderne n'existe que depuis 1969 date à laquelle les premières unités de rayons x dédiées à l'imagerie mammaire furent disponibles. En 1976 le mammogramme devint un test standard pour détecter le cancer du sein.

Même si la mammographie joue un rôle primordial dans le dépistage du cancer du sein, son utilisation présente des risques faibles, mais non négligeables, de carcinogenèse induite par les rayonnements associés à l'examen par rayons x du sein, l'un des tissus les plus sensibles aux effets des radiations. Il est donc essentiel que les rayons x auxquels le patient est exposé soient délivrés de manière optimale afin d'obtenir la meilleure qualité d'image possible et de réduire au maximum la dose de rayonnement délivrée. C'est pourquoi la surveillance de la dose de rayonnement, de façon régulière et au niveau d'exactitude requis, est un aspect fondamental de la mammographie. En effet cette surveillance est recommandée par les instances internationales et dans la plupart des pays développés il existe une législation la concernant.

Les tissus glandulaires, principaux tissus à risque, constituent presque toujours le site de carcinogénèse. La dose moyenne glandulaire (DMG) est ainsi le meilleur indicateur parmi les différentes grandeurs dosimétriques utilisées pour évaluer le risque de cancer chez un patient. La méthode de référence pour estimer la DMG chez les personnes passant une mammographie par rayons x se fonde sur des mesures du rayonnement émis par le tube à rayons x, ainsi que sur l'utilisation de facteurs de conversion appropriés afin d'obtenir la dose glandulaire.

Dosimétrie de référence pour la mammographie

En radiologie de diagnostic, la grandeur dosimétrique liée au rayonnement émis par le tube à rayons x est le kerma dans l'air, K_{air} , mesuré en gray. Le kerma, acronyme de *kinetic energy released per mass (of material)*, est l'énergie cinétique libérée par unité de masse. En pratique, le kerma dans l'air est mesuré à l'aide d'une chambre d'ionisation. Les chambres d'ionisation du commerce, utilisées par les services de radiologie de diagnostic, doivent être étalonnées dans des laboratoires d'étalonnage de référence, de préférence dans le même type de faisceaux de rayonnement que celui utilisé pour le diagnostic, car la réponse des détecteurs de ce type dépend de l'énergie et peut varier en fonction de la nature des faisceaux de rayonnement.

Dans un pays donné, les laboratoires d'étalonnage de référence en dosimétrie des rayonnements sont généralement rattachés au laboratoire national de métrologie ; ce sont des laboratoires de référence primaires (PSDL) ou secondaires (SSDL) de dosimétrie. Les laboratoires primaires peuvent étalonner des chambres d'ionisation directement par rapport à leurs propres étalons, ou l'instrument de référence d'un laboratoire secondaire de dosimétrie qui est alors en mesure d'étalonner à son tour les chambres des utilisateurs.

Un étalon primaire est un instrument de la plus haute qualité métrologique qui permet de réaliser l'unité d'une grandeur à partir de sa définition. En radiologie de diagnostic, l'étalon primaire pour réaliser le gray, l'unité de la grandeur « kerma dans l'air », est une chambre d'ionisation à paroi d'air.

Les faisceaux de rayonnement couramment utilisés en mammographie sont délivrés par des tubes à rayons x à anode et dispositif de filtration en molybdène. À une tension de fonctionnement entre 25 kV et 35 kV, le seuil d'absorption des rayons x du filtre en

molybdène permet d'éliminer les énergies spectrales les plus élevées émises par la cible en molybdène et de privilégier les émissions de rayons x caractéristiques (17,5 kV et 19,6 kV). Le domaine d'énergie de rayonnement ainsi obtenu est idéal pour que les images de la mammographie des tissus mous soient assez contrastées pour pouvoir effectuer un diagnostic adapté, tout en garantissant que les rayons x aux basses énergies délivrés ne dépassent pas la dose exactement nécessaire.

Certains laboratoires d'étalonnage de référence sont équipés de tubes à rayons x à anode en molybdène équivalents à ceux utilisés pour la mammographie clinique. Ces laboratoires établissent des qualités de rayonnement de référence similaires à celles utilisées en mammographie, à l'aide de leur étalon de kerma dans l'air aux caractéristiques parfaitement déterminées dans ces faisceaux de rayonnement. Les laboratoires de référence non équipés de matériel pour la mammographie mais disposant de tubes à rayons x à anode en tungstène, à savoir ceux utilisés en radiologie conventionnelle, peuvent également établir des qualités de rayonnement de référence similaires à celles utilisées pour la mammographie en ajoutant aux tubes des filtres en molybdène ou en rhodium et en les faisant fonctionner dans la même gamme d'énergie que celle utilisée pour la mammographie. Ces qualités de rayonnement sont également désignées sous le terme de « faisceaux simulés pour la mammographie ». L'utilisation de qualités de rayonnement provenant d'une anode en tungstène pour étalonner des chambres d'ionisation qui serviront à réaliser des mesures dosimétriques dans des faisceaux de rayonnement délivrés par une anode en molybdène nécessite des études supplémentaires afin de déterminer la réponse des chambres aux faisceaux de rayonnement en fonction de la distribution spectrale [2].

Les étalonnages des chambres d'ionisation doivent être effectués dans des faisceaux de rayons x parfaitement définis, la réponse des dosimètres dépendant de la distribution spectrale du faisceau de rayons x. Le matériau de l'anode, la tension produite, le taux de kerma dans l'air, la filtration, la première couche de demi-atténuation et la distribution en énergie des photons (spectre) constituent les principaux paramètres ayant un impact sur les caractéristiques d'un faisceau de rayons x. Il est important que les laboratoires d'étalonnage de référence soient équipés de générateurs de tension stable afin d'éviter toute fluctuation de la distribution spectrale du faisceau de rayons x ; des mesures exactes de la tension produite sont nécessaires pour déterminer la qualité du faisceau de rayonnement, et des systèmes stables de contrôle et de mesure du courant traversant l'anode permettent d'évaluer les corrections à appliquer à d'éventuelles fluctuations du taux de kerma dans l'air mesuré.

Les déterminations exactes du kerma dans l'air nécessitent que les caractéristiques de l'étalon primaire soient parfaitement définies ou que des chambres étalonnées et traçables à des étalons primaires soient utilisées. Le moyen de vérifier l'exactitude de mesures est de participer à des comparaisons avec d'autres étalons dans des faisceaux de rayonnement bien définis. Les comparaisons en dosimétrie sont considérées comme un élément important des programmes d'assurance qualité et sont également recommandées dans des guides normatifs internationaux édités notamment par l'Organisation internationale de normalisation (ISO) [3], la Commission électrotechnique internationale (IEC) [4], la Commission internationale des unités et mesures radiologiques (ICRU) [5] et l'Agence internationale de l'énergie atomique (IAEA) [6].

Rôle du BIPM

Des comparaisons internationales d'étalons primaires et des étalonnages d'étalons secondaires dans le domaine de la dosimétrie des rayonnements ionisants ont été effectués au Bureau international des poids et mesures (BIPM) pour le compte des laboratoires nationaux de métrologie depuis le début des années 60. Le BIPM maintient des étalons de référence stables, met à disposition de ses États Membres des équipements internationaux de comparaison et assure l'unification mondiale des mesures et leur traçabilité au Système international d'unités (SI). Les comparaisons internationales bilatérales organisées par le BIPM permettent aux laboratoires nationaux de métrologie de démontrer leurs aptitudes en matière de mesures et d'étalonnages, tel que cela est défini dans l'Arrangement de reconnaissance mutuelle du CIPM (CIPM MRA). Le CIPM MRA a été mis en place en 1999 par le Comité international des poids et mesures (CIPM), l'organe de supervision du BIPM, afin d'établir le degré d'équivalence des étalons de mesure nationaux maintenus par les laboratoires nationaux de métrologie, de reconnaître les aptitudes en matière de mesures et d'étalonnages (CMCs) de ces laboratoires et de mettre en place un système de traçabilité des mesures au SI.

Le BIPM travaille en étroite collaboration avec les Comités consultatifs, dont les membres sont les laboratoires nationaux de métrologie des États Parties à la Convention du Mètre (1875). Le Comité consultatif pour les étalons de mesure des rayonnements ionisants (CCEMRI) a été créé en 1958, suite aux recommandations de l'International Commission for Radiation Units and Measurements (ICRU); il a été renommé Comité consultatif des rayonnements ionisants (CCRI) en 1997. Sa mission est de conseiller le BIPM sur son

programme de travail scientifique en matière de rayonnements ionisants, et de fixer les conditions de référence pour toutes les comparaisons de dosimétrie.

Les comparaisons d'étalons nationaux primaires par rapport à ceux du BIPM sont désignées sous le terme de « comparaisons clés » et ont pour référence BIPM.RI(I)- K_n , (n étant le nombre associé à chaque comparaison clé). La détermination par le BIPM de la grandeur dosimétrique a été établie par le CCRI(I) en 1999 comme la valeur de référence de la comparaison clé (KCRV), x_R , à partir de laquelle les laboratoires nationaux de métrologie participant à la comparaison clé établissent les degrés d'équivalence. Les résultats de comparaison sont publiés dans la base de données du BIPM sur les comparaisons clés KCDB [7] du CIPM MRA.

Le Département des rayonnements ionisants a effectué les premières comparaisons internationales dans des faisceaux de rayons x aux basses énergies en 1966 [8] dans les qualités de rayonnement de référence recommandées par le CCEMRI [9] : ces comparaisons sont identifiées sous la référence BIPM.RI(I)-K2. Les faisceaux de rayonnement de référence ont été établis au BIPM à l'aide d'un tube à rayons x à anode en tungstène et filtre en aluminium, fonctionnant de 10 kV à 50 kV. Une chambre à parois d'air libre a été mise au point au BIPM au début des années 60 afin de servir d'étalon primaire pour ces faisceaux de rayonnement ; elle est depuis utilisée pour toutes les comparaisons en continu de kerma dans l'air dans ce domaine.

En 2001, la Section I du CCRI, (CCRI(I)), a pour la première fois proposé que le BIPM étende ses activités à la mammographie, afin de répondre aux besoins des laboratoires nationaux de métrologie en matière de comparaisons dans ce domaine, et afin de déterminer les caractéristiques des étalons nationaux et de les étalonner en garantissant leur traçabilité au Système international d'unités (SI).

J'ai entrepris ce travail en établissant un ensemble de neuf qualités de rayonnement à l'aide du tube à rayons x à anode en tungstène existant, équipé de filtres en molybdène ou rhodium, afin de simuler les faisceaux de rayonnement utilisés en mammographie clinique [10]. En 2005 et 2007, un programme à moyen terme visant à mettre en place au BIPM un équipement de comparaison et d'étalonnage dans les faisceaux mammographiques a été présenté au CCRI(I). En 2009, après l'installation d'un tube à rayons x à anode en molybdène, quatre qualités de rayonnement ont été établies comme faisceaux de référence pour les comparaisons

et étalonnages en mammographie [11], suite aux recommandations faites par la Section I du CCRI lors de la 19^e réunion du Comité au BIPM, en mai 2009. Par ailleurs, une nouvelle chambre à parois d'air libre a été conçue et fabriquée au BIPM afin d'être utilisée comme étalon primaire pour la dosimétrie dans les faisceaux mammographiques. Il a été établi que les qualités de rayons x simulés pour la mammographie étaient appropriées pour étalonner quatre chambres d'ionisation similaires à celles couramment utilisées par les laboratoires nationaux de métrologie pour la dosimétrie en mammographie en comparant la réponse des chambres aux qualités de rayonnement déterminées par la combinaison tungstène/molybdène ou molybdène/molybdène.

Les paragraphes suivants décrivent brièvement le travail effectué au BIPM pour disposer d'équipements internationaux de comparaison et d'étalonnage dans le domaine de la mammographie, et sont répartis en cinq parties : l'établissement des faisceaux de rayonnement simulés pour la mammographie ; la conception, la construction et la détermination des caractéristiques d'un étalon primaire ; la mise en place de qualités de rayonnement de référence pour la mammographie ; l'étude de la réponse de chambres d'ionisation à différents faisceaux de rayonnement ; et enfin, le programme de comparaisons internationales constituant une nouvelle comparaison clé du BIPM, ayant pour référence BIPM.RI(I)-K7. Les détails complets sont donnés dans les différents chapitres de ce mémoire, qui peuvent être lus de manière indépendante ; toutes les références sont fournies dans le dernier chapitre.

Qualités de faisceaux de rayonnement simulés pour la mammographie

Afin de disposer de qualités de rayonnement similaires à celles utilisées pour la mammographie, tout en se servant de son tube à rayons x à anode en tungstène, j'ai mis en place un nouvel ensemble de qualités de rayonnement en remplaçant la filtration en aluminium utilisée pour les qualités de rayonnement de référence recommandées par le CCRI par des filtres en molybdène et en rhodium de 0,06 mm et 0,05 mm d'épaisseur respectivement, et en faisant fonctionner le tube à diverses tensions spécifiques à la mammographie clinique.

La détermination de la qualité d'un faisceau, exprimée en termes d'épaisseur d'aluminium nécessaire pour réduire de moitié le taux de kerma dans l'air par rapport à sa valeur initiale, dénommée couche de demi-atténuation (CDA), a été réalisée à l'aide de l'étalon du BIPM, à

savoir la chambre à parois d'air libre L-01. Des facteurs de correction ont été appliqués aux mesures pour déterminer le débit de kerma dans l'air. Comme ces facteurs de correction dépendent de l'énergie, ils doivent être déterminés pour chaque qualité de rayonnement, de façon expérimentale ou au moyen de calculs, à l'aide du spectre correspondant à chaque qualité.

Le facteur de correction k_s (défaut de saturation dû à la recombinaison et à la diffusion des ions) a été déterminé à l'aide de la méthode proposée par De Almeida et Niatel [12] et mise en œuvre par Boutillon [13] ; les corrections k_{pol} (polarité) et k_p (transmission de photons par la paroi avant de la chambre) ont été déterminées aux moyen de mesures ; les facteurs de correction k_e (perte d'électrons), k_{sc} (diffusion des photons), k_{fl} (fluorescence) et k_{dia} (diffusion et transmission des photons à partir du diaphragme) ont été calculés à l'aide des techniques de Monte Carlo ; à cet effet le programme de calcul Monte Carlo PENELOPE [14] a été utilisé pour des photons monoénergétiques de 2 keV à 50 keV, par pas de 2 keV ; une simulation complète de l'étalon du BIPM a été réalisée avec le programme de géométrie du code PENELOPE, PENGEO. Les résultats des calculs pour les photons monoénergétiques ont été convolués avec le spectre correspondant à chaque qualité de rayonnement, déterminée de façon expérimentale et par simulation, tel que cela sera ultérieurement expliqué.

Les spectres ont été mesurés à l'aide de la méthode de diffusion Compton, qui consiste à placer un matériau de diffusion dans le faisceau primaire, puis à mesurer les photons déviés sous un certain angle, et enfin à reconstruire le faisceau primaire. Un spectromètre Compton du commerce construit pour diffuser les photons sous un angle de 90° a été utilisé pour cette étude ; les photons déviés ont été identifiés à l'aide d'un détecteur au germanium pur adapté à la mesure des basses énergies associé à un analyseur multicanaux. Le détecteur au germanium a été étalonné aux énergies connues des rayons x et γ émis par des sources radioactives de ^{125}I et ^{241}Am . Les spectres primaires de rayons x ont été reconstruits à partir de la distribution de l'amplitude des impulsions à l'aide d'un logiciel du commerce [15].

Deux des spectres mammographiques ont également été obtenus par simulation à l'aide des techniques de Monte Carlo en utilisant le programme PENELOPE. La configuration du tube à rayons x (source d'électrons, cible, fenêtre du tube, système du collimateur et filtres) a été simulée en détail à l'aide du programme de géométrie de PENELOPE. Une interface utilisateur a été écrite : elle appelle les sous-programmes définis dans PENELOPE pour simuler le transport d'électrons se propageant dans le vide et frappant la cible où ils induisent un

rayonnement de freinage, ainsi que le transport de photons à travers les collimateurs et les filtres, afin d'enregistrer, au niveau du plan de mesure de référence, l'énergie des photons ainsi que les coordonnées associées et la direction de chaque photon traversant ce plan.

Les spectres mesurés présentent un bon accord avec les spectres calculés, la déviation maximale étant inférieure à 0,35 keV ; ces différences n'ont pas d'effet significatif sur le calcul des facteurs de correction à appliquer à l'étalon. Les débit de kerma dans l'air ont ensuite été mesurés à l'aide de la chambre à parois d'air libre L-01.

L'utilisation des faisceaux produits par la combinaison tungstène/molybdène pour l'étalonnage de chambres qui seront utilisées ensuite pour la dosimétrie de faisceaux produits par la combinaison molybdène/molybdène doit être évalué en comparant la réponse de ces chambres dans ces deux types de faisceaux de rayonnement. En préambule à la présente étude, trois chambres d'ionisation couramment utilisées pour la dosimétrie en mammographie ont été étalonnées de régulièrement pendant plusieurs années, dans les faisceaux simulés pour la mammographie, afin de déterminer leur réponse.

Étalon primaire pour la mammographie

Un nouvel étalon primaire pour la dosimétrie dans les faisceaux mammographiques a été conçu et fabriqué au BIPM. Ce nouvel étalon, appelé L-02, est une chambre à paroi d'air libre à plaques parallèles conçue pour être utilisée jusqu'à 50 kV et réduire au maximum l'amplitude des facteurs de correction appliqués pour la détermination du kerma dans l'air.

Le nouvel étalon L-02 a été comparé à l'étalon actuel L-01, à l'aide du tube à rayons x à anode en tungstène, dans les qualités de rayonnement de référence du CCRI. À cette fin, les facteurs de correction à appliquer au nouvel étalon pour déterminer le taux de kerma dans l'air ont dû être définis pour ces faisceaux de référence ; comme cela a été expliqué dans la section précédente, ces facteurs ont été obtenus soit par des calculs à l'aide des techniques de Monte Carlo, soit de façon expérimentale au moyen de mesures ionométriques. Le nouvel étalon a été simulé de façon exhaustive à l'aide du programme de géométrie PENELOPE permettant de reproduire les dimensions et les matériaux. Les facteurs de correction ont été calculés pour des photons monoénergétiques de 2 keV à 50 keV, par pas de 2 keV. Les résultats des calculs pour les photons monoénergétiques ont été convolués avec les spectres spécifiques aux qualités du CCRI.

Ces spectres ont été mesurés à l'aide du spectromètre Compton du BIPM et ont également été simulés en utilisant le programme PENELOPE.

Étant donné que la comparaison des étalons L-01 et L-02 a fait ressortir des différences de l'ordre de 4×10^{-3} , une série d'études visant à déterminer la cause de ce désaccord ont été entreprises : elles concernent la détermination du volume de la chambre, les potentiels de contact entre le collecteur et la plaque de garde, ainsi que la température et sa stabilité au sein de la chambre. Aucune de ces études n'a permis d'expliquer les différences initiales qui ont pu atteindre 8×10^{-3} au cours de certaines mesures. La planéité de la plaque du collecteur a été vérifiée en utilisant un instrument de mesure de coordonnées tridimensionnelles (MMT) une fois la chambre constituée, puis à chacun de ses démontages et réassemblages, une tolérance de $50 \mu\text{m}$ étant acceptée. Afin d'évaluer si cette tolérance convient, le bord supérieur du collecteur a été surélevé puis abaissé de près de $100 \mu\text{m}$ par rapport à la plaque de garde. On a alors observé des différences allant jusqu'à 3×10^{-2} , ce qui indique que la tolérance de $50 \mu\text{m}$ est trop élevée et pourrait expliquer la variation des résultats. Un nouveau support a donc été conçu pour que l'électrode de collecte puisse être ajusté par rapport à la plaque de garde à mieux que $5 \mu\text{m}$. L'électrode de collecte et la plaque de garde, tous deux en aluminium, ont été nettoyés puis à nouveau assemblés à l'aide du nouveau support. Avec cette configuration, la différence entre les étalons a été réduite à 1×10^{-3} , mais ce résultat ne s'est pas avéré stable, atteignant trois mois plus tard 4×10^{-3} sans modification de la co-planéité. Ce n'est qu'en revêtant le collecteur et la plaque de garde de graphite que cette différence a pu être à nouveau réduite à 1×10^{-3} ; elle est depuis restée stable.

Qualités de rayonnement de référence pour la mammographie

Un tube à rayons x à anode en molybdène a été installé dans le laboratoire des rayons x pour les basses énergies du BIPM ; des équipements tels que le générateur à haute tension, le stabilisateur de tension ou le système de mesure du courant traversant l'anode, peuvent ainsi être utilisés soit avec le tube à anode en tungstène existant, soit avec le nouveau tube à anode en molybdène.

Le plan de référence est établi à 600 mm du centre du tube. Des films radiographiques ont été utilisés pour l'étude du champ de rayonnement (taille, forme et axe du faisceau) et des mesures des profils de faisceaux horizontaux et verticaux effectuées à l'aide d'une chambre d'ionisation en forme de dé. Grâce à ces radiographies et profils de faisceaux, un système

équipé de deux collimateurs en plomb a été conçu et usiné afin de produire un champ circulaire de 10 cm de diamètre dans le plan de référence.

Quatre qualités de rayonnement, de 25 kV à 35 kV, ont été choisies comme faisceaux de référence pour les comparaisons et étalonnages. La qualité du faisceau, exprimée en termes de couche de demi-atténuation d'aluminium (CDA), a été déterminée pour chaque faisceau à l'aide du nouvel étalon primaire. Le courant traversant l'anode a été sélectionné pour chaque qualité afin d'obtenir un débit de kerma dans l'air de 2 mGy s^{-1} dans le plan de référence. Un filtre en molybdène de $30 \mu\text{m}$ d'épaisseur est utilisé pour l'ensemble des qualités.

Les spectres en énergie de photons ont été mesurés à l'aide de la méthode de diffusion Compton précédemment décrite. Deux spectres mammographiques ont également été obtenus par simulation à l'aide des techniques de Monte Carlo en utilisant le programme PENELOPE. La configuration du tube à rayons x (cible en molybdène, filtre en molybdène, et collimateur) a été simulée à l'aide du programme de géométrie PENELOPE.

Les facteurs de correction à appliquer aux mesures réalisées avec l'étalon utilisé pour la détermination de K_{air} ont été obtenus par des calculs de Monte Carlo, ou de façon expérimentale par mesures ionométriques. Les résultats pour les photons monoénergétiques ont été convolués avec les spectres mesurés à l'aide du spectromètre Compton du BIPM et également avec les spectres simulés à l'aide du programme PENELOPE. Quoiqu'il existe des différences entre les amplitudes du pic pour les spectres mesurés et pour ceux calculés, la détermination des facteurs de correction applicable à l'étalon y demeure insensible.

Étude de la réponse d'une chambre aux faisceaux de rayonnement simulés pour la mammographie

La pertinence des faisceaux simulés pour la mammographie, établis à l'aide d'un tube à rayons x à anode en tungstène et filtre en molybdène, pour étalonner des chambres d'ionisation a été étudiée pour quatre types de chambres couramment utilisées pour la dosimétrie en mammographie. Les chambres d'ionisation étudiées, une Radcal RC6M, une Exradin A11TW, une Exradin Magna 92650 et une PTW 34069 ont été étalonnées au BIPM dans des faisceaux utilisant la combinaison tungstène/molybdène, puis les réponses obtenues ont été comparées avec celles résultant de l'étalonnage de ces chambres dans des faisceaux de qualité mammographique utilisant la combinaison molybdène/molybdène. Les coefficients d'étalonnage mesurés dans les faisceaux simulés pour la mammographie sont en accord avec

ceux obtenus dans les faisceaux provenant de tubes à rayons x à anode en molybdène au niveau de 1×10^{-3} pour les chambres Exradin, 3×10^{-3} pour la chambre Radcal et 5×10^{-3} pour la chambre PTW. Par conséquent, les laboratoires nationaux de métrologie non équipés de tubes à rayons x à anode en molybdène peuvent, à ce niveau d'incertitude, mettre en place des faisceaux utilisant la combinaison tungstène/molybdène pour étalonner des chambres devant être utilisées dans des faisceaux délivrés par des tubes à rayons x à anode en molybdène. Toutefois, cette méthode ne doit pas être appliquée à d'autres types de chambre sans une vérification similaire préalable dans des faisceaux utilisant la combinaison tungstène/molybdène et la combinaison molybdène/molybdène.

Comparaisons internationales

Une nouvelle série de comparaisons en continu du BIPM, identifiées dans la KCDB sous la référence BIPM.RI(I)-K7, a commencé en 2009 ; elle consiste en des comparaisons bilatérales d'étalons primaires pour la dosimétrie en mammographie entre les laboratoires nationaux de métrologie NMI et le BIPM.

Les comparaisons d'étalons de kerma dans l'air dans les faisceaux de rayons x de qualité mammographique peuvent être effectuées directement au BIPM ou indirectement à l'aide des chambres d'ionisation de transfert appartenant au NMI. Dans le premier cas, le kerma dans l'air est déterminé en comparant l'étalon d'un laboratoire national de métrologie à celui du BIPM, les résultats de comparaison étant exprimés suivant le rapport $K_{\text{NMI}}/K_{\text{BIPM}}$. Dans le cas d'une comparaison indirecte, le laboratoire national de métrologie étalonne un étalon de transfert (chambre d'ionisation) par rapport à son propre étalon primaire, en déterminant le coefficient d'étalonnage $N_{K,\text{NMI}}$, défini comme la moyenne des mesures effectuées avant et après les celles réalisées au BIPM ; entre-temps, l'instrument de transfert est étalonné au BIPM, ce qui permet de déterminer le coefficient $N_{K,\text{BIPM}}$. Le résultat de la comparaison s'obtient alors en évaluant le rapport des coefficients d'étalonnage déterminés dans chacun des laboratoires, $N_{K,\text{NMI}}/N_{K,\text{BIPM}}$. Si l'utilisation de chambres de transfert peut induire une incertitude plus élevée dans les résultats de la comparaison que lors d'une comparaison directe d'étalons primaires, cela permet également d'obtenir de précieuses informations sur la reproductibilité des coefficients d'étalonnage et sur le comportement des instruments de transfert utilisés dans la chaîne de dissémination. Le bilan d'incertitude est analysé en profondeur afin de calculer l'incertitude-type composée des résultats de la comparaison, en prenant en considération les corrélations entre les étalons.

Les résultats de chaque comparaison sont analysés en termes de degré d'équivalence par rapport à la valeur de référence de la comparaison clé pour chaque étalon national, x_R , avec $x_R = 1$. Pour chaque laboratoire, i , pour lequel un résultat de comparaison, x_i , avec une incertitude-standard composée u_i , a été obtenu, le degré d'équivalence, D_i , établi par rapport à la valeur de référence, s'écrit $x_i - 1$ avec une incertitude étendue $U_i = 2 u_i$. Ces données permettent de créer des tableaux de valeurs et graphiques de résultats qui sont enregistrés dans la base de données du BIPM sur les comparaisons clés (KCDB).

Pour chaque comparaison un rapport correspondant est écrit décrivant les conditions de mesure dans chaque laboratoire, les instruments de transfert utilisés dans le cas d'une comparaison indirecte, les facteurs de correction utilisés dans la détermination du débit de kerma dans l'air et les facteurs d'étalonnage pour les comparaisons indirectes, les résultats de la comparaison avec leurs incertitudes. Les rapports de comparaisons sont examinés par le CCRI : une fois approuvés, ils sont publiés dans *Metrologia* et leurs résultats sont enregistrés dans la KCDB. Ces rapports sont publiés sur internet par IOP Publishing, en version électronique, et sont en accès libre sur le site Web du BIPM.

La première comparaison d'étalons pour le kerma dans l'air dans les faisceaux de rayons x de qualité mammographique a été effectuée avec le NRC (Canada) en mars 2007 dans le faisceau utilisant la combinaison tungstène/molybdène. Il s'agissait d'une comparaison indirecte utilisant un jeu de quatre chambres d'ionisation appartenant à ce laboratoire, mesurées à deux distances différentes.

La comparaison suivante a été conduite avec le NMIJ (Japon) en novembre 2009. Il s'agissait de la première comparaison dans des faisceaux de rayons x utilisant la combinaison molybdène/molybdène effectuée à l'aide d'un ensemble de trois chambres d'ionisation appartenant au NMIJ.

La troisième demande de participation à la comparaison clé BIPM.RI(I)-K7 a été formulée par le NIST (États-Unis) ; cette comparaison a été effectuée de façon indirecte à l'aide d'un instrument de transfert en janvier 2010.

En septembre 2010, une nouvelle comparaison a été programmée avec la PTB (Allemagne), non seulement dans les faisceaux de rayonnement de qualité mammographique (qualités de faisceaux utilisant la combinaison molybdène/molybdène) mais aussi dans les faisceaux

simulés pour la mammographie (qualités de faisceaux utilisant la combinaison tungstène/molybdène) ; deux instruments de transfert ont été utilisés pour cette comparaison.

Une comparaison directe et une autre indirecte ont été réalisées avec l'ENEA (Italie) dans les faisceaux simulés pour la mammographie (qualités de faisceaux utilisant la combinaison tungstène/molybdène) car l'ENEA dissémine les coefficients d'étalonnage dans ces faisceaux. Les mesures effectuées avec l'étalon primaire de l'ENEA et avec une chambre d'ionisation de transfert ont été faites au BIPM en février 2011.

Les résultats des comparaisons avec le NRC, le NMIJ, le NIST et la PTB ont été publiés dans les suppléments techniques de la revue *Metrologia*, *Metrologia Technical Supplements* ; le graphique indiquant les degrés d'équivalence, tel qu'il apparaît dans la KCDB est présenté Figure 1.

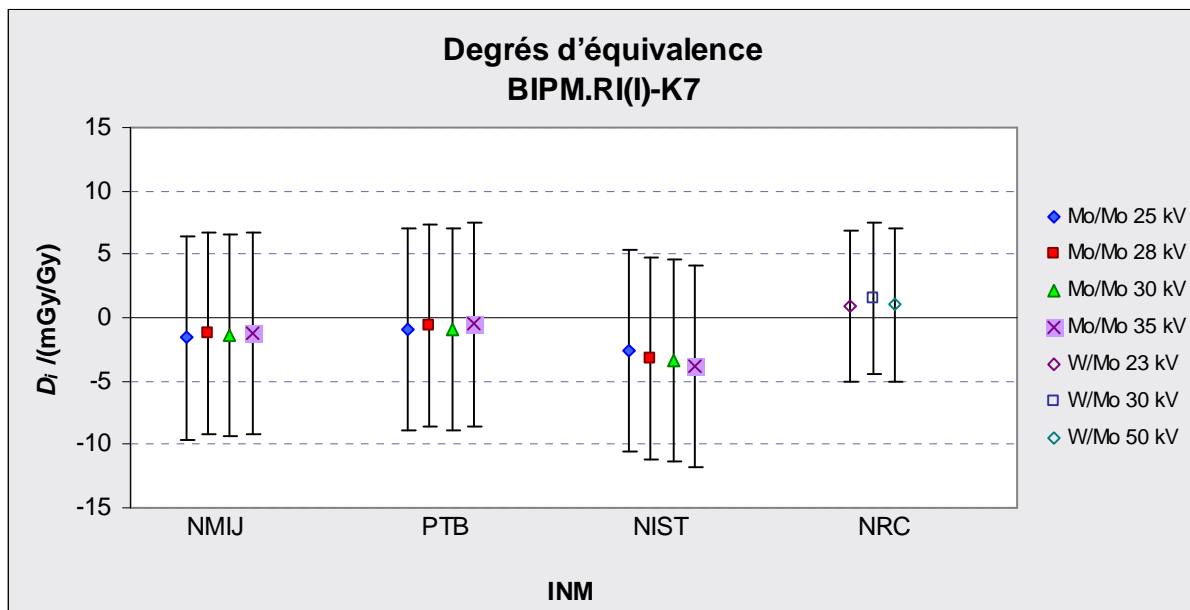


Figure 1. Degrés d'équivalence D_i et leurs incertitudes U_1 ($k = 2$), in mGy/Gy

L'ENEA a accepté de répéter leur comparaison dans un proche avenir eu égard aux différentes conditions d'étalonnage qui sont utilisées dans ce laboratoire pour étalonner leurs chambres d'ionisation.

L'Agence internationale de l'énergie atomique (AIEA), qui est traçable à la PTB, a demandé au BIPM de lancer une comparaison bilatérale dans des faisceaux de rayons x utilisant la combinaison molybdène/molybdène pour soutenir ses « aptitudes » en matière de mesures et

d'étalonnages (CMC) publiées dans l'appendice C de la base de données de l'Arrangement de reconnaissance mutuelle du CIPM, CIPM MRA KCDB. Les mesures ont été effectuées en 2012 et le rapport de la comparaison a été envoyé au CCRI(I) pour approbation puis publication.

Une comparaison récente avec le VNIIM (Fédération de Russie) a été entreprise dans les faisceaux de rayons x utilisant la combinaison molybdène/molybdène avec une chambre de transfert ; des étalonnages successifs de cette chambre sont encore en cours de réalisation au VNIIM, après que les mesures ont été menées à bien au BIPM.

Chapter 1. Breast cancer and mammography: the role of the BIPM

Introduction

1.1. Breast cancer

Breast cancer is a malignant disease that starts with the transformation of cells of the breast tissues to form a tumour. A malignant tumour is a group of cancerous cells that may grow into (invade) surrounding tissues or spread (metastasize) to distant areas of the body. The disease occurs almost entirely in women, but men can get it, too.

Breast cancer is by far the most frequent cancer among women with an estimated 1.38 million new cancer cases diagnosed worldwide in 2008 (23% of all cancers), and ranks second overall (10.9% of all cancers). It is now the most common cancer both in developed and developing regions of the world with around 690,000 new cases estimated in each of these regions.

Incidence rates vary from 19.3 per 100,000 women in Eastern Africa to 89.7 per 100,000 women in Western Europe, and are high (greater than 80 per 100,000) in developed regions of the world (except Japan) and low (less than 40 per 100,000) in most of the developing regions.

The range of mortality rates is much less (approximately 6 to 19 per 100,000) because of the more favourable survival of breast cancer in (high-incidence) developed regions, due to early detection and treatment. As a result, breast cancer ranks globally as the fifth cause of death from cancer overall (458,000 deaths), but it is still the most frequent cause of cancer death in women in both developing (269,000 deaths, 12.7% of total) and developed regions, where the estimated 189,000 deaths is almost equal to the estimated number of deaths from lung cancer (188,000 deaths) for women [1].

As the causes of breast cancer are poorly understood, prevention is problematic. Although several risk factors for breast cancer have been well documented, including genetic make-up, it is not possible to identify specific risk factors for the majority of women with breast cancer.

Therefore, detection of the disease at an early stage is the only way to control breast cancer and reduce mortality.

1.2. Mammography

Mammography is considered to be the most sensitive technique currently available for early detection of breast cancer. It is an imaging technique that uses x rays to provide a picture of the internal structure of the breast. The x rays can show abnormal growths or changes in breast tissue before they can be identified by any other method, including breast self-examination. It is considered to be the best technique for detecting non-palpable, subtle breast cancers and serves also as means of localization for biopsy and therapy.

Mammography started in 1960, but modern mammography has existed only since 1969 when the first x-ray units dedicated to breast imaging were available. By 1976, the mammogram became the standard test for breast cancer detection.

Although mammography plays an important role in the detection of breast cancer, there are small but non-negligible risks of radiation-induced carcinogenesis associated with an x-ray examination of the breast, one of the more radiosensitive tissues. Thus, it is essential that the x rays to which the patient is exposed are used efficiently and effectively to optimize the image quality and minimize the radiation dose delivered to the breast. Therefore, the routine and accurate monitoring of radiation dose is an important aspect in mammography. Indeed, this is recommended internationally and in most developed countries there is a legislation regarding this.

In terms of the tissues at risk, the glandular tissue is nearly always the site of carcinogenesis. Thus, among the different dosimetric quantities used in risk assessment, the mean glandular dose (MGD) is the best indicator of patient risk. The standard method of estimating the MGD on patients undergoing mammography x-ray examinations is based on measurements of the output of the x-ray tube and the use of appropriate conversion factors to obtain the glandular dose.

1.3. Reference dosimetry for mammography

The dosimetric quantity related to the output of the x-ray tube used in diagnostic radiology is the air kerma, K_{air} , measured in gray. The kerma is the acronym for the kinetic energy

released per mass (of material). The air kerma is readily measured in practice using ionization chambers. Commercial ionization chambers used in diagnostic radiology departments need to be calibrated at standard reference laboratories; this calibration should be preferably in the same type of radiation beams as used for diagnosis as these types of detectors are generally energy dependent and may have different responses to different radiation beams.

Standards reference laboratories for radiation dosimetry are usually part of the National Metrology Institute (NMI) of each country; they can either be a Primary Standard Dosimetry Laboratory (PSDL) or a Secondary Standard Dosimetry Laboratory (SSDL). Primary laboratories can calibrate the user's chamber directly against their primary standards, or they can calibrate reference instruments belonging to a Secondary Standard Laboratory, which in turn calibrates the users' chambers.

A primary standard is an instrument of the highest metrological quality that permits determination of the unit of the quantity from its definition. In diagnostic radiology, the primary standard for realizing the unit gray for the quantity air kerma is a free-air ionization chamber.

The radiation beams in common use for mammography are based on molybdenum anode x-ray tubes with molybdenum filtration. When operated at voltages between 25 kV and 35 kV, the x-ray absorption edge of the Mo filter cuts out the higher spectral energies from the Mo target while the emissions of characteristic x-rays of 17.5 keV and 19.6 keV from the target are favoured and photons with energy less than 10 keV are absorbed. This provides the ideal radiation energy range to provide good diagnostic contrast in soft tissue images while ensuring that low-energy x-rays do not contribute to unnecessary patient dose.

Some of the standards laboratories are indeed equipped with molybdenum-anode x-ray tubes, like the ones used in clinical mammography. The laboratories establish reference radiation qualities similar to those used in mammography, using their standard to determine the air kerma characterized in these radiation beams. Those reference laboratories with no mammography facilities but having tungsten-anode x-ray tubes, the type of tube used in conventional radiology, can also establish similar reference radiation qualities as used for mammography by adding molybdenum or rhodium filters and operating the tube in the same energy range used in mammography. These radiation qualities are referred to as simulated mammography beams. The use of tungsten-anode radiation qualities to calibrate ionization

chambers that will be used for the dosimetry of molybdenum-anode radiation beams requires additional studies to determine the response of the chambers to radiation beams with different spectral distribution [2].

Calibrations of ionization chambers have to be made in well defined x-ray beams, as the response of the dosimeters depends on the spectral distribution of the x-ray beam. The anode material, the generating voltage, the air kerma rate, the filtration, the first half value layer and the photon-energy distribution (spectrum) are the main parameters that determine the x-ray beam characteristics. It is important that standard reference laboratories are equipped with stable voltage generators in order to avoid fluctuations in the spectral distribution of the x-ray beam; accurate measurements of the generating voltage are needed in order to determine the quality of the radiation beam, and stable monitoring and measuring systems for the anode current allow corrections to be applied for possible fluctuations to the measured output (air-kerma).

Accurate air-kerma determinations require a full characterization of the primary standard or the use of calibrated chambers traceable to primary standards. The way to verify the accuracy of measurements is by participating in comparisons with other standards in well defined radiation beams. The concept of dosimetry comparisons is recognized as an important element in quality assurance programmes and is also recommended in international guides like the International Organization of Standardization (ISO) norm [3], International Electrotechnical Commission (IEC) series [4], International Commission on Radiation Units and Measurements (ICRU) report [5] and the International Atomic Energy Agency (IAEA) Code of Practice [6].

1.4. The role of the BIPM

International comparisons of primary standards and calibrations of secondary standards of the National Metrology Institutes for radiation dosimetry have been carried out at the Bureau International des Poids et Mesures (BIPM) since the early 1960s. The BIPM maintains stable reference standards, provides an international facility for comparisons and ensures world-wide uniformity of measurements and their traceability to the International System of Units (SI). International bilateral comparisons organized by the BIPM enable the NMIs to demonstrate their calibration and measurement capabilities as presented in the CIPM Mutual Recognition Arrangement (CIPM MRA database). The CIPM MRA was established in 1999 by the

International Committee for Weight and Measurements CIPM, the supervisory body of the BIPM, to establish the degree of equivalence of national measurement standards maintained by the NMIs, to recognize the calibration and measurement capabilities of the NMIs (CMCs) and to provide a system of traceability to the international system of units (SI).

The BIPM operates through a series of Consultative Committees, whose members are the national metrology institutes of the States that are party to the Metre Convention of 1875. A Consultative Committee for Ionizing Radiation (CCRI) was established in 1958 following recommendations of the International Commission on Radiation Units and Measurements (ICRU) to advise on the programme of work of the BIPM Ionizing Radiation Department and also to determine the reference conditions for all dosimetry comparisons.

Comparisons of national primary standards with the BIPM primary standards are designated as key comparisons with reference BIPM.RI(I)-K n , (n is the number for each key comparison). The CCRI(I) took the decision at its meeting in 1999 to use the BIPM determination of air-kerma rate as the basis of the key comparison reference value (KCRV), x_R , to which the degrees of equivalence are established for the NMIs that participate. The comparison results are published in the BIPM key comparison data base KCDB [7] of the CIPM MRA.

The Ionizing Radiation (RI) Department started international comparisons in low-energy x-ray beams in 1966 [8] in the reference radiation qualities recommended by the CCRI [9], and these are identified as BIPM.RI(I)-K2 comparisons. These reference radiation beams were established at the BIPM using a tungsten-anode x-ray tube with aluminium filtration and the tube is operated in the range from 10 kV to 50 kV. A free-air chamber was developed at the BIPM as the primary standard for these beams in the early 1960s and it has been used for all the ongoing air-kerma comparisons in these reference beams to date.

In 2001, the CCRI(I) first proposed that the BIPM extend these activities to mammography, to meet the needs of the National Metrology Institutes for comparisons in this domain and to provide characterizations and calibrations of national standards traceable to the International System of Units (SI).

I began this work at the BIPM by establishing a set of nine radiation qualities using the existing tungsten-anode x-ray tube with molybdenum and rhodium as filters to simulate the radiation beams used in clinical mammography [10]. In 2005 and 2007, a medium-term

programme was presented to the CCRI to implement a facility for comparisons and calibrations in clinical-type mammography beams at the BIPM. In 2009, after the installation of a molybdenum-anode x-ray tube, a set of four radiation qualities was established as reference beams for mammography comparisons and calibrations [11], following the recommendations made by the Consultative Committee for Ionizing Radiation, Section I (CCRI(I)) during the 19th meeting (May 2009) held at the BIPM. In addition, a new free-air chamber primary standard for air kerma was designed and constructed at the BIPM to be used for the dosimetry of these beams. The suitability of the simulated mammography x-ray qualities for the calibration of four ionization chambers of the type currently used by NMIs for mammography dosimetry was carried out by comparing their responses to both tungsten/molybdenum and molybdenum/molybdenum sets of radiation qualities.

A brief description of the work carried out at the BIPM to provide an international facility for comparisons and calibrations in the mammography field is presented in the following paragraphs, divided into five stages: establishment of simulated mammography beams; design, construction and characterization of a primary standard; set-up of reference mammography radiation qualities; study of the response of ionization chambers to different radiation beams; and finally, the international comparison programme running as a new BIPM on-going key comparison with reference BIPM.RI(I)-K7 and characterization of national standards. Full detail is presented in the subsequent chapters of this thesis, each of which is stand-alone; all the references are given in the final chapter.

1.4.1. Simulated mammography radiation qualities

In order to have radiation qualities similar to those used in mammography but using the tungsten-anode x-ray tube at the BIPM, a new set of qualities was implemented by replacing the aluminium filtration used for the CCRI reference radiation qualities by molybdenum and rhodium filters of 0.06 mm and 0.05 mm thickness, respectively, and operating the tube at the different voltages used in the clinical mammography range.

The determinations of the beam quality, expressed in terms of the aluminium thickness needed to reduce the air kerma rate to half its initial value, known as the half-value layer (HVL), were made using the BIPM primary standard, the free air chamber L-01. A set of correction factors for the free air chamber is involved in the determination of the air kerma rate. As these correction factors are energy-dependent, they have to be determined for each

radiation quality, either experimentally or by calculation, using the spectrum corresponding to each quality.

The factor that corrects for the lack of saturation due to ion recombination and diffusion k_s was determined following the method proposed by De Almeida and Niatel [12] as implemented by Boutillon [13]; the polarity correction k_{pol} and the correction for photon transmission through the front wall of the chamber k_p were determined by measurements; the correction factors for electron loss k_e , photon scatter k_{sc} , fluorescence k_{fl} and photon scatter and transmission from the diaphragm k_{dia} were calculated using Monte Carlo techniques. The factors were calculated using the Monte Carlo code PENELOPE [14] for monoenergetic photons from 2 keV to 50 keV, with steps of 2 keV; a detailed simulation of the BIPM standard was performed with the PENELOPE geometry package. The results for monoenergetic photons were convoluted with the spectrum corresponding to each radiation quality, which were determined experimentally and by simulation, as explained in the following paragraph.

The spectra were measured using the Compton scattering method, which consists of placing a scattering material in the primary beam, measuring the scattered photons at a certain angle and then reconstructing the primary beam. A commercial Compton spectrometer with a scatter angle of 90° was used for this study; the scattered photons were detected using a low-energy pure germanium detector coupled to a multichannel analyser. The Ge detector was calibrated using the known energies of the x- and γ -rays emitted by radioactive sources of ^{125}I and ^{241}Am . The primary x-ray spectra were reconstructed from the resulting pulse height distribution using commercial software [15].

Two of the mammography spectra were also obtained by simulation with Monte Carlo techniques using the code PENELOPE. The x-ray tube configuration (electron source, target, tube window, collimator system and filters) was simulated in detail using the PENELOPE geometry code. A user code was written which calls the subroutines defined in PENELOPE to simulate the transport of electrons travelling in vacuum and striking the target to produce bremsstrahlung and the transport of photons through the collimators and filters, to record at the reference measurement plane, the photon energy together with the corresponding coordinates and direction of each photon crossing this plane.

The measured spectra agree well with the calculated spectra, the maximum deviation between them being less than 0.35 keV; these differences have no significant effect in the calculation

of the standard's correction factors. The air kerma rates were then determined using the free air chamber L-01.

The suitability of these tungsten/molybdenum beams for the calibration of chambers that will then be used for the dosimetry of molybdenum/molybdenum beams has to be studied by comparing the response of such chambers in the two sets of radiation beams. To start this study, three ionization chambers currently used in mammography dosimetry were calibrated periodically in the simulated mammography beams over several years to determine their response in these beams.

1.4.2. Primary standard for mammography

A new primary standard was designed and constructed at the BIPM to be used for the dosimetry of the mammography beams. The new standard, designated as L-02, is a parallel-plate free-air chamber designed to be used up to 50 kV and to minimize the correction factors involved in the air-kerma determination.

A comparison with the existing standard L-01 for the tungsten-anode x-ray tube was made at the CCRI reference radiation qualities. To be able to carry out this comparison, the correction factors involved in the air kerma rate determination for the new standard needed to be determined for these reference beams; as explained in section 1.4.1, these factors were obtained either by calculation using Monte Carlo techniques or experimentally by ionometric measurements. The new standard was simulated in detail using the PENELOPE geometry code, reproducing dimensions and materials. The correction factors were calculated for mono-energetic photons from 2 keV to 50 keV in steps of 2 keV. The results for mono-energetic photons were folded with the spectra corresponding to the CCRI qualities.

These spectra were measured with the BIPM Compton spectrometer and also simulated with the PENELOPE Monte Carlo code.

Initial discrepancies between the standards of the order of 4 parts in 10^3 motivated a series of studies to investigate the cause of this disagreement: a study of the volume determination, a study of contact potentials between the collector and the guard plate and a study of the temperature measurement and its stability inside the chamber. None of these studies could explain the initial discrepancy, which increased to as much as 8 parts in 10^3 during some of these measurements. When the chamber was first constructed and each time that it was

dismantled and reassembled, the planarity of the collector-guard plate was checked using the coordinate measuring machine (CMM) and a tolerance of 50 μm was accepted. To examine this choice, the upstream edge of the collector was raised and lowered by around 100 μm with respect to the guard plate. This resulted in discrepancies of up to 3 parts in 10^2 , indicating that the tolerance of 50 μm was too high and might explain the fluctuating results. A new collector support was designed, allowing the collector to be adjusted to better than 5 μm with respect to the guard plate. The collector and guard plate, both of aluminium, were cleaned and mounted again with the new support. With this configuration, the discrepancy between the standards was reduced to 1 part in 10^3 , but it was not stable, increasing to 4 parts in 10^3 three months later with no change in the co-planarity. Finally, once the collector and guard plate were coated with graphite the discrepancy was reduced again to 1 part in 10^3 and has since remained constant.

1.4.3. Reference radiation qualities for mammography

A molybdenum-anode x-ray tube was installed in the low-energy x-ray laboratory at the BIPM, sharing the facilities with the tungsten-anode tube, using the same high-voltage generator, voltage stabilization and anode current measuring system.

The reference plane is established at 600 mm from the tube centre. Radiographic films were used for the study of the radiation field (size, shape and beam axis). Horizontal and vertical radial profiles were measured using a thimble ionization chamber. Using the data from the radial profiles and the radiographic images, a system of two lead collimators was designed and machined to produce a circular field 10 cm in diameter at the reference plane.

Four radiation qualities were set up as reference beams for comparisons and calibrations, in the range from 25 kV to 35 kV. The beam quality, expressed in terms of the aluminium half-value layer (HVL), was determined for each beam using the new primary standard. The anode current for each quality was chosen to give an air-kerma rate of 2 mGy s^{-1} in the reference plane. A molybdenum filter 30 μm in thickness is used for all the qualities.

The Mo-target photon energy spectra were measured using the Compton scattering method, described previously. Two mammography spectra were also obtained by simulation with Monte Carlo techniques using the code PENELOPE. The x-ray tube configuration (Mo target, Mo filter and collimation) was simulated using the PENELOPE geometry code.

The correction factors for the standard involved in the determination of K_{air} were obtained either by calculation using Monte Carlo techniques or experimentally by ionometric measurements. The results for mono-energetic photons were folded with the spectra measured with the BIPM Compton spectrometer and also using the spectra simulated with PENELOPE. In spite of some differences in the peak height between the measured and the calculated spectra, the correction factors for the standard were insensitive to these differences.

1.4.4. Study of chamber response to the simulated mammography beams

A study of the suitability of the simulated mammography beams established using the tungsten-anode x-ray tube and molybdenum filter for the calibration of ionization chambers was carried out for four types of ionization chamber commonly used for mammography dosimetry. The ionization chambers used in this study were a Radcal RC6M, an Exradin A11TW, an Exradin Magna 92650 and a PTW 34069; they were calibrated in the BIPM W/Mo beams and the responses compared with those obtained through their calibration in Mo/Mo mammography beams. The calibration coefficients measured in the simulated mammography beams are in agreement with those obtained in the Mo-anode beams at the level of 1 part in 10^3 for the Exradin chambers, 3 parts in 10^3 for the Radcal and 5 parts in 10^3 for the PTW. Consequently, national standards laboratories not equipped with Mo-anode x-ray tubes can, at this level of uncertainty, implement W/Mo beams to calibrate these types of chamber for subsequent use in Mo-anode beams. This method, however, should not be extended to other chamber types without similar verification in W/Mo and Mo/Mo beams.

1.4.5. International comparisons and characterization of national standards

A new BIPM ongoing series of comparisons, identified as BIPM.RI(I)-K7 in the KCDB, was started in 2009 for the bilateral comparisons of primary standards for mammography dosimetry between the National Metrology Institutes (NMIs) and the BIPM.

Comparisons of the standards for air kerma in mammography x-ray beams can be carried out directly at the BIPM or indirectly using transfer ionization chambers belonging to the NMIs. In the first case, the quantity air kerma is determined with the NMI and the BIPM standards and the comparison result is expressed as the ratio $K_{\text{NMI}} / K_{\text{BIPM}}$. In the case of an indirect comparison, the NMI calibrates the transfer standard (ionization chamber) against its primary standard in its laboratory, determining the calibration coefficient $N_{K,\text{NMI}}$, taken as the mean of

measurements performed before and after the measurements at the BIPM; the transfer instrument is calibrated in between at the BIPM, determining the $N_{K,BIPM}$; the comparison result is taken as the ratio of the calibration coefficients determined at each laboratory as $N_{K,NMI} / N_{K,BIPM}$. While the use of transfer chambers might introduce more uncertainty in the comparison results than for a direct comparison of the primary standards, useful information is gained on the reproducibility of calibration coefficients and on the behaviour of transfer instruments of the type used in the dissemination chain. A detailed analysis of the uncertainty budget is made in order to calculate the combined standard uncertainty of the comparison results, taking into account correlations between the standards.

The results of each of the comparisons are analysed in terms of the degree of equivalence of each national standard with respect to the key comparison reference value x_R . It follows that $x_R = 1$. For each laboratory i , with a comparison result x_i determined with combined standard uncertainty u_i , the degree of equivalence D_i with respect to the reference value is therefore simply $x_i - 1$ with expanded uncertainty $U_i = 2 u_i$. The results of the degrees of equivalence D_i and the expanded uncertainties U_i are entered in the form of tables and graph in the BIPM key comparison data base (KCDB).

For each comparison, the corresponding report is produced describing the measurement conditions at each lab, details of the standards, the transfer instruments in the case of an indirect comparison, correction factors involved in the determination of the air-kerma rate and calibration coefficients for indirect comparisons, the comparison result and the corresponding uncertainties. Reports of the comparisons are reviewed by the CCRI and once approved are published in *Metrologia*, and the results included in the KCDB. The reports are published electronically by IOP Publishing on the internet and are freely available through the BIPM web site.

The first comparison of standards for air kerma in mammography x-ray beams was carried out with the NRC (Canada) in March 2007 in the W/Mo beams; this was an indirect comparison using a set of four transfer ionization chambers belonging to the NRC, and was made at two different distances.

The following comparison was with the NMIJ (Japan) in November 2009; it was the first comparison in the Mo/Mo beams and used a set of three transfer ionization chambers belonging to the NMIJ.

The third request for participating in the BIPM.RI(I)-K7 comparison was made by the NIST (USA); this was carried out indirectly using one transfer instrument in January 2010.

In September 2010, a new comparison was scheduled with the PTB (Germany), not only in the mammography radiation beams (Mo/Mo qualities) but also in the simulated mammography beams (W/Mo qualities); two transfer instruments were used for this comparison.

A direct and indirect comparison was carried out with the ENEA (Italy) in the simulated mammography beams (W/Mo qualities) as the ENEA disseminates the calibration coefficients in these beams. Measurements with the ENEA primary standard and one transfer ionization chamber were made at the BIPM during February 2011.

The results of the comparisons with the NRC, NMIJ, NIST and the PTB have been published in the Metrologia Technical Supplement; the graph of degree of equivalence, as presented in the KCDB, is shown in Figure 1.1.

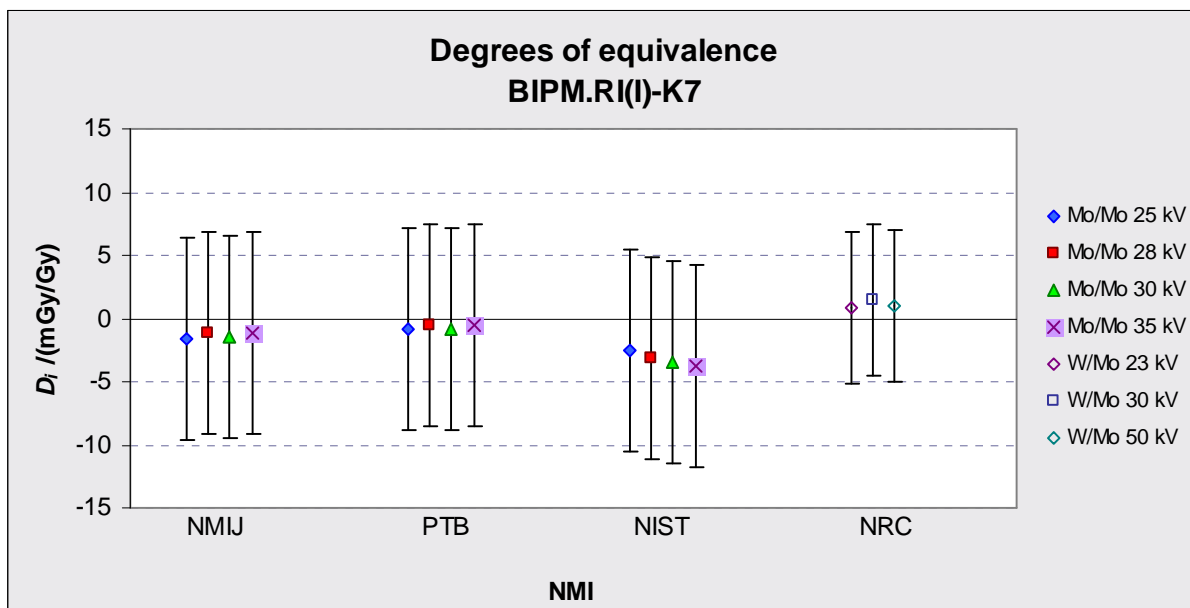


Figure 1.1. Degrees of equivalence D_i and uncertainty U_i ($k = 2$), in mGy/Gy

The ENEA agreed to repeat the comparison in the near future, because of the different calibration conditions used at the ENEA to calibrate the transfer chambers.

The International Atomic Energy Agency, traceable to the PTB, asked the BIPM to run a bilateral comparison in the Mo/Mo beams in order to support their dosimetry calibration and

measurement capabilities (CMCs), published in Appendix C of the CIPM MRA key comparison database. The measurements were performed in 2012 and the comparison report has been sent to the CCRI(I) for approval and future publication.

A recent comparison with the VNIIM (Russian Federation) has been carried out in the Mo/Mo beams using two transfer chambers; repeat calibrations of the transfer chambers are still being carried out at the VNIIM, after the measurements made at the BIPM.

Comparisons with other countries are anticipated in the coming years.

Up to now, five national standards belonging to the CMI (Czech Republic), HIRCL (Greece), ININ (Mexico), ITN (Portugal) and NIM (China) were characterized in the mammography beams and two of them, also in the simulated mammography beams. The corresponding calibration certificates issued for each NMI contain information on the calibration coefficient determined under the measuring conditions described in [16] together with the corresponding uncertainties, the uncertainty budget and the details concerning the calibration.

Chapter 2. Establishment of simulated mammography radiation qualities using a tungsten target x-ray tube with molybdenum and rhodium filters

2.1. Introduction

Mammography is an imaging technique that uses x rays to examine the human breast, specifically for detecting breast pathology. Breast radiography requires a special x-ray spectrum to fulfill two important requirements: provide a good subject contrast of soft tissues and, keep the radiation dose as low as possible. Adequate subject contrast is necessary to distinguish between normal and diseased tissues and to detect calcifications within breast tissue, as there is a high correlation between the presence of calcification and disease. As breast tissue is one of the more radiosensitive tissues, the x-ray dose delivered during the examination must be kept as low as possible in order to reduce the risks of radiation-induced carcinogenesis. These requirements are difficult to accomplish: a reduction of the beam energy improves the subject contrast at the expense of increasing the dose to tissue; this indicates mono-energetic x rays in the energy range from 17 keV to 25 keV as the best choice. Unfortunately, the output of an x-ray tube is poly-energetic, but a good approximation to mono-energetic beams at these energies can be achieved using x-ray tubes with molybdenum or rhodium targets and filters.

As mentioned above, it is essential in mammography to minimize the radiation dose delivered to the breast because of the risk of inducing a breast cancer associated with the use of ionizing radiation. Thus, an accurate dose determination is an important aspect in mammography. The mean glandular dose is usually used to evaluate the risk of carcinogenesis, and this is calculated from measurements of the radiation output of the x-ray tube and applying conversion factors. The output of the x-ray tube is determined from measurements using radiation detectors called ionization chambers. As mentioned in the first chapter, commercial ionization chambers used in diagnostic radiology departments need to be calibrated at standard reference laboratories in the same mammography energy range and preferably in the

same type of radiation beams used in mammography. This is because the response of these detectors can be energy dependent and thus be sensitive to radiation beams with different spectral distributions.

At present, a few national reference standards laboratories are equipped with mammography x-ray tubes. These laboratories can establish reference radiation qualities in the same energy range used in clinical mammography to calibrate the users' ionization chambers. However, those standard dosimetry laboratories with neither a molybdenum- nor rhodium-anode x-ray tube but having a tungsten-anode x-ray tube, the type of tube used in conventional radiology, can also establish similar reference radiation qualities as used for mammography by adding molybdenum or rhodium filters and operating the tube in the same energy range used in mammography. These qualities are referred to as simulated mammography beams and are usually denoted as W/Mo or W/Rh beams.

In order to meet the needs of the National Metrology Institutes for comparisons of standards belonging to Primary Standard Dosimetry Laboratories in mammography radiation beams, and to provide characterizations and calibrations for Secondary Standard Dosimetry Laboratories traceable to the International System of Units (SI), the BIPM was asked to extend the international programme of ongoing comparisons and calibrations to this domain.

Initially, a set of nine x-ray qualities using a combination of the tungsten-anode low-energy x-ray tube and molybdenum or rhodium as additional filtration was established [10]. A description of the work I carried out at the BIPM to provide an international facility for comparisons and calibrations in mammography radiation beams is presented in this chapter.

The suitability of these simulated mammography x-ray qualities for the calibration of ionization chambers currently used in mammography was investigated and the results of this work are presented in Chapter 5 "A study of the response of commercial ionization chambers to mammography beams".

Three comparisons of primary standards have been carried out in these simulated mammography beams, with the National Research Council NRC (Canada), the Physikalisch-Technische Bundesanstalt PTB (Germany) and the Istituto Nazionale di Metrologia delle Radiazioni Ionizzanti ENEA (Italy). Details of the comparisons are presented in Chapter 6 "Implementation of an international comparison and calibration facility for mammography dosimetry at the BIPM".

2.2. Establishing new radiation beams: determination of the beam quality and the air kerma rate

2.2.1. X-ray production

X rays are produced by energy conversion when a fast-moving stream of electrons interacts with the anode target of an x-ray tube. X rays are generated by two different processes, resulting in the production of a continuous spectrum (bremsstrahlung) and characteristic x rays.

Bremsstrahlung: when the electron passes near the nucleus, an inelastic radiative interaction occurs in which an x-ray photon is emitted. The electron is not only deflected in this process but gives a significant fraction (up to 100 %) of its kinetic energy to the photon, slowing down in the process. Such x-rays are referred to as bremsstrahlung, the German word for “braking radiation”.

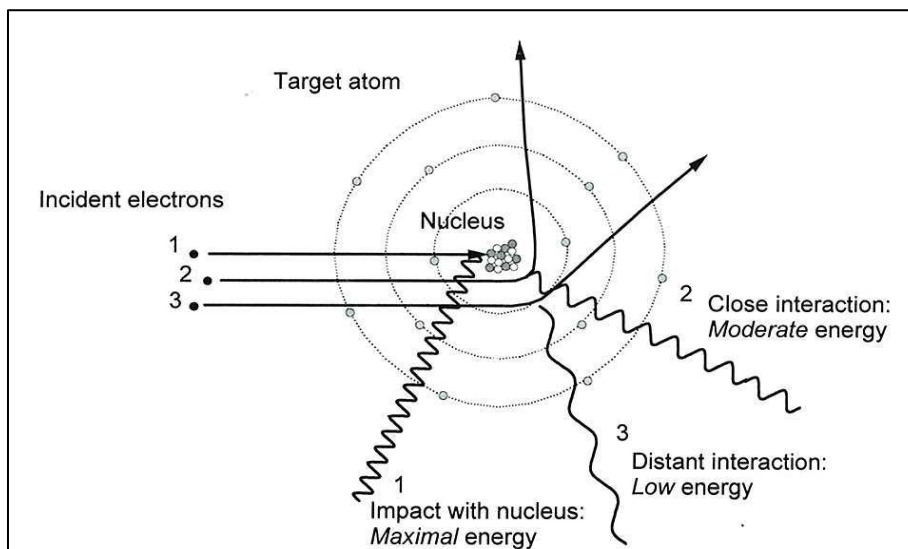


Figure 2.1. Fast electrons in the proximity of a nucleus are deflected and the emission of x-rays is produced in this process.

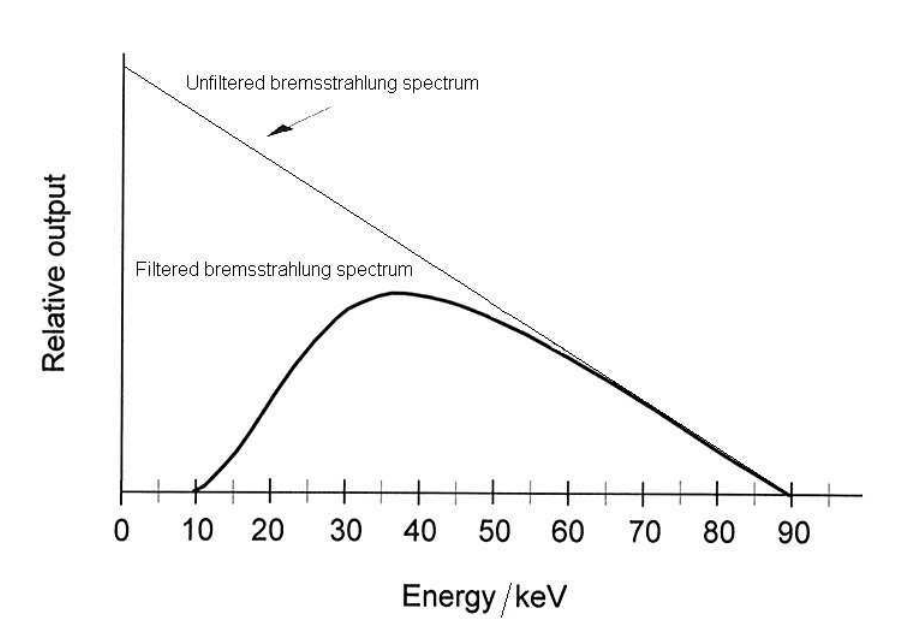


Figure 2.2. The resulting bremsstrahlung radiant energy spectrum (unfiltered and filtered), generated in a thick target of any atomic number Z by an electron beam of incident energy T_0 .

Characteristic x rays: electrons with energy exceeding the binding energy of an inner shell electron of the target atom can eject it, leaving an ionized atom with an unfilled inner shell. Electrons from an outer shell will fill this vacancy with the release of a “characteristic” x-ray photon; this is identified as a K x ray when the innermost shell is filled, L x ray for the next electron shell, etc.

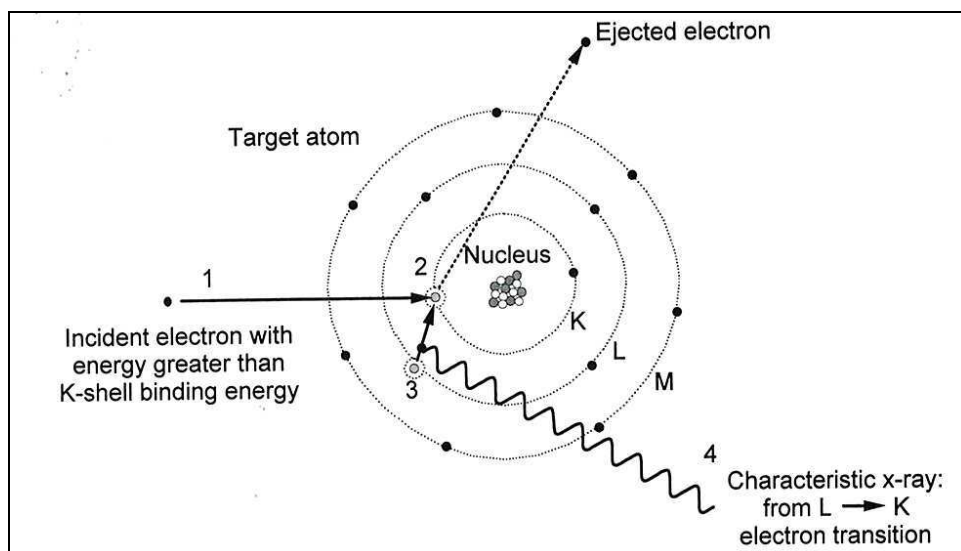


Figure 2.3. Following the creation of a K-shell vacancy, an electron from another higher shell fills it, and emits a fluorescence photon having a quantum energy equal to the difference in the two energy levels involved.

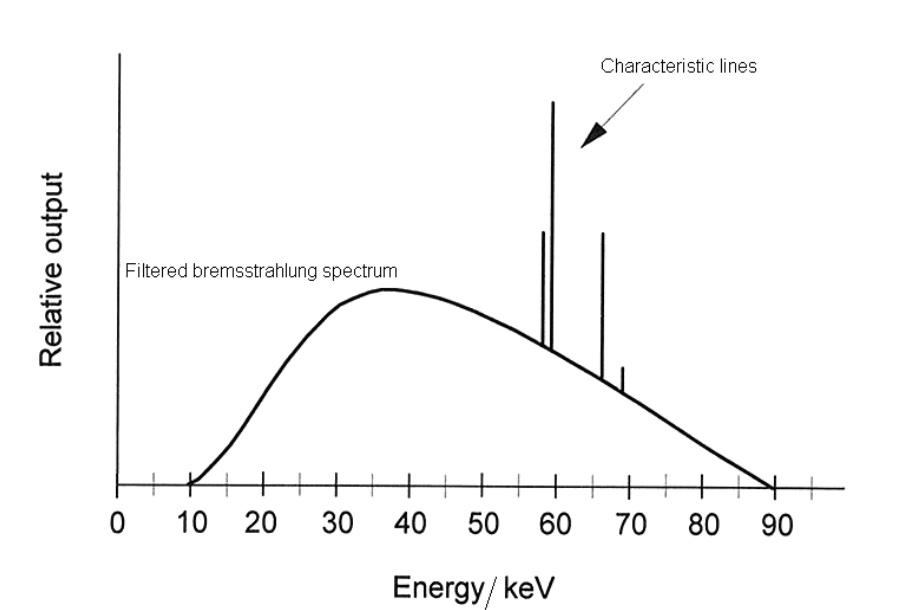


Figure 2.4. The characteristic lines at these specific energies (difference in the two energy levels involved) and the continuous spectrum.

The contribution of each of these two interaction processes to the production of the x-ray spectrum depends on the electron energy and on the atomic number Z of the target material.

With a high atomic number anode like tungsten, the x-ray beam consists almost entirely of bremsstrahlung radiation and the contribution from characteristic radiation is negligible in the diagnostic energy range. Some diagnostic examinations like mammography require x-ray spectra with a minimal bremsstrahlung contribution, the best choice being a monoenergetic x-ray beam. When operating x-ray tubes at low voltages, such as the values required in mammography, and having lower atomic number anodes, bremsstrahlung production is less efficient to the point at which characteristic radiation assumes an overriding importance. To take advantage of this principle, approximation of the ideal monoenergetic beam can be achieved with x-ray tubes with molybdenum and rhodium targets, whose characteristic x rays occur in the energy range needed for mammography. Filters of molybdenum or rhodium are commonly added to attenuate bremsstrahlung produced at energies higher than the K-absorption edge of the anode materials, such filters being transparent to their own characteristic radiation.

An illustration of the production of bremsstrahlung and characteristic radiation can be seen in Figure 2.5: the first graph shows a measured spectrum corresponding to a radiation quality produced with a W-anode x-ray tube and Al filtration whereas the second one is a spectrum

corresponding to a Mo-anode x-ray tube and Mo filtration, both x-ray spectra are obtained using the same generating voltage of 30 kV.

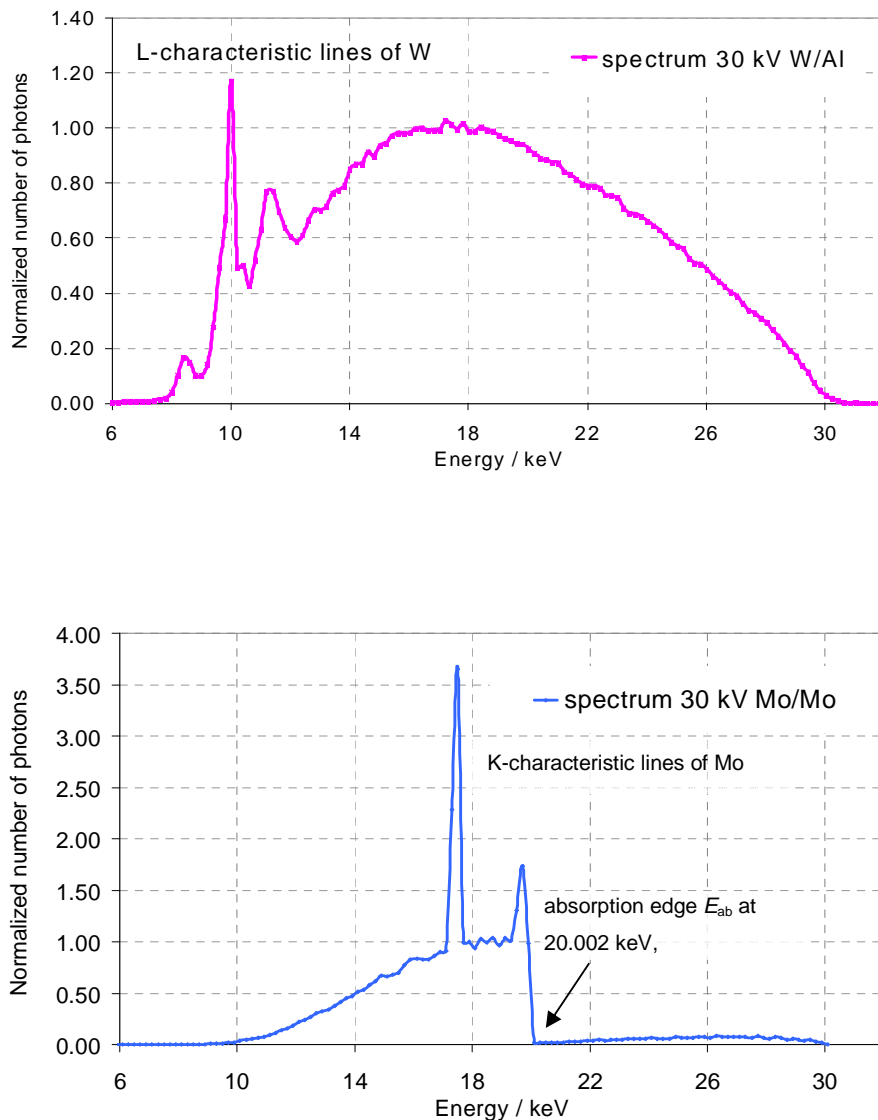


Figure 2.5. BIPM spectra corresponding to a W anode (top) and Mo anode (bottom) x-ray tube operated at 30 kV (spectra measured at the BIPM using the Compton scatter method).

Spectra consisting almost entirely of bremsstrahlung like the one produced with a W-anode x-ray tube (normally operated in the range from 10 kV to 50 kV) can be modified significantly depending on the filtration added in the beam. Taking advantage of the K-absorption edges E_{ab} of the filter material, the filters will attenuate both low and high energy photons and thus transmit a narrowed spectrum, as illustrated in Figure 2.6. This spectrum is obtained from the

one shown at the top of Figure 2.5 by simply replacing the Al filter with a 60 μm Mo filter that has its K-absorption edge at 20.002 keV. The Mo filter attenuates x rays strongly just above the 20 keV K-edge where its mass attenuation coefficient increases considerably, as can be seen in the second graph of Figure 2.6.

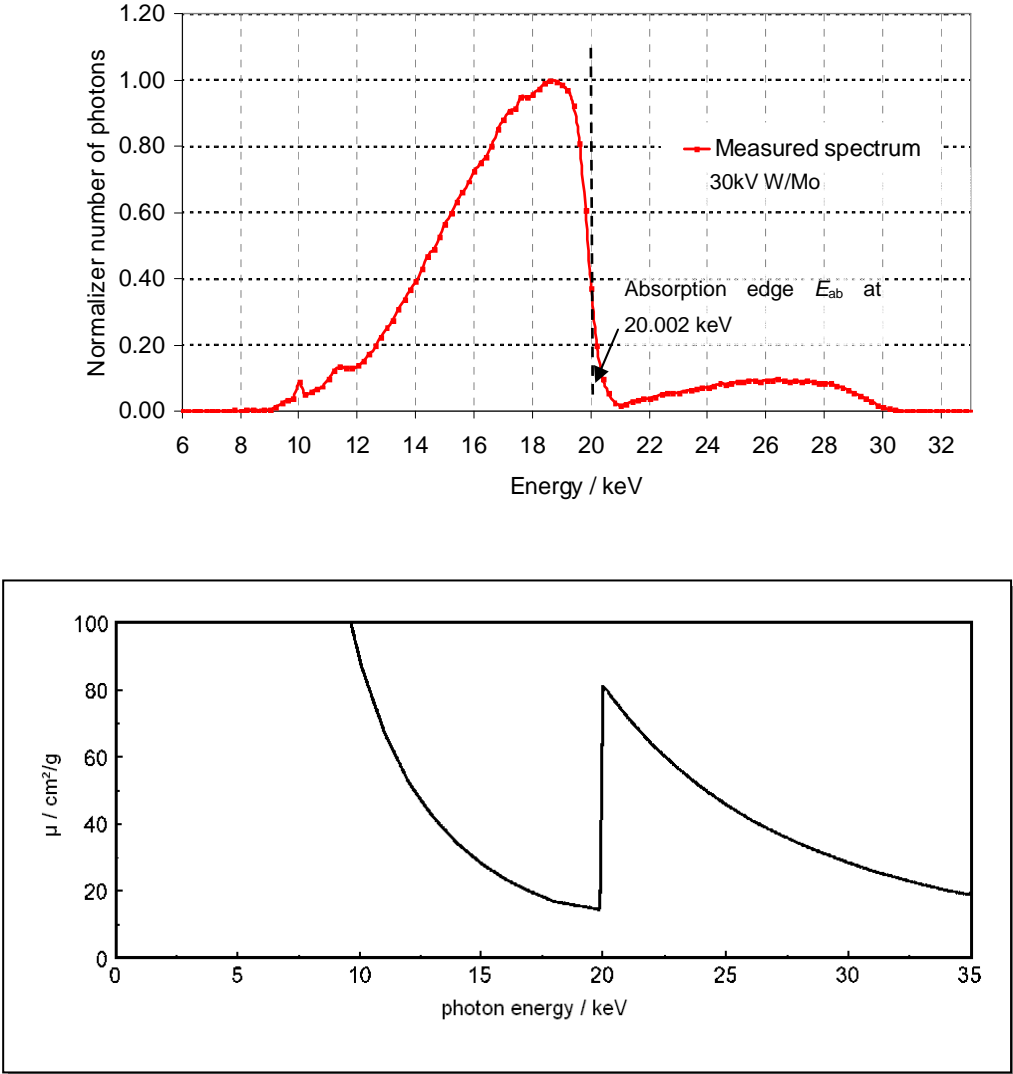


Figure 2.6. Spectra corresponding to a W anode x-ray tube with Mo filtration operated at 30 kV (top) and the mass attenuation coefficient, μ , for molybdenum (bottom)

2.2.2 X-ray tube

The x-ray tube is made of glass that encloses a vacuum containing two electrodes. The electrodes are designed so that electrons produced at the cathode (negative electrode or filament) can be accelerated by a high potential difference toward the anode (positive

electrode or target). The basic elements of a stationary target x-ray tube are shown in Figure 2.7.

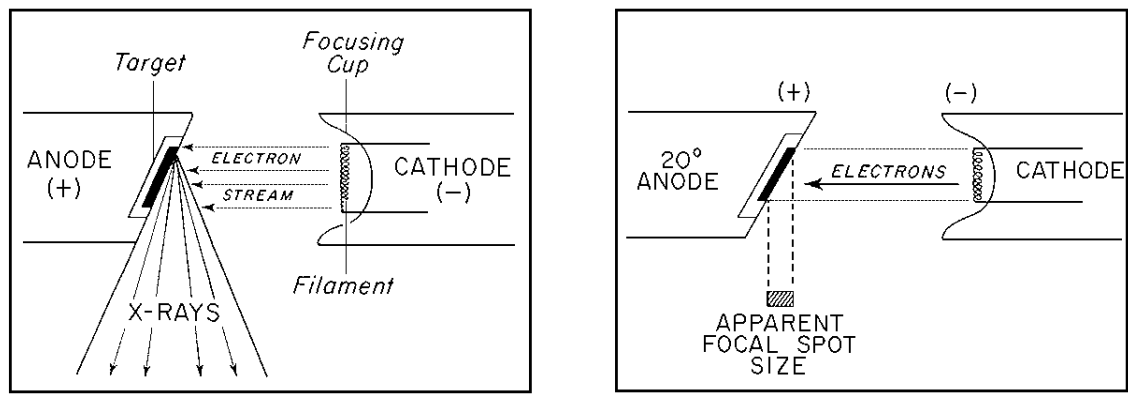


Figure 2.7. Schema of an x-ray tube

Electrons are produced by the heated filament and accelerated across the tube to hit the target, where x rays are produced. The vacuum is needed to avoid that electrons collide with gas molecules, lose energy and cause secondary interaction. The filament, which is the source of electrons, is a tungsten wire that is coiled to form a vertical spiral.

The focal spot is the area of the target that is bombarded by electrons from the cathode. As most of the energy of the electrons is converted into heat, a large focal spot is needed to dissipate the heat and thus avoid damage of the target. Alternatively, in a clinical situation, the target may be rotated to dissipate the heat. This is necessary when using generating voltages above 60 kV. But to produce good radiography, a small focal spot is necessary. To solve this conflict, the angle that the target forms with the plane perpendicular to the incident beam should be small so that the apparent focal spot size becomes smaller.

2.2.3 X-ray characterization

It is worth introducing few concepts related to the characterization of an x-ray beam. The main parameters that determine the x-ray beam characteristics are the target material, the generating voltage, the anode current, the filtration, all of which together will define the air kerma rate. An important additional parameter is the first half value layer that is a measure of the additional material needed to halve the air kerma rate and will depend on the photon-energy distribution (spectrum). All these parameters are used to define the quality of the x-ray

beam. The word quality may be taken as synonymous with hardness, that is, the penetrating ability of the radiation beam. This comes from the early days of radiotherapy when orthovoltage x rays (200 kV to 400 kV) were used to treat deep seated tumours; the effectiveness of the treatment depended on the ability of the x rays to penetrate to the tumour: the more penetrating the beam, the higher its quality. The same term quality is also applied to diagnostic radiology.

- The generating voltage determines the maximum energy of the electrons and hence the x rays produced, while the anode current determines the output intensity or number of photons of the beam.
- The dosimetric quantity related to the intensity of the output of the x-ray tube used in diagnostic radiology is the air kerma, K_{air} , acronym for the kinetic energy released per mass (of material). Primary determinations of air kerma are made using free-air ionization chambers (FAC).
- The quality of the beam is usually expressed in terms of the aluminium half value layer (HVL), defined as the aluminium thickness needed to reduce the air-kerma rate to half its initial value.
- The spectrum is needed for several dosimetric applications such as, for example, the calculation of the correction factors for the free air chamber entering in the determination of air-kerma rate or the calculation of the conversion factors to determine the mean glandular dose in mammography.
- Filtration of the emitted x rays is caused by inherent attenuators and added filters in the path of the x-ray beam. Inherent filtration comes from the thickness of the x-ray tube window and its material, often beryllium, whereas added filtration refers to any filters placed in the beam in order to modify the spectrum for a particular application.

To produce well defined x-ray beams it is necessary to have stable voltage generators to avoid fluctuations in the spectral distribution, accurate measurements of the generating voltage to determine the quality of the radiation beam, and stable monitoring and measuring systems for the anode current to allow corrections for possible fluctuations to the measured output (air-kerma).

2.2.4 X-ray irradiation facility at the BIPM

The low-energy x-ray laboratory at the BIPM is equipped with a high-voltage generator and a tungsten-anode x-ray tube with an inherent filtration of 1 mm beryllium, comprising the tube window. The main characteristics are listed in Table 2.1.

Table 2.1. Main characteristics of the W-anode x-ray tube

Tube MXR-160/0.4-1.5 COMET	
Nominal x-ray tube voltage	160 kV
Max. tube current at nominal voltage	10 mA
Power	1.6 kW
Inherent filtration (window)	1 mm Be
Target angle	20°
Focal spot diameter	1.5 mm

The generating potential is stabilized using an additional feedback system designed and constructed by the BIPM. Monitoring is done using a voltage divider built and regularly calibrated at the BIPM [17]. Using this, the generator runs approximately 10 V below the desired potential, and a programmable voltage supply is inserted between the anode and the ground. This is operated in a feedback arrangement by the controlling computer; the difference between the measured voltage and the desired voltage being programmed into the voltage supply approximately once per second. Using this system, stability of a few tenths of a volt is achieved.

As an alternative to using a transmission ionization chamber monitor to track the radiation output stability, the anode current is measured. The anode current is monitored by placing a calibrated 200 ohm resistor between the anode and the ground, and the voltage across this resistor is read using a voltmeter with a high impedance. This gives a measure of the anode current to be used either just for information or to actually normalize the measured ionization current (in the standard, for example) to a reference value for the anode current.

This method provides a more stable reference output of the tube. The tube is operated using a high tension in the range from 10 kV to 50 kV.

As the kerma measured in air depends on the mass of the measuring volume, the temperature and pressure must be known. The irradiation area is temperature controlled at around 20 °C; two thermistors, calibrated by the BIPM to a few mK, measure the temperature of the ambient air and the air inside the BIPM standard used for the dosimetry of the x-ray qualities. Air pressure is measured by means of a BIPM-calibrated barometer positioned at the height of the beam axis. The relative humidity is controlled within the range 47 % to 53 %.

2.2.5 The BIPM standard

The BIPM low-energy x-ray standard used for the dosimetry of the W-anode radiation qualities is a free-air chamber of the conventional parallel-plate design [8], identified as L-01. A full description of a free-air chamber is presented in Chapter 3 “Design and construction of a primary standard for mammography”. The measuring volume V is defined by the diameter of the chamber aperture and the length of the collecting region. The main dimensions, the measuring volume and the polarizing voltage for the standard are shown in Table 2.2.

Table 2.2. Main characteristics of the standard

Standard	L-01
Aperture diameter / mm	9.941
Air path length / mm	100.0
Collecting length / mm	15.466
Electrode separation / mm	70
Collector width / mm	71
Measuring volume / mm ³	1 200.4
Polarizing voltage / V	1 500

2.2.6 New radiation qualities

In order to have radiation qualities similar to those used in mammography but using the W-anode x-ray tube, a new set of qualities was implemented. This was achieved by replacing the Al filtration with Mo and Rh filters of 0.06 mm and 0.05 mm thick, respectively, and

operating the tube at the different voltages as used in the clinical mammography range. The characteristics of these beams are given in Table 2.3.

Table 2.3. Characteristics of the simulated mammography radiation qualities

Radiation quality	W/Mo 23	W/Mo 25	W/Mo 28	W/Mo 30	W/Mo 35	W/Mo 40	W/Mo 50	W/Rh 25	W/Rh 30
Generating potential / kV	23	25	28	30	35	40	50	25	30
Additional filtration	60 μ m Mo							50 μ m Rh	
HVL /mm Al	0.332	0.342	0.356	0.364	0.388	0.417	0.489	0.464	0.505

* 0.423 mm of Be was added to all the qualities for reasons of consistency related to the measurement of air attenuation, as explained in 2.2.6.2.

2.2.6.1 Half value layer

The determinations of the beam qualities, expressed in terms of the aluminium half-value layer (HVL) were made with the BIPM standard L-01. The air kerma rate was measured with no added attenuator in the beam and for three different combinations of attenuators placed on the beam axis; the attenuated air-kerma rate values were normalized to the value measured with no attenuator, and they were plotted as a function of the corresponding numbered attenuators' thickness as illustrated in Figure 2.8. A quadratic fit was made to the measured values, the fit being constrained to unity at zero attenuator thickness. The HVL for each radiation quality was derived from this fit. The uncertainty arising from the fitting procedure is taken as the root mean square (r.m.s.) deviation of the measured values from the fitted line. This is evaluated as 8 parts in 10^5 .

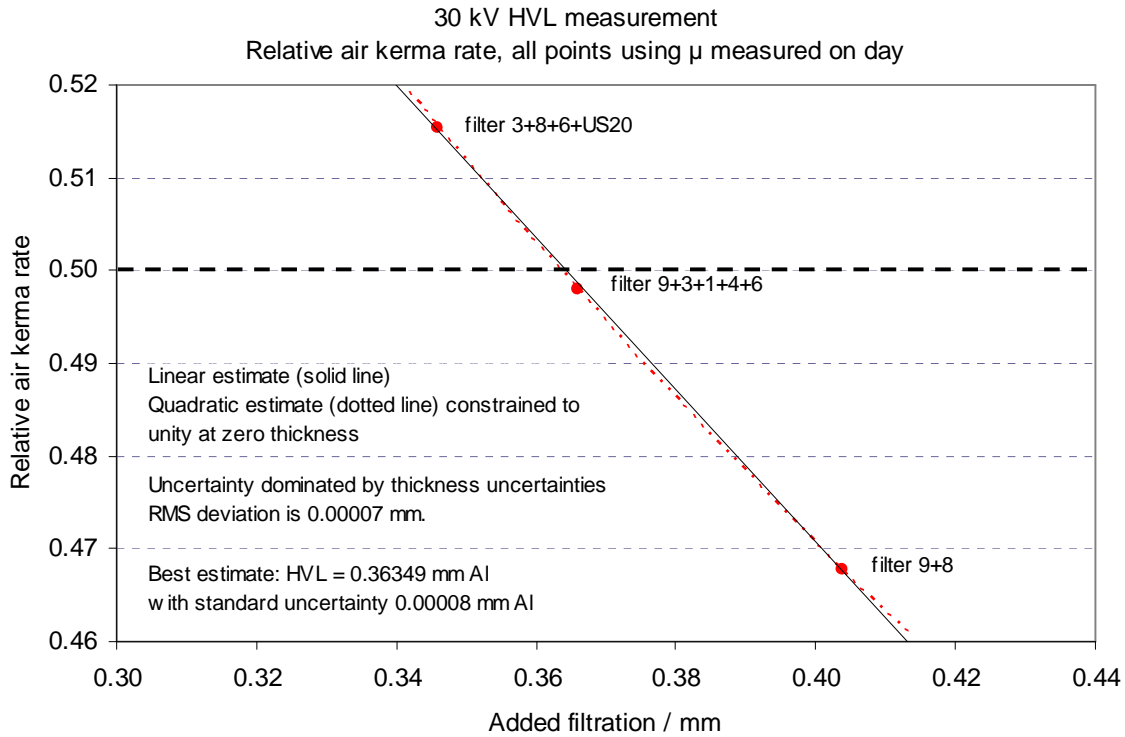


Figure 2.8. Half value layer determination

2.2.6.2 Air kerma rate

The air kerma rate was measured using the standard L-01 under the reference conditions described in [16]; the most important details are produced here. The reference plane for the BIPM standard was positioned at 500 mm from the radiation source, with a reproducibility of 0.03 mm. The standard remains in a fixed position and it was aligned on the beam axis to an estimated uncertainty of 0.1 mm; the positioning of the standard was done at the time of the installation of the W-anode x-ray tube, previously to this work, using a method similar to the one described in 4.2.4. The beam diameter in the reference plane is 84 mm for all radiation qualities.

For a free-air ionization chamber standard with measuring volume V , the air-kerma rate is determined by the relation

$$\dot{K} = \frac{I}{\rho_{\text{air}} V} \frac{W_{\text{air}}}{e} \frac{1}{1 - g_{\text{air}}} \prod_i k_i \quad (2.1)$$

where ρ_{air} is the density of air under reference conditions, I is the ionization current under the same conditions, W_{air} is the mean energy expended by an electron of charge e to produce an ion pair in air, g_{air} is the fraction of the initial electron energy lost by bremsstrahlung

production in air, and Πk_i is the product of the correction factors to be applied to the standard. The values used for the physical constants ρ_{air} and W_{air}/e are given in Table 2.4. For use with this dry-air value for ρ_{air} , the ionization current I must be corrected for humidity and for the difference between the density of the air of the measuring volume at the time of measurement and the value given in the table.¹

Table 2.4. Physical constants used in the determination of the air-kerma rate

Constant	Value	u_i^a
ρ_{air}^b	1.2930 kg m ⁻³	0.000 1
W_{air}/e	33.97 J C ⁻¹	0.001 5

^a u_i is the relative standard uncertainty.

^b Density of dry air at $T_0 = 273.15$ K and $P_0 = 101.325$ kPa.

The correction factors listed in Table 2.5 for the standard were determined by interpolation in terms of HVL from the existing data for the CCRI reference qualities [9].

Table 2.5. Interpolated correction factors for the BIPM standard

Radiation quality	W/Mo 23	W/Mo 25	W/Mo 28	W/Mo 30	W/Mo 35	W/Mo 40	W/Mo 50	W/Rh 25	W/Rh 30
Scattered radiation k_{sc}	0.9974	0.9974	0.9974	0.9974	0.9974	0.9974	0.9975	0.9975	0.9975
Fluorescence k_{fl}	0.9972	0.9972	0.9972	0.9972	0.9973	0.9973	0.9975	0.9974	0.9975
Electron loss k_e	1.0000	1.0000	1.0000	1.0000	1.0000	1.0000	1.0000	1.0000	1.0000
Saturation k_s	1.0007	1.0007	1.0007	1.0007	1.0007	1.0007	1.0007	1.0007	1.0007
Polarity k_{pol}	1.0005	1.0005	1.0005	1.0005	1.0005	1.0005	1.0005	1.0005	1.0005
Wall transmission k_p	1.0000	1.0000	1.0000	1.0000	1.0000	1.0000	1.0000	1.0000	1.0000
Field distortion k_d	1.0000	1.0000	1.0000	1.0000	1.0000	1.0000	1.0000	1.0000	1.0000
Diaphragm k_{dia}	0.9995	0.9995	0.9995	0.9995	0.9995	0.9995	0.9994	0.9995	0.9994

¹ For an air temperature $T \sim 293$ K, pressure P and relative humidity ~ 50 % in the measuring volume, the correction for air density involves a temperature correction T/T_0 , a pressure correction P_0/P and a humidity correction $k_h = 0.9980$. At the BIPM, the factor 1.0002 is included to account for the compressibility of dry air between $T \sim 293$ K and $T_0 = 273.15$ K.

Air attenuation k_a^a	1.0218	1.0213	1.0208	1.020	1.0195	1.0187	1.0169	1.0159	1.0150
-------------------------	--------	--------	--------	-------	--------	--------	--------	--------	--------

^a Values for 293.15 K and 100.0 kPa; each measurement is corrected using the air density measured at the time.

The factors for the free-air chamber at the CCRI qualities for electron loss k_e , photon scatter k_{sc} and fluorescence k_{fl} and photon transmission and scatter from the diaphragm were calculated by Burns [18] and by Burns et al [19, 20] using Monte Carlo techniques for monoenergetic photons and the results were convoluted using spectral measurements performed previously with the spectrometer belonging to the Dutch Metrology Institute (VSL), The Netherlands, that was used at the BIPM. The correction for photon transmission through the front wall of the chamber k_p was measured. The correction factor for the lack of saturation due to ion recombination and diffusion k_s was determined following the method proposed by De Almeida and Niatel [12] as detailed by Boutillon [13]. The polarity correction k_{pol} was determined by measurements. The air attenuation factor k_a was measured for each quality using the method of reduction of the air pressure in a tube placed between the filter and the free-air chamber [21] (the beryllium windows for this tube, of total thickness 0.423 mm, are used as additional filters at all times for all the qualities, for consistency).

A detailed description of the correction factors and their evaluation is presented in Chapter 3 “Design and construction of a primary standard for mammography dosimetry”.

By using a suitable choice for the anode current, the air kerma rate was set to 1.00 mGy s⁻¹ for all the radiation qualities.

2.2.6.3 Re-evaluation of the correction factors for the BIPM standard L-01

The correction factors to be applied to the BIPM standard for the determination of the air-kerma rate for the new set of radiation qualities were recalculated using the Monte Carlo code PENELOPE [14].

The Monte Carlo code PENELOPE is a subroutine package that simulates the transport of photons and electrons in arbitrary material systems consisting of a number of regions (bodies) limited by interfaces. The PENELOPE code cannot operate by itself; the subroutines have to be called from a main program written by the user, who also defines two input files needed by PENELOPE to perform the particle transport: the geometry file created using the package

The main program, written in Fortran, calls the subroutines defined in PENELOPE; controls the evolution of the tracks; identifies the type of particle and interaction taking place; scores the energy deposition in the bodies of interest; and calculates the correction factors required in the determination of air kerma for monoenergetic photons from 2 keV to 50 keV, with steps of 2 keV. The simulation starts with a divergent beam of monoenergetic photons at 500 mm from the reference measuring plane of the standard.

The results for monoenergetic photons were convoluted with the spectra measured with the BIPM Compton spectrometer and simulated using Monte Carlo techniques, described in section 2.3.

The calculated values, obtained either using the experimental or the simulated spectra, are in agreement with those obtained by interpolation (Table 2.5), at the level of 2 to 4 parts in 10^4 , as can be seen in Table 2.6, for the photon scatter k_{sc} and fluorescence k_{fl} correction factors.

Table 2.6. Comparison between interpolated and calculated correction factors for the BIPM standard

Radiation quality	W/Mo 23	W/Mo 25	W/Mo 28	W/Mo 30	W/Mo 35	W/Mo 40	W/Mo 50	W/Rh 25	W/Rh 30
Interpolated k_{sc}	0.9974	0.9974	0.9974	0.9974	0.9974	0.9974	0.9975	0.9975	0.9975
Calculated k_{sc}	0.9976	0.9977	0.9977	0.9977	0.9977	0.9977	0.9978	0.9978	0.9978
Interpolated k_{fl}	0.9972	0.9972	0.9972	0.9972	0.9973	0.9973	0.9975	0.9974	0.9975
Calculated k_{fl}	0.9975	0.9976	0.9976	0.9976	0.9977	0.9977	0.9979	0.9978	0.9978

2.2.6.4 Uncertainties in the BIPM determination of the air-kerma rate

The uncertainties associated with the primary standard are listed in Table 2.7.

The uncertainties for the physical constants are those internationally accepted as advised by the CCRI [22]. The Type B uncertainty values in the second column for the correction factors are based on best estimates derived using different parameters in the MC calculations and different MC codes while the Type A uncertainty values in the first column are all based on measurement uncertainties.

Table 2.7. Relative standard uncertainties in the BIPM determination of air kerma rate for mammography x-ray qualities

Symbol	Parameter / unit	Relative standard uncertainty	
		$s_i^{(1)}$	$u_i^{(2)}$
Physical constants			
ρ_a	dry air density (273.15 K, 101 325 Pa) / (kg m ⁻³)	-	0.01
W/e	mean energy per charge / (J C ⁻¹)	-	0.15
g	fraction of energy lost in radiative processes	-	0.01
Correction factors			
k_{sc}	scattered radiation	-	0.03
k_e	electron loss	-	0.05
k_{fl}	fluorescence	-	0.01
k_s	saturation	0.01	0.01
k_{pol}	polarity	0.01	-
k_a	air attenuation	0.02	0.01
k_d	field distortion	-	0.07
k_{dia}	diaphragm	-	0.01
k_p	transmission through walls of standard	0.01	-
k_h	humidity	-	0.03
Measurement of I/v			
v	volume /cm ³	0.03	0.05
I	ionization current (T, P , air compressibility)	0.02	0.02
	positioning of standard	0.01	0.01
<i>Combined uncertainty of the BIPM determination of air-kerma rate</i>			
	quadratic summation	0.05	0.19
	combined relative standard uncertainty	0.20	

⁽¹⁾ s_i represents the relative standard Type A uncertainty, estimated by statistical methods;

⁽²⁾ u_i represents the relative standard Type B uncertainty, estimated by other means.

2.3. Determination of spectra

An accurate knowledge of each spectrum is required to evaluate the energy-dependent correction factors involved in the air kerma determination. Spectra can be determined either experimentally or by simulation using Monte Carlo techniques.

2.3.1 Experimental spectra determination

One of the problems in determining the spectra experimentally is the high photon fluence of the x-ray beams. While several techniques exist to solve this problem, the Compton scattering method was chosen for the present work as being the most practical. The Compton scattering method consists of placing a scattering material in the primary beam, measuring the scattered photons at a certain angle and then reconstructing the primary beam. A commercial spectrometer system was used for this study, consisting of a Compton spectrometer and a spectral reconstruction program, to be used together with a high purity planar germanium detector and a multichannel analyser (MCA). The Compton spectrometer diagram is shown in Figure 2.10.

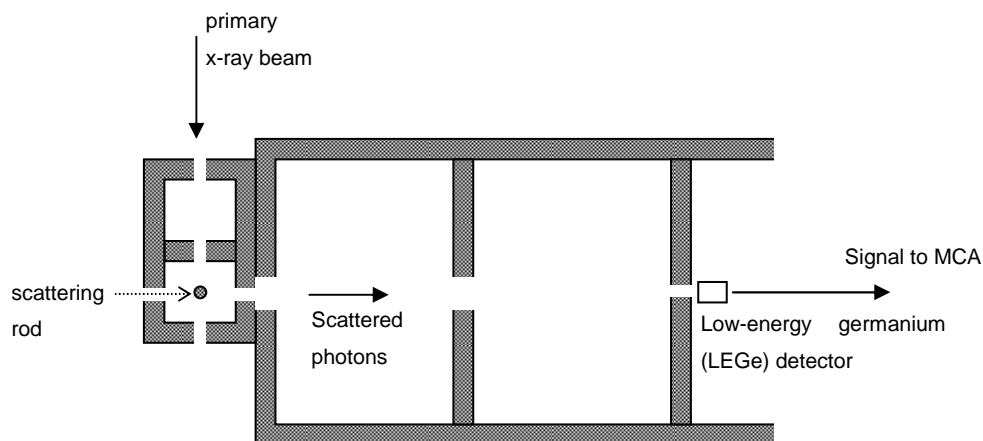


Figure 2.10. Schematic diagram of the Compton spectrometer

- *Compton spectrometer*: this consists of a scattering chamber with lead walls, lead collimators, a lucite² rod of circular cross section used as the scatterer and the spectrometer tube, designed to be used with the detector placed at 90° to the beam axis.

² A commercial name for polymethylmethacrylate

The scattering chamber has three collimators, which facilitate the alignment of the spectrometer with the primary beam. The first two collimators of the scattering chamber define the direction of the primary beam; the third collimator is needed to let those photons which do not interact with the scatterer to escape from the chamber, minimizing backscattering. The lucite rod used as scatterer is placed in the scattering chamber on the beam axis and aligned with the collimation system. It is a cylindrical rod of 2 mm diameter. The spectrometer tube is made of aluminium covered with 5 mm lead. Inside the tube there are two collimators; the first collimator is used to reduce the number of photons scattered inside the tube from reaching the detector and the second defines the effective detector area. The detector is fitted into the spectrometer tube with a special mounting ring so that the central part of the detector is in the scattered beam.

- *Detector*: the spectrometer is designed to be used with a planar germanium detector (cooled to liquid N₂ temperature) placed at 90° with respect to the primary beam axis coupled to a multichannel analyser (MCA).
- *Data acquisition*: the pulse height distribution was obtained and analyzed with the software GENIE 2000 [23]
- *Spectral reconstruction program*: The primary x-ray spectra are reconstructed from the resulting pulse height photon distribution detected at 90° using a program developed by Matscheko [15].

Calibration of the MCA

The energy calibration of the MCA was performed using the known energies of the x- and γ -rays emitted by radioactive sources of ¹²⁵I and ²⁴¹Am, in the form of liquid-filled ampoules. The centre of each ampoule was positioned at about 500 mm from the centre of the Ge detector entrance window. The pulse height distribution was acquired with the software GENIE 2000, where the detector and the MCA are defined and configured.

The x- and γ -ray energies used for the calibration of the detector are listed in Table 2.8.

The energy calibration of the MCA was made prior to any x-ray spectral measurements and it was checked regularly during the period of the spectral determinations. No deviation of the channel number assigned to each energy peak was observed during the repeated calibration checks.

Table 2.8. Characteristics of the radionuclides used for the Ge detector calibration

Radionuclide [24]	¹²⁵ I				²⁴¹ Am		
	x-rays			γ -rays	x-rays		γ -rays
Energy / keV	27.2	27.4	30.9	35.49	13.9	17.8	59.54
Emission probability %	39.6	73.8	21.3	6.7	12.5	18.0	35.9

The spectrum obtained with these radioactive sources is shown schematically in Figure 2.11, superposed on the energy calibration curve for the MCA as a function of the channel number.

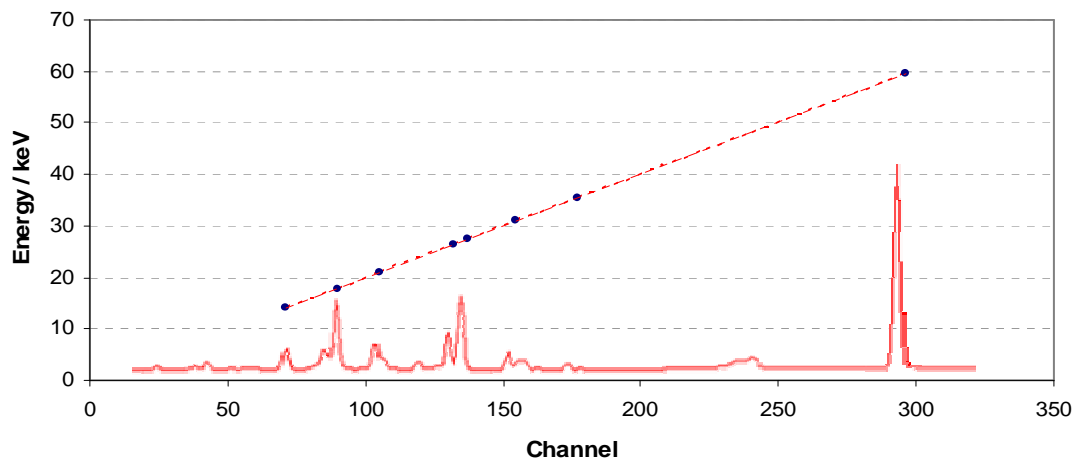


Figure 2.11. Energy calibration curve for the multichannel analyzer

X-ray spectral measurements

The Compton spectrometer was positioned on the x-ray calibration bench to have the scatterer placed inside the scattering chamber at the reference distance of 500 mm from the exit tube window, perpendicular to the beam axis. The experimental set-up is shown in Figure 2.12.

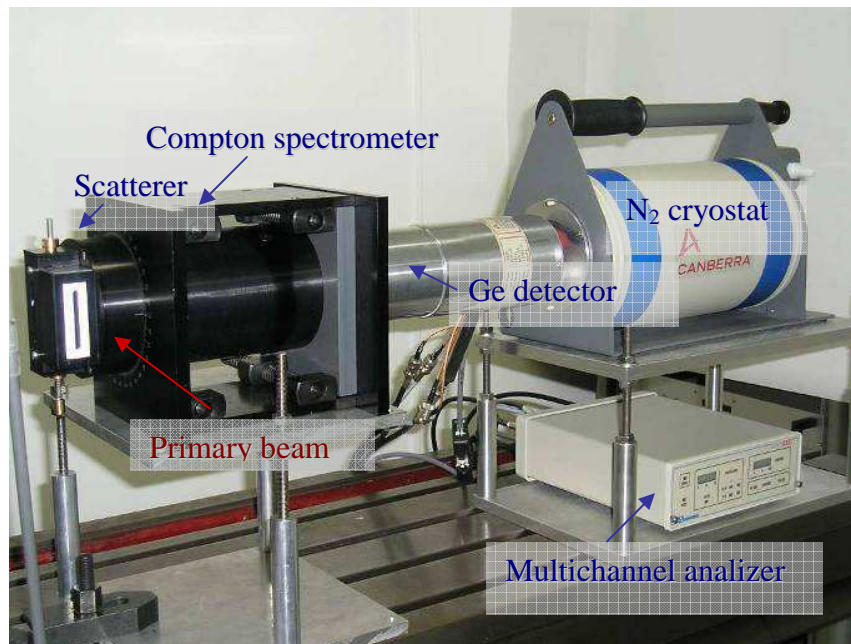


Figure 2.12. Compton spectrometer, low-energy Ge detector and multichannel analyser

Using this configuration, the spectrum at 90° was measured for the nine radiation qualities listed in Table 2.3. The photon energy distributions obtained were used as the input files for the COMPTON deconvolution software to reconstruct the primary spectra.

2.3.2 Spectra determination by simulation

The mammography spectra were also obtained by simulation using Monte Carlo techniques using the code PENELOPE. As mentioned earlier, a realistic model of the x-ray tube geometry is needed in order to achieve reliable results in the simulation of the particle transport. The geometry has been simulated with the PENELOPE geometry code; it consists of a set of bodies limited by quadratic surfaces and identified by their composition (material). The x-ray tube configuration (target, tube window, collimator system and filters) is shown in Figure 2.13. The simulated geometry reproduces the target angle, tube window and filter thicknesses, collimator dimensions as well as the exact location of each component. The electron source, represented as a cylinder of finite dimensions, and the tungsten target are enclosed in a vertical cylinder, with its volume defined as vacuum, while the rest of the geometry is in a horizontal cylinder containing air.

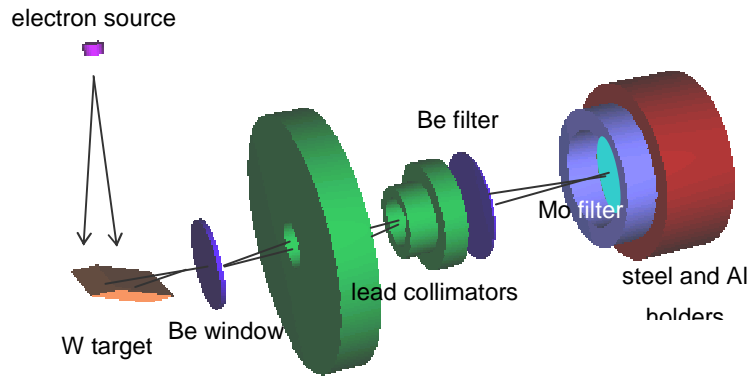


Figure 2.13. Model of the x-ray tube, filters and collimators

The transport of electrons, travelling in vacuum and striking the target to produce bremsstrahlung, and the subsequent transport of photons, passing through the beryllium window, lead collimators and the added filtration (beryllium and molybdenum filters), was made in two steps.

In the first step, this model was used to create a phase-space file of photons crossing the first lead collimator (plane at 5 cm from the centre of the target), including the energy, angle and position of each particle. The photon and electron cut-off energies were set to 1 keV. The following values were chosen for the electron transport parameters in PENELOPE³: $C1 = C2 = 0.2$, $W_{cc} = W_{cr} = 1$ keV. To improve the efficiency of bremsstrahlung emission, a method of variance reduction was used in the main program to force primary electrons to interact in the target.

In the second step, this phase-space file was used as the input for the transport of photons in air through the collimators and filters. The photon cut-off energy was also set to 1 keV, while the electron transport cut-off was raised to the maximum photon energy value (that is, no electron transport). The energy, position and angle of each photon crossing a plane defined at 500 mm from the centre of the target was saved in the output file, which was then used as the input file for the program that generates the distribution of the photon numbers with energy at the reference distance.

³ C1 and C2 determine the cut-off angle that separates hard from soft elastic interactions; W_{cc} and W_{cr} are the cut-off energies for the production of hard inelastic and bremsstrahlung events, respectively.

2.4. Results

2.4.1 Spectral measurements

The measured spectra corresponding to 23 kV, 30 kV, 50 kV with the Mo filter and 30 kV with the Rh filter are shown in Figure 2.14. The energy bins are 0.2 keV. No correction was made for the small Ge escape peak at 10 keV. Each spectrum has been normalized to the maximum number of photons in the peak channel. The spectra are effectively cut at 20 keV and at 23.2 keV, the K-absorption edges of molybdenum and rhodium, respectively.

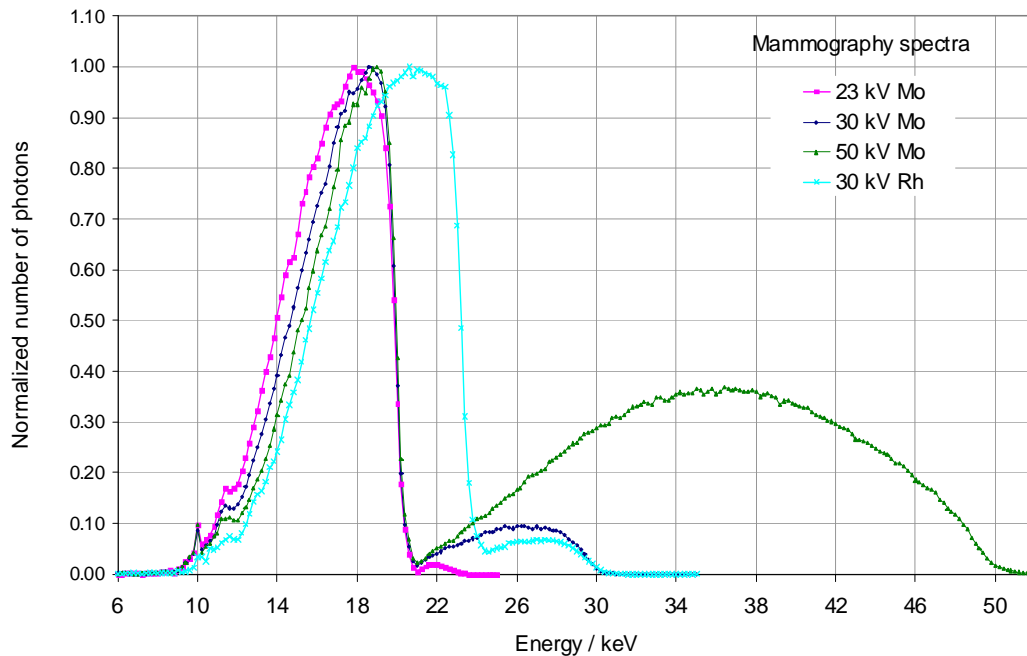


Figure 2.14. Tungsten target spectra measured with the Compton spectrometer

2.4.2 Spectral simulations

Figures 2.15 and 2.16 show the spectra for the 30 kV qualities with Mo and Rh filters, respectively, simulated with the PENELOPE code. Each spectrum is compared with that measured using the Compton spectrometer.

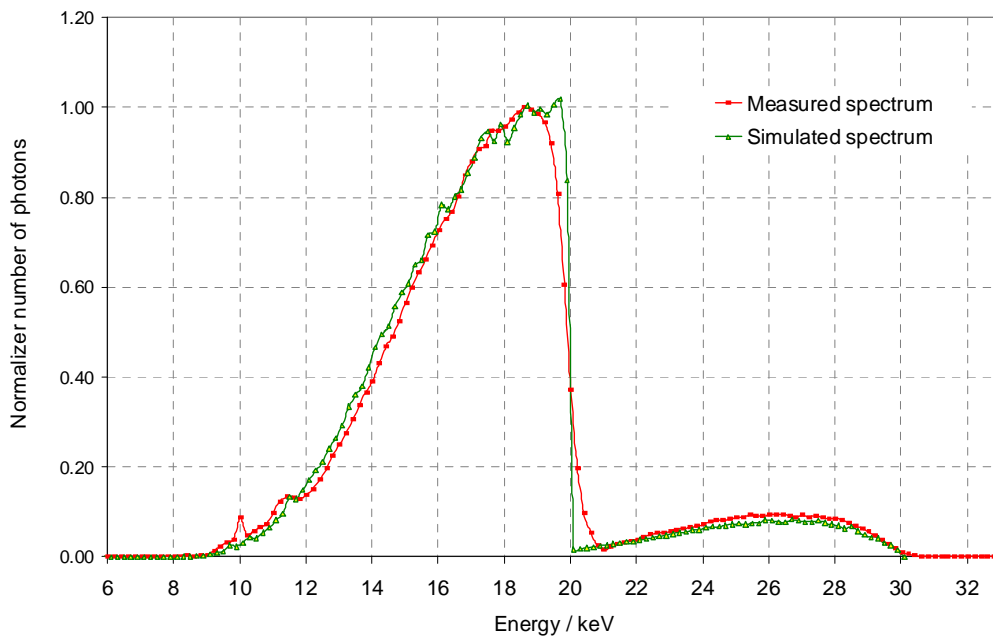


Figure 2.15. Comparison of the simulated and measured spectra for the 30 kV, Mo filter quality

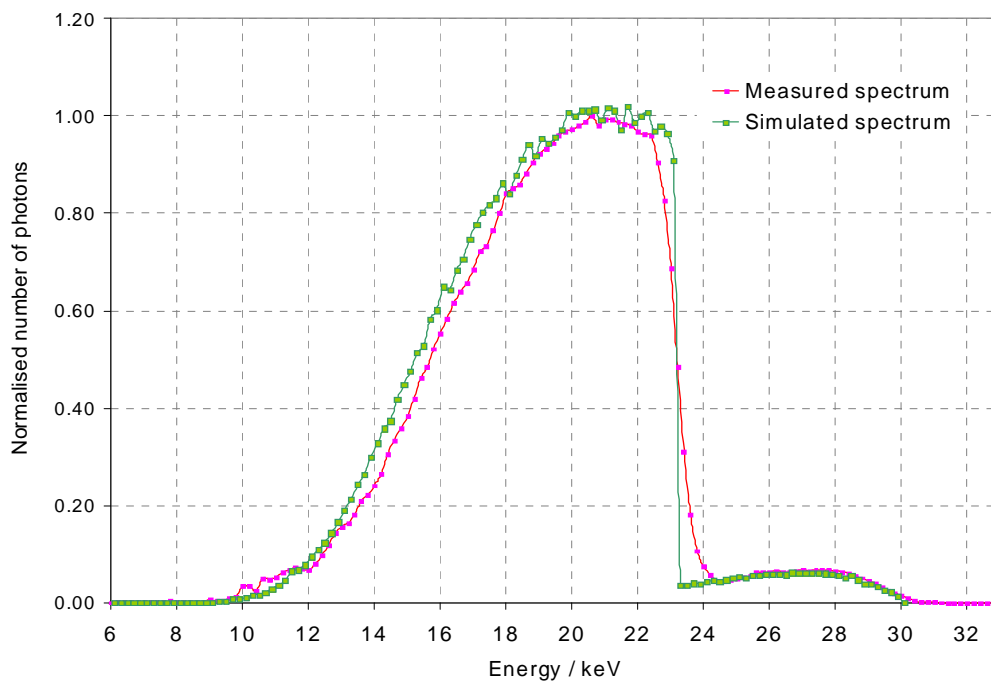


Figure 2.16. Comparison of the simulated and measured spectra for the 30 kV, Rh filter quality

The measured and calculated spectra for the 30 kV, Mo filter quality show slightly better agreement than those for the Rh filter qualities, although the maximum deviation between the curves in the latter case remains less than 0.35 keV. This deviation might be due to statistical fluctuations, which could be improved with further calculations. The energy broadening observed in the measured spectra at the absorption edge of the two filters is likely to be from the energy resolution of the Compton spectrometer. The 10 keV escape peak from the Ge is clearly visible in Figure 2.15.

The agreement between the calculated and measured spectra gives confidence in using the measurements for the input to the MC calculations of the correction factors needed for the primary standard FAC.

2.5. Calibration of transfer ionization chambers

Three commercial ionization chambers of two different types (two Radcal⁴ RC6M and one Exradin A11TW), typically used for mammography dosimetry in hospitals, are calibrated periodically in the simulated mammography beams to study their stability and, in particular, to study their responses in these beams. Technical details of the chambers are presented in Chapter 5 “A study of the response of commercial ionization chambers to mammography beams”.

The main characteristic of these chambers, as informed by the manufacturers, is their “flat” energy response over the energy range used in mammography. Figure 2.17 shows the calibration coefficients for the Radcal RC6M, serial number 9112, measured at the BIPM in the simulated mammography beams, normalized to the CCRI 25 kV reference quality [9]. The response of the chamber changes smoothly with energy, the relative energy dependence being 6×10^{-3} in the range 23 kV to 50 kV for the W/Mo radiation qualities, a non-negligible energy response for this type of chamber.

The calibration coefficients measured for the W/Rh beams are not included in the graph; surprisingly, it was observed that the calibration coefficients for the W/Rh beams were up to 8×10^{-3} greater than the ones measured for the W/Mo beams (the same effect measured also

⁴ The use of these two commercial ionization chambers does not indicate that the BIPM endorses their use for metrological purposes.

for other chamber types). Further studies were undertaken and it was identified that the calibration coefficient depends on the angle of rotation of the filter about the beam axis. Even more, the increases and decreases in current that are seen when the filter is rotated are not the same for the free-air chamber and the chamber under calibration; in some cases the changes are even in the opposite sense. The results of the studies made with the commercial ionization chambers of the BIPM and with those belonging to the NMIs in the simulated mammography beams are presented in Chapter 5 “A study of the response of commercial ionization chambers to mammography beams”.

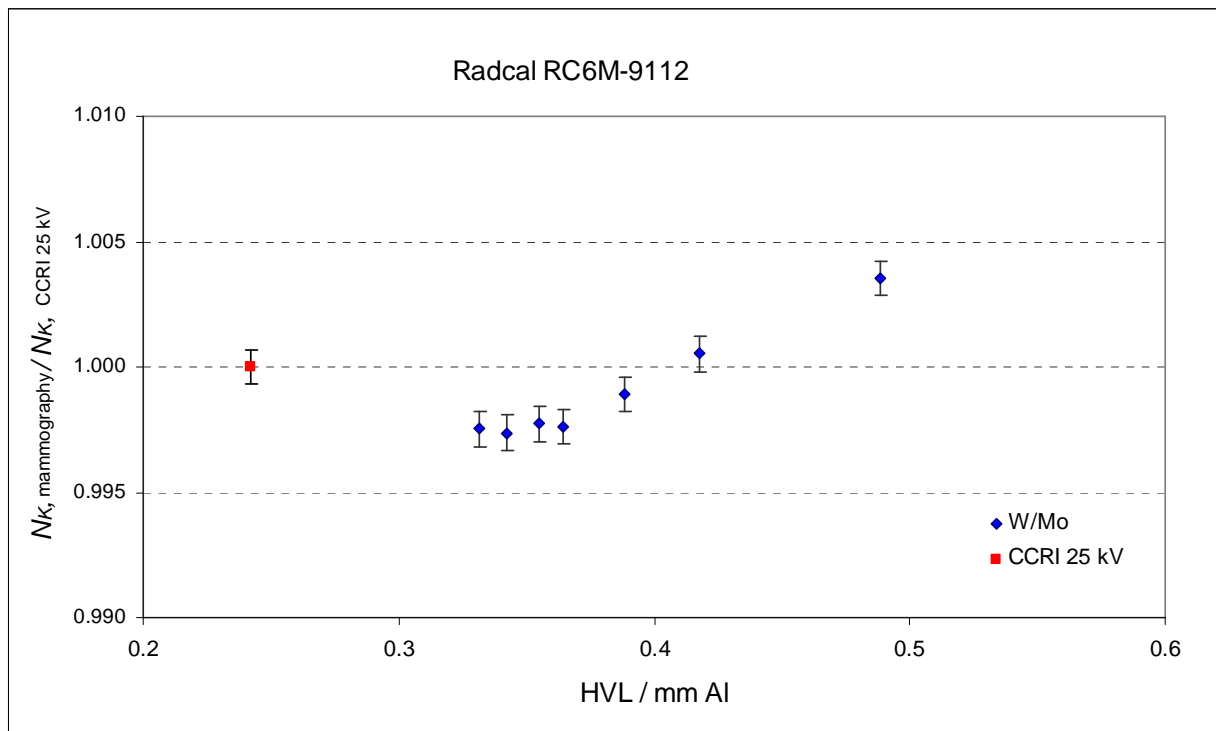


Figure 2.17. Normalized calibration coefficients for the Radcal chamber RC6M s.n. 9112

2.6. Summary

The correction factors used for the primary air kerma determination were derived by interpolation in terms of the HVL from the correction factors calculated for the CCRI qualities. The subsequent recalculation of these factors using the measured spectra with Mo and Rh filters and an improved model of the standard showed the factors to be insensitive at the level of 4×10^{-4} .

In order to calculate the correction factors for the standard L-01 for the new radiation qualities, the spectra were measured using the Compton scattering method and also simulated

using Monte Carlo techniques. Discrepancies up to 0.35 keV were observed between the measured and simulated spectra for a given quality. However, these differences have no significant effect on the calculation of the standard's correction factors.

The suitability of these simulated mammography x-ray qualities for the calibration of ionization chambers currently used in mammography was investigated and the study is described in Chapter 5 "A study of the response of commercial ionization chambers to mammography beams".

2.7. Conclusions

A set of nine radiation qualities in the mammography energy range has been established at the BIPM, using a W-anode x-ray tube and Mo and Rh filters in order to simulate the beams used in clinical mammography. These reference radiation beams are available to the National Metrology Institutes either to undertake primary comparisons in this domain or to have their secondary standards characterized and calibrated at the BIPM, ensuring traceability to the International System of Units (SI).

Chapter 3. Design and construction of a primary standard for mammography dosimetry

3.1. Introduction

Radiation physics is the branch of physics that studies ionizing radiation, its interaction with matter and the way that it transfers energy to a given medium. The amount of energy absorbed in the medium is called absorbed dose and the determination of such dose, either by measurements or by calculations, is referred to as radiation dosimetry. Any detector capable of providing a reading r that is a measure of the dose deposited in its sensitive volume v is defined as a dosimeter. The most common dosimeter used to make precise measurements of dose, as required in medical applications such as radiotherapy or x-ray diagnostic examinations, is the ionization chamber.

An ionization chamber is a device that consists of a gas-filled enclosure between two conducting electrodes. The electrodes can be in the form of parallel plates, coaxial cylinders or coaxial spheres. When the incident ionizing radiation passes through the chamber, it ionizes the gas inside its volume. If an electric field is present, the ions will move apart, each moving in opposite directions along the electric field lines until they encounter the electrodes that are producing the electric field. An ionization current is thus created which may be measured using an electrometer. If the ion-collecting gas volume can be determined absolutely, that is by means other than ionometric calibration in a known radiation field, then the chamber is an absolute dosimeter, becoming a primary reference standard when it is fully characterized for the radiation beam that is intended to be measured. When the gas volume of the ionization chamber is unknown, which is the case for commercial ionization chambers, then the detector needs to be calibrated ionometrically in known radiation fields under certain reference conditions, traceable to a primary standard.

A primary standard is an instrument of the highest metrological quality that permits determination of the unit of the specified quantity from its definition. In diagnostic radiology, the primary standard for realizing the unit gray for the quantity air kerma is a free-air

ionization chamber. When absorbed dose is the quantity required, this can be estimated within acceptable uncertainties from the air-kerma measurements.

The BIPM has maintained in the domain of low-energy x-ray beams (10 kV to 50 kV) an international reference standard since the early 1960s. This is used for the international comparisons of primary standards held by the National Metrology Institutes (NMIs) in well defined x-ray beams at the BIPM. It is also used for the dissemination of the dosimetry quantity air kerma by characterizing and calibrating commercial ionization chambers against the BIPM primary standard in these BIPM reference beams for those NMIs who use such chambers as their national reference standard when they do not have primary standards for such dosimetry.

Following the establishment of new radiation facilities for mammography at the BIPM [11], to be used as reference beams for comparisons and calibrations in this domain, it is evident that a new primary standard was necessary for the dosimetry of these specific beams. This new free air chamber was designed, constructed and assembled at the BIPM. Mechanical measurements of the critical dimensions of the chamber were made using a three-dimensional co-ordinate measuring machine; a full characterization of the standard was made for the reference x-ray beams by determining the necessary correction factors using ionometric measurements for certain factors and calculations using Monte Carlo techniques where this approach was more appropriate. The new standard was then compared against the existing standard in the CCRI reference beams [9] to confirm its behaviour prior to use in the mammography reference beams.

3.2. Definitions

Terminology for radiation interaction products

The free-air chamber consists of a volume of air contained within a chamber body with an entrance aperture that is irradiated by photons coming from an x-ray tube. Photons coming directly from the radiation source (x-ray tube) and entering through the aperture into the volume of air without any interaction are called *primary photons*. Photons interacting with the surrounding walls or the aperture of this body are referred to as *transmitted photons*. Interactions of the primary photons in the air generate *secondary electrons* resulting from photoelectric or Compton processes. The subsequent interactions of secondary electrons result

in a large number of electrons of lower energies. The secondary electrons and their progeny are called *liberated electrons* and the total charge of all electrons, *liberated charge*.

Primary photons scattering in the air volume are called *scattered photons*; the relaxation of atoms excited during primary photon interactions results in the emission of *fluorescence photons* and *photoelectrons*; the slowing down of liberated electrons whether from this process or from Compton scatter generates *bremsstrahlung* radiation.

The term *secondary photons* refers to transmitted, scattered and fluorescence photons as well as bremsstrahlung.

Exposure and air kerma

An early quantity used in diagnostic radiology dosimetry is the exposure [25], defined only for photons as the mean quotient of dQ by dm , where dQ is the total charge of a given sign produced when the liberated charge arising from the interactions of primary photons in a mass dm of dry air is allowed to come to rest in air. It follows that any charge resulting from the interaction of secondary photons, including bremsstrahlung, is not included in the definition of exposure, X :

$$X = \frac{dQ}{dm_{\text{air}}} \quad (3.1)$$

The more general quantity, defined for uncharged particles in any material, is kerma (kinetic energy released per mass), defined as the mean quotient of T by m , where T is the total kinetic energy given to charged particles produced in the interaction of primary uncharged particles in a mass m of material, in this case, air [25].

However, both quantities are closely related, as kerma is the dissipation of the kinetic energy of secondary electrons that gives rise to the liberated charge. The difference between them is related to the radiative losses: the slowing down of the liberated electrons producing radiated photons, mainly bremsstrahlung. As this radiation generally escapes from the region of interest, it does not produce any appreciable measured charge and is not included in the definition of exposure. However, radiative photons take some of the initial kinetic energy of the secondary electrons and this energy is included in the air kerma definition. A correction for the energy given to radiative photons in air is thus required in the determination of air

kerma from the measured exposure. Thus, the relationship between these two quantities can be expressed as

$$K_{\text{air}} = \frac{(W_{\text{air}}/e)}{(1-g)} X \quad (3.2)$$

where W_{air} is the mean energy required to create an ion pair in air and e is the electronic charge.

According to the definition of exposure, the total liberated charge due to photons interacting in a known mass of air has to be measured. Such a requirement is difficult to realize in practice, but it can be achieved with a detector of special design working under conditions where charged-particle equilibrium (CPE) exists. That means that for a volume v , each charged particle of a given type and energy leaving v is replaced by an identical particle of the same energy entering v . This concept can be understood by considering a homogeneous, semi-infinite slab of material irradiated by a parallel beam of photons. At the surface, energy deposition will be relatively small, especially at photon energies for which the secondary electrons are preferentially forward-directed. As the depth is increased, energy deposition will increase until the depth is equivalent to the maximum secondary-electron range. At this depth, the spectrum of liberated electrons reaches an equilibrium state such that, ignoring photon attenuation, the electron spectrum is the same at all points beyond this depth.

3.3. Free air chamber

3.3.1. Principle of operation

An instrument to measure exposure has to allow the primary photons and the liberated electrons to interact only in air; such a requirement is accomplished by using a free-air chamber, in which the volume of interaction has no « walls ». The general characteristics are indicated in Figure 3.1.

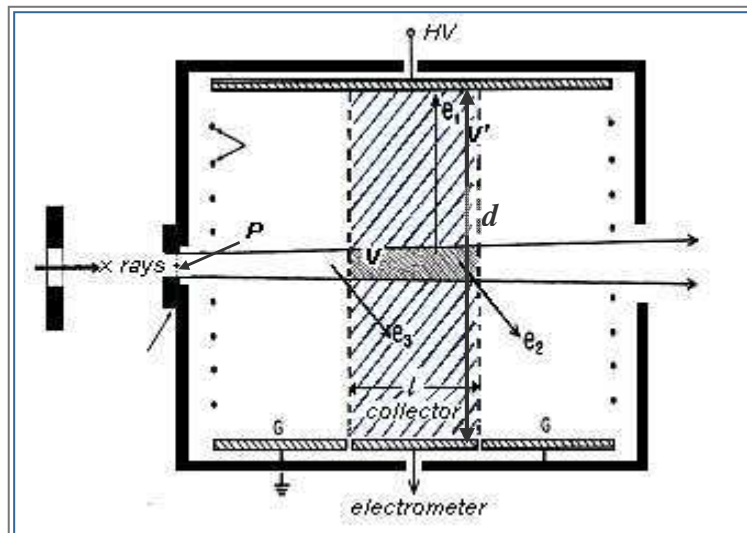


Figure 3.1. Schematic diagram of a free-air chamber [26]

The chamber is enclosed in a radiation-shielding box with an entrance diaphragm aligned with the x-ray beam central axis. The diaphragm with cross-sectional area A_0 defines a reference plane at point P at which exposure (and thus kerma) will be determined. Inside the box, a pair of planar electrodes separated by a distance d produces an electric field when a polarizing voltage is applied to one of the electrodes and the other is kept at ground potential.

The latter electrode contains a plate of length l_c in the beam direction isolated by a thin air gap of length l_g . This plate is connected to a measuring device and is called the collecting electrode (or simply, collector). The remaining plate is the guard electrode. To provide a uniform electric field between the electrodes, a set of strips encircles the space between them. These strips are electrically biased in uniform steps to establish parallel equipotential planes between the electrodes. Under these conditions, it is assumed that the electric lines of force go straight across the chamber, perpendicular to the electrodes. With this assumption, the electric field lines at the centre of the air gap and the collecting electrode define the region where charge is collected and this is referred to as the collecting volume V' (blue shaded region in Fig 3.1). The reason why half of the air gap length is included as part of the collecting length in defining the collecting volume is explained in section 3.3.2. The volume V (grey shaded region in Fig 3.1) is where secondary electrons are produced whose ionization must be measured.

The primary photons entering the chamber through the aperture will interact with the air and generate secondary electrons. If the electrode separation d is larger than the range of the most energetic electrons generated in V , these electrons will not strike either electrode and will

come to rest in the air of the chamber, like electron e_1 , converting all of their kinetic energy into ionizations inside the collecting volume V' . Electrons like e_2 are generated inside the volume V but produce ionization outside the collecting volume V' ; under conditions of charged particle equilibrium this loss is compensated by electrons like e_3 . That implies that the length between the defining plane of the diaphragm and the centre of the collecting region must be at least equivalent to the maximum range of the secondary electrons. Under these conditions, the charge collected is a measure of the total charge liberated in photon interactions over the length l of the collecting region.

If Φ_0 is the photon fluence (photons/m²) at the reference plane of the aperture of area A_0 (m²), then $\Phi_0 A_0$ is the number of photons entering in the chamber. Ignoring air attenuation effects, the fluence Φ decreases, in proportion to the inverse square of the distance from the source, as the beam proceeds through the chamber. Simultaneously the beam area A increases in proportion to the square of the distance from the source; thus ΦA remains constant and equal to $\Phi_0 A_0$ through the chamber. The number of electrons produced by ΦA photons in traversing the volume V of length l will be constant, irrespective of the actual cross-sectional area A of the beam in V (strictly, for a photon with angle θ to the beam axis it is the interaction length $l/\cos\theta$ that is relevant. However, for typical geometries the maximum angle is less than 1° ; so the uncertainty of the assumption of constancy is less than 1 part in 10^4). Consequently one can replace the actual volume V by a cylindrical volume $V_c = A_0 l$ (m³); multiplying V_c by the air density ρ (kg/m³), gives the air mass m_{air} (kg) by which the measured charge Q (C) is to be divided to obtain the exposure at point P. One important approximation made in the above argument is the neglect of the air attenuation of the primary photon fluence. The exposure at point P must include a correction to the measured charge for photon attenuation between the reference plane and the collecting region.

In practice, it is usual to determine the exposure rate by measuring ionization current I rather than charge. The air kerma rate is derived from the exposure rate determination using the equation:

$$\dot{K}_{\text{air}} = \frac{(W_{\text{air}}/e)(I/m_{\text{air}})}{(1-g)} \prod_i k_i, \quad (3.3)$$

where Πk_i is the product of a set of correction factors introduced to account for the limitations of the free-air chamber in measuring the exposure rate. The correction factors k_i are mentioned in the section 3.3.2 and are fully explained in section 3.5.

3.3.2. Design of a free-air chamber

The main factors that must be investigated for the optimum design of a free-air chamber are described in the following paragraphs: the electrode separation, the distance between the diaphragm and the collector (air attenuation length), the diaphragm system, the effective length of the region of ion collection (collecting electrode length), the electric field and the temperature of the air volume inside the chamber.

Electrode separation

According to the definition of exposure, the electrode separation has to be greater than the range of the most energetic secondary electrons to allow them to come to rest in the air of the chamber and produce all their ionization inside the collecting volume. The range for electrons in the continuous slowing-down approximation (csda), in air is given in ICRU Report 37 [27]. For x-ray spectra up to 50 kV, the maximum electron range is that for electrons of 50 keV, namely 4.9 mg cm^{-2} , which at ambient temperature and pressure is equivalent to 41 mm, but such spectra actually contain very few photons above 40 keV. This can be considered also as an overestimation because the csda assumes that the electrons travel in straight lines. So, under these considerations, a separation of 70 mm between the electrodes is sufficient to avoid secondary electrons reaching either electrode ; this has the effect of minimizing a correction usually introduced in (3.3) as the electron loss correction factor k_e to account for this effect.

Attenuation length

As mentioned in section 3.2, charged particle equilibrium (CPE) is an essential condition for the measurement of exposure. The length between the reference plane defined by the aperture and the centre of the collecting region required for CPE is referred to as the attenuation length A . In the design of a free-air chamber, the attenuation length must be defined taking into account the maximum range of the secondary electrons in air [27], following the argument outlined in the preceding section. Nevertheless, the attenuation length must be kept short in order to minimize the correction applied for attenuation of the primary photon fluence

over this length; the attenuation correction k_a is calculated from measurements of the air attenuation coefficient μ as $\exp[\mu A]$. Another reason to keep this length short is to minimize the scattered photons generated along this air path, as these scattered photons can liberate electrons that reach the collecting region but these are not part of the exposure definition. A factor to correct for photon scatter k_{sc} along the attenuation length is introduced in (3.3).

Diaphragm system

The diaphragms of free-air chambers are normally made of tungsten (or an alloy of tungsten), with, usually, cylindrical apertures. The area of the aperture defines, together with the length of the collecting electrode and half of the air gap length, the air volume (mass) by which the measured charge is to be divided to determine the kerma. To minimize the uncertainty contribution of the area aperture to the kerma uncertainty, accurate mechanical measurements of the order of few micrometres are required.

The diameter of the aperture has to be greater than the focus of the x-ray tube to avoid the photons emitted from the limits of the focus being attenuated by the upstream edge of the aperture and those emitted from the centre, by its downstream edge. As focus diameters are usually not greater than 4 mm, the aperture diameter can range from 5 mm up to 12 mm. The diaphragm should be thick enough to reduce photon transmission through its body to a negligible level. A correction factor $k_{tr,dia}$ is calculated to account for this effect. The diaphragm correction factor k_{dia} introduced in (3.3) takes into account not only photon transmission $k_{tr,dia}$ but also the fact that photons can be scattered by the diaphragm $k_{sc,dia}$ and that fluorescence photons $k_{fl,dia}$ from the tungsten or alloy material can also be produced. These three factors are calculated using Monte Carlo techniques.

Collecting electrode length

As mentioned previously, the length of the collecting electrode (including half of the air gap length, as explained in the following paragraph) and the aperture area A define the volume V where the secondary electrons are generated. Mechanical measurements of the order of a few micrometres are also required for the determination of the collector length. The collector length is typically in the range from 10 mm to 20 mm for free air chambers used for low-energy x-ray beams. The choice of the length involves many compromises: a greater length is better to minimize the uncertainty in the mechanical measurements as well as to increase the

ion collection, whereas a shorter length is desired in order to minimize distortions in the electric field, as explained in the following section.

It is usual to consider the collecting length l as the sum of the collector length l_c and half of the air gaps surrounding the collector; in other words, if l_g is the the air gap length, then the length of the collecting region is $l_c + l_g/2 + l_g/2$, that is $l = (l_c + l_g)$. The reason for this is because it is assumed that the charge produced at the positions corresponding to the air gaps is shared equally between the collector and the guard electrode.

Electric field

The ionization is measured for a length l , determined by the limiting lines of force to the centre of the air gap surrounding the collector, assuming that the lines are perpendicular to both electrodes. Several aspects have to be considered in designing the chamber in order to achieve this requirement: a high degree of parallelism between the electrodes, co-planarity of the collecting electrode and the guard plate and no perturbation due to the chamber enclosure. The first two aspects demand that each component be machined as flat as achievable; studies presented in [28] have shown that for a chamber with $l_c = 100$ mm and $l_g = 0.9$ mm, the ionization current changes by 1×10^{-3} per 25 μm of misalignment. Studies made at the BIPM, for the particular case of $l_c = 15$ mm, $l_g = 0.5$ mm and $d = 70$ mm, showed that the ionization current varies by 4 parts in 10^3 when the co-planarity is at the level of 30 μm . The results of this study are presented in section 3.6. The chamber enclosure itself will perturb the electric field at the edges of the polarizing plate and it can also make perturbations in the collecting region. This effect can be minimized by inserting a system of horizontal guard strips, or guard wires surrounding the air volume of the chamber. The guard strips are electrically isolated from each other and uniformly spaced between the ground and high-voltage electrodes and are parallel to the electrodes. Their potentials are fixed by a suitable chain of resistors which increases the potential linearly from the guard plate at the bottom to the high-voltage electrode at the top. The resistor chain needs to be placed outside the chamber in order to avoid temperature fluctuations in the air volume, as the heat dissipated in the resistors can be significant. However, some electrical distortions are still present due to the guard strips themselves. Many studies have been made in order to evaluate these remaining distortions of the electric field. The results presented in [29, 30] showed that the separation of the strip centres should be not more than one tenth of the attenuation length in order to minimize the remaining distortions and a theoretical study [31] showed that field uniformity can be

improved by increasing the thickness of the strips, reducing the insulators between them. A simulation of the electric field has been made using commercial software based on finite element analysis, as presented in section 3.5.

Temperature

Apart from air pressure, the air mass inside the chamber is influenced by fluctuations of the air temperature and these variations must be measured with a calibrated sensor inside the chamber (variations of the air pressure, which also influence the air mass, do not need to be measured by a sensor inside the chamber). A temperature sensor must be placed preferably inside the chamber rather than outside as the air mass may be slow to respond to variations of the laboratory ambient temperature. The sensor position is not trivial, as it should measure the temperature of the collecting volume but it should not interfere with the primary beam and not introduce distortions of the electric field. For these reasons, it is positioned distant from the collecting region although still within the chamber. In order to determine if a temperature gradient exists between that measured by the sensor and that in the region of interest, a second sensor was placed temporarily in the centre of the collecting region, with no radiation present. As the resistor chain may heat the air of the chamber, this test had to be made with the polarizing voltage applied and after reaching a thermal stability. By comparing the responses of the two sensors, an appropriate correction may be deduced and applied to the temperature measured by the distant sensor to correct for this effect.

3.4. The BIPM free-air chamber design

Once all the influence parameters had been studied and their effects characterized, I designed a new primary standard and this was machined and constructed at the BIPM. It is a parallel-plate free-air chamber, identified as L-02, designed to be used for x-ray beams operating up to 50 kV and to minimize the correction factors k_i and their uncertainties, involved in the air-kerma determination, as explained in section 3.5.

A schematic diagram of the L-02 chamber is shown in Figure 3.2.

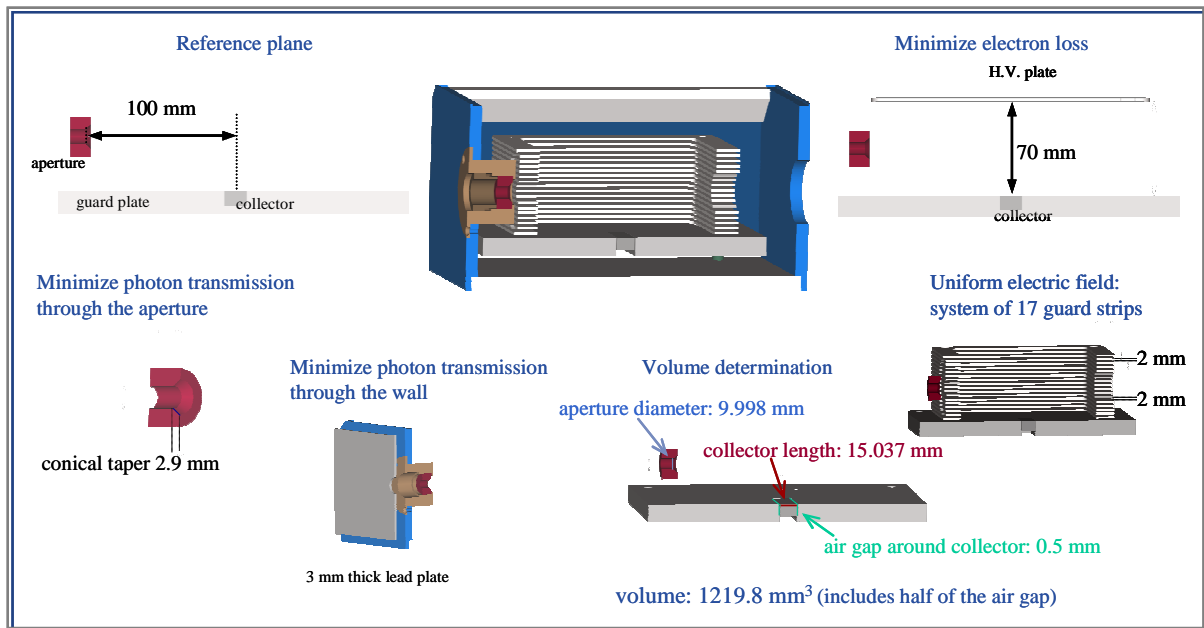


Figure 3.2. The new free-air chamber, L-02. A schematic representation (not to scale) showing the various components and important dimensions.

Electrode separation

The separation between the high-voltage plate and the collector is 70 mm; this separation was calculated in order to reduce electron loss to a negligible amount for a radiation quality corresponding to a generating voltage of 50 kV, using the tungsten-anode x-ray tube, known as the CCRI 50 kVa quality [9]. This radiation quality was chosen to ensure that the L-02 chamber could be used at the maximum likely beam energy for mammography and also to serve as a replacement in the event of a failure of the existing standard L-01 for the tungsten-anode radiation qualities.

Attenuation length

The attenuation length, defined as the distance between the reference plane of the diaphragm and the centre of the collecting region is 100.20(5) mm; this length is identified as sufficient to ensure that charged-particle equilibrium exists in the collecting volume.

Diaphragm

The diaphragm is made of a tungsten-alloy. Mechanical measurements of the diaphragm were made using a three-dimensional co-ordinate measuring machine (CMM), calibrated at the

1 μm level using reference blocks. The diaphragm is 13.04(1) mm thick with an aperture 9.998(1) mm in diameter. In order to reduce photon transmission, the innermost 2.90(1) mm forms a conical section that increases the diameter to 15.8 mm. The effective aperture length is therefore 10.14(1) mm.

Collecting electrode and guard plate

The collector and the guard plate are made of aluminium with a thin graphite coating. The collector is placed in the centre of the guard plate and is surrounded by an air gap of 0.5 mm. The CMM was used for the measurements of the critical dimensions of the collector and to assure the co-planarity of the collector and the guard plate. The collector length is 15.037(1) mm. The collector support was designed to allow the co-planarity to be adjusted with a tolerance of around 5 μm as this had proved to be critical.

Electric field

A system of 17 guard strips, uniformly spaced between the ground and high-voltage plates and parallel to them, surrounds the air cavity in order to produce a uniform electric field in the collecting region. The individual strips are 20 mm wide and 2 mm thick and are spaced by gaps of 2 mm. Plastic discs are placed between the guard strips to fix their position and their spacing, and to avoid electrical contact between the strips. Their potentials are fixed by a chain of 18 resistors which increases the potential linearly from the guard plate at the bottom to the high-voltage electrode at the top. The resistor chain is located outside the chamber in order to avoid temperature fluctuations inside the chamber.

Volume determination

The collecting volume defined by the aperture diameter and the collector length is 1219.8(4) mm^3 . As is normal for a chamber of this type, the effective collector length (15.537(2) mm) includes half of the front and rear air gaps.

Air temperature

A thermistor, calibrated to a few mK, measures the air temperature inside the chamber. The thermistor is placed just above the high-voltage plate, laterally centred, 20 mm behind the front wall. This position was chosen after studying the temperature distribution within the

chamber; measurements at this location best represent the temperature of the collecting air volume, as explained in section 3.6.

Front wall

A 3 mm thick lead plate with an aperture 20 mm in diameter, centred on the diaphragm aperture was added to the front wall to minimize photon transmission through the aluminium wall.

3.5. Correction factors

As explained in section 3.3, the design of a free air chamber involves many compromises. As some of the requirements are constrained by others, an optimum compromise is reached to minimize the necessary correction factors, which are then determined either by measurements or calculations. A description of the correction factors applied to the new standard L-02 and the methods used to determine them are presented in this section.

Polarity

Free-air chambers must be operated with both positive and negative polarizing voltages and the mean current I_{mean} is calculated, correcting in this way for possible variations in the response of the chamber to both polarities. Also, certain effects related to field distortion are reversed when changing polarity and are therefore accounted for when taking the mean response. Care must be taken to ensure that the chamber has stabilized after a change in polarity and that any variation in the x-ray output during the duration of the measurements is taken into account. In practice, it is more efficient to use always the same polarity and apply a pre-measured correction factor k_{pol} ; if the chamber is going to be operated with positive polarity, then k_{pol} is defined as

$$k_{\text{pol}} = I_{\text{mean}} / I_{+} \quad (3.4)$$

This polarity correction for the standard L-02 is 1.0004(2).

Lack of saturation

The charge collected and measured using an ionization chamber is less than the charge produced in the air volume of the chamber because of recombination of some positive and

negative ions within the air. An ionization chamber is said to be saturated when such ionic recombination is absent, achieved by increasing the potential applied to the chamber. As it is not possible to increase the applied potential indefinitely to eliminate recombination, a correction factor for the lack of saturation is calculated. It is usual to distinguish between initial and volume recombination; initial recombination, correction k_{init} , occurs when the positive and negative ions formed in the same charged-particle track meet and recombine and volume recombination, correction k_{vol} , occurs when ions of different tracks encounter each other on their way to the electrodes. Initial recombination is independent of the kerma rate whereas volume recombination depends on how many ions are created per unit volume and per unit time and hence on the air kerma rate.

The correction for ion recombination was determined following the method proposed by De Almeida and Niatel [12] as implemented by Boutillon [13]. It consists of determining the chamber response to different air kerma rates when applying two different polarizing voltages, V and V/n , where n is not necessarily an integer. The ratio between the currents I_V and $I_{V/n}$ can be expressed as

$$\frac{I_V}{I_{V/n}} = 1 + (n-1)\frac{A}{V} + (n^2 - 1)m^2\left(\frac{g}{V^2}\right)I_V \quad (3.5)$$

where A is a constant depending on the chamber type and m^2 is a parameter that takes into account the mobilities of ions and g is a factor depending on the geometry of the chamber; the first variable term describes the initial recombination and the second, the volume recombination.

The measured current ratio $I_V / I_{V/n}$ plotted as a function of the current I_V measured at the standard polarizing potential V , is used to determine k_{init} and k_{vol} : for a linear fit with intercept $(1 + a_0)$ and gradient a_1 , the component of initial recombination at voltage V is given by

$$k_{\text{init}} = \frac{a_0}{n-1} \quad (3.6)$$

and that for volume recombination by

$$k_{\text{vol}} = \frac{a_1}{n^2 - 1} \quad (3.7)$$

The total recombination is then calculated as $k_s = 1 + k_{\text{init}} + k_{\text{vol}} \cdot I$.

As ion recombination does not depend on the radiation quality (energy spectrum) [13], measurements can be made for any generating voltage at different air kerma rates, achieved either by varying the anode current or by adding filtration in the beam. Ion recombination for the standard L-02 was determined using a generating voltage of 30 kV, a combination of different filters and applying a positive polarizing voltage V of 1500 V and V/n of 500 V. Polarity corrections k_{pol} were determined for both polarizing voltages prior to the ion recombination measurements and these were applied to the measured currents. The results are shown in Figure 3.3 and the initial and volume recombination obtained from the linear fit are presented in Table 3.1.

Table 3.1. Ion recombination for the FAC-L-02

Initial recombination, k_{init}	0.0006
Volume recombination, k_{vol} / pA	1.0×10^{-5}
k_s for $I = 90 \text{ pA}$	1.0015(1)

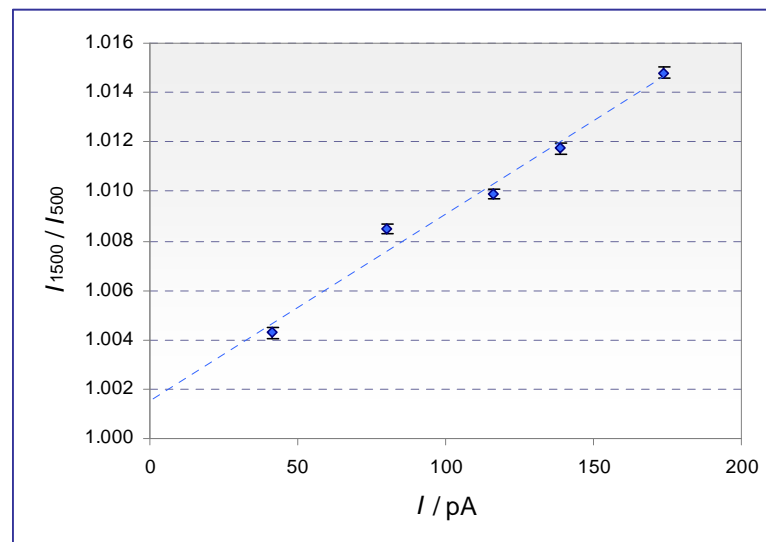


Figure 3.3. Linear fit to the measured points to calculate k_{init} and k_{vol}

Field distortion

A simulation of the electric field was made using the Quick Field software, a program based on finite element theory, developed for electromagnetic, thermal and stress analysis. A two-dimensional simulation of the chamber was made using the geometry editor provided by the

software, reproducing the actual dimensions of collector, guard plate, guard strips and high-voltage (HV) plate, as well as the location of each component of the chamber. The corresponding potential values were assigned to each guard strip, increasing linearly from 0 V for collector and guard-plate to 1800 V for the HV plate at the top of the chamber. To build the finite element mesh, the element sizes were chosen by the program, resulting in an uniform mesh. The electric field was simulated for the central plane of the chamber; a graphical representation of the field strength and the lines of equal potential is shown in Figure 3.4.

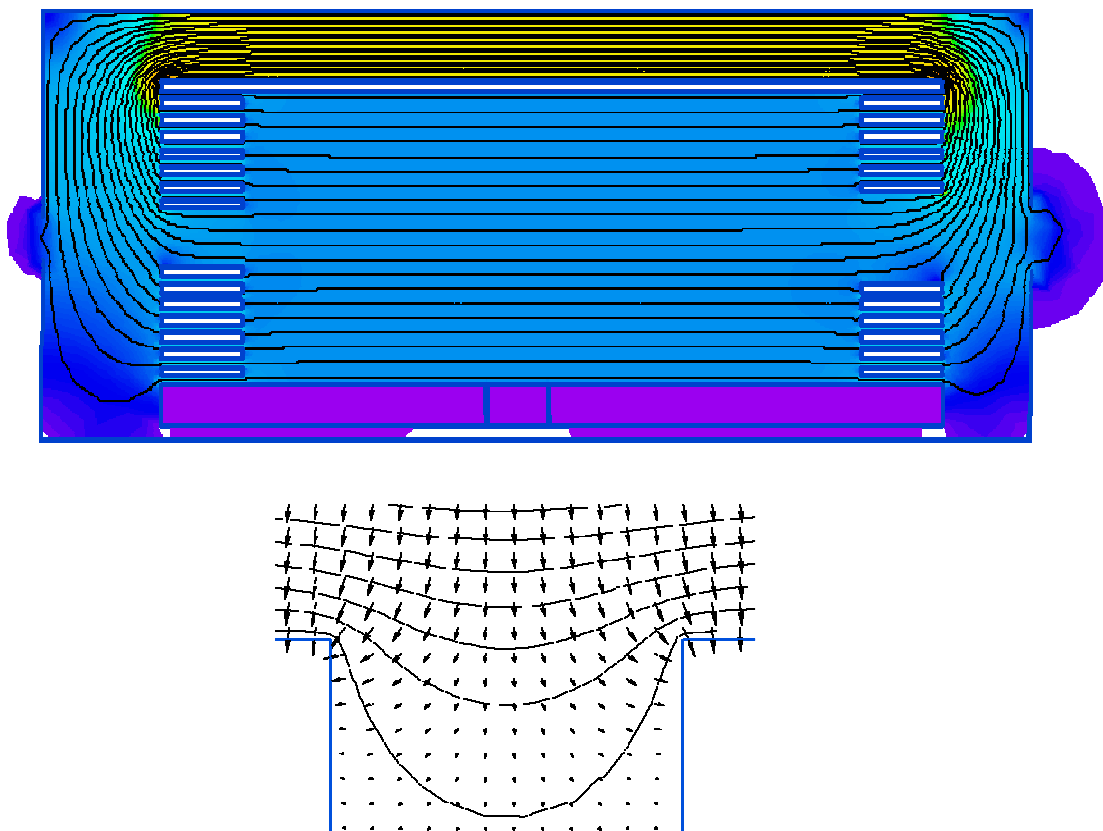


Figure 3.4. Mapping of the field strength (upper graph) and electric field vectors in the air gap between collector and guard plate (lower graph); lines of equal potential are also plotted.

No field distortion is observed from the graphical representation near the collecting volume; the directions of the electrical vectors are perpendicular to the beam axis in the defined volume and equally distributed to the collector and guard plate in the air gap between them, confirming the assumption of considering half of the air gap as part of the effective collector length.

Photon attenuation

The air between the reference plane defined by the aperture and the collecting region attenuates the primary photons and a factor k_a that corrects for this effect must be determined for each radiation quality at which the chamber is to be used. There are several methods to determine this correction [21]. In the present work, the photon attenuation correction was derived by using the reduced air pressure pipe method. This consists of placing an enclosed pipe with thin beryllium windows on the beam axis, in front of the free-air chamber. Air is aspirated from the pipe, reducing the effective length of the air column traversed by the primary photons, until it is equivalent to the attenuation length A . The consequent increase in the ionization current is a measure of the mean attenuation coefficient for the air removed. A diagram of the experimental arrangement is shown in Figure 3.5.

The pipe length is 30 cm, that is, 3 times the attenuation length A of the FAC L-02; this implies that the air to be removed is equivalent to a reduction of the pressure inside the tube to around 67 kPa. Ionization current is measured when the pipe is open to the ambient conditions and when air is removed. Under these two conditions, the current corrected by the air attenuation must be equal to the current measured when air is removed. Typical values for the air attenuation coefficient μ in the energy range 20 kV to 50 kV are from 0.20 m^{-1} to 0.15 m^{-1} , giving an air attenuation correction from 1.022 to 1.017 for the BIPM reference beams qualities for mammography.

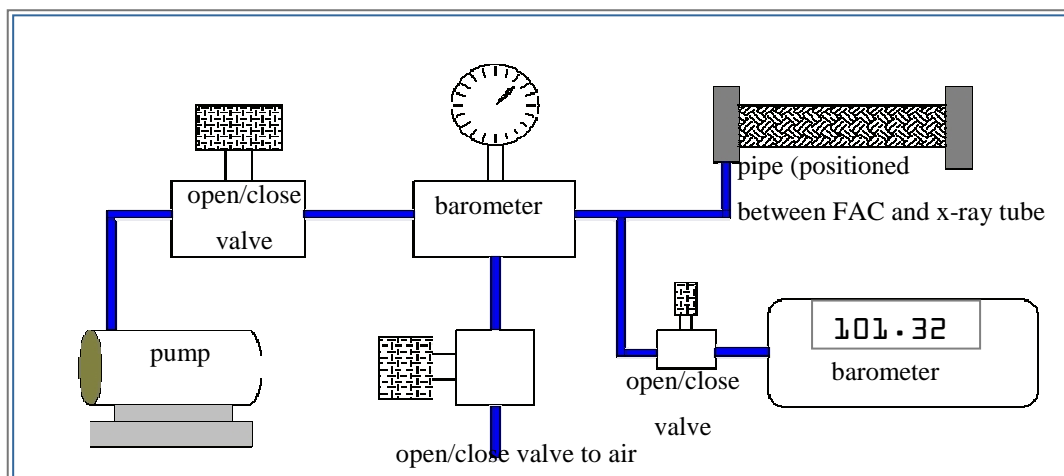


Figure 3.5. Schematic representation of the experimental arrangement for air attenuation measurements

Electron loss

The electron loss correction factor k_e corrects for any loss of charge due to electrons that originate within but do not come to rest in the air volume, that is, they have enough energy to reach the electrodes or the side walls of the free-air chamber. This factor was calculated using Monte Carlo techniques.

Scattered and fluorescence photons

Primary photons entering the chamber that are scattered within the air volume are not considered as primary photons anymore and consequently the ionization produced by electrons generated by these scattered photons should not be included in the definition of kerma. Similarly, fluorescence photons, emitted by atoms excited during primary photon interactions, can generate electrons and the ionization produced by them must be excluded from the kerma determination. The correction factors for scattered photons k_{sc} and for fluorescence emission k_{fl} were calculated using Monte Carlo techniques.

Diaphragm transmitted and scattered photons, wall transmission

Primary photons passing through the aperture and interacting with the diaphragm or those photons transmitted through the diaphragm or the front wall are not part of the primary fluence and the correction factors k_{dia} and k_{wall} are calculated using Monte Carlo methods to correct for the contribution of these photons to the measured ionization current.

Monte Carlo calculations

The correction factors for the L-02 standard involved in the determination of K_{air} for electron loss, photon scatter and fluorescence inside the chamber, bremsstrahlung production, photon transmission through the diaphragm edge, photon scatter and fluorescence from the diaphragm, photon scatter from the diaphragm holder and front wall transmission, were all calculated using the Monte Carlo code PENELOPE [14]. For these calculations, I made a detailed simulation of the new L-02 standard using the PENELOPE geometry package PENGEOM. The FAC geometry consists of 45 bodies defined by their composition (material) and 62 limiting quadratic surfaces, reproducing the actual dimensions of the standard. An example of the way that the surfaces and bodies are defined is shown Figure 3.6 together with the resulting geometry, as displayed by the program GVIEW3D and GVIEW2D.

```

XXXXXXXXXXXXXXXXXXXXXXXXXXXXXXXXXXXXXXXXXXXX
*****
Pengeom geometry - facmam.geo
*****
BIPM mammography FAC-L-02
0000000000000000000000000000000000000000
SURFACE ( 1)  CYLINDER R=1.5 sup
ap
INDICES=( 1, 0, 1, 0,-1)
X-SCALE=( 1.5000000000000000E+00,  0)
Z-SCALE=( 1.5000000000000000E+00,  0)
0000000000000000000000000000000000000000
-----
0000000000000000000000000000000000000000
SURFACE ( 43)  PLANE X=3.55 pair
air gap-collector
INDICES=( 1, 0, 0, 0,-1)
X-SCALE=( 3.5500000000000000E+00,  0)
0000000000000000000000000000000000000000
-----
0000000000000000000000000000000000000000
SURFACE ( 60)  PLANE Y=46.2
shielding Pb
INDICES=( 0, 0, 0, 0, 0)
      AY=( 1.0000000000000000E+00,  0)
      A0=(-4.6200000000000000E+01,  0)
0000000000000000000000000000000000000000
-----
BODY ( 5)  collecting region
air
MATERIAL( 3)
SURFACE ( 36), SIDE POINTER=( 1)
SURFACE ( 37), SIDE POINTER=(-1)
SURFACE ( 33), SIDE POINTER=(-1)
SURFACE ( 38), SIDE POINTER=(-1)
0000000000000000000000000000000000000000
-----
BODY ( 6)  air around
coll.region for ke
MATERIAL( 4)
SURFACE ( 36), SIDE POINTER=( 1)
SURFACE ( 37), SIDE POINTER=(-1)
SURFACE ( 33), SIDE POINTER=(-1)
SURFACE ( 35), SIDE POINTER=(-1)
BODY ( 5)
0000000000000000000000000000000000000000
-----
BODY ( 37)  guard plate graphite
MATERIAL( 8)
SURFACE ( 11), SIDE POINTER=( 1)
SURFACE ( 15), SIDE POINTER=(-1)
SURFACE ( 34), SIDE POINTER=(-1)
SURFACE ( 39), SIDE POINTER=(-1)
SURFACE ( 44), SIDE POINTER=( 1)
BODY ( 31)
BODY ( 32)
BODY ( 33)
0000000000000000000000000000000000000000
-----

```

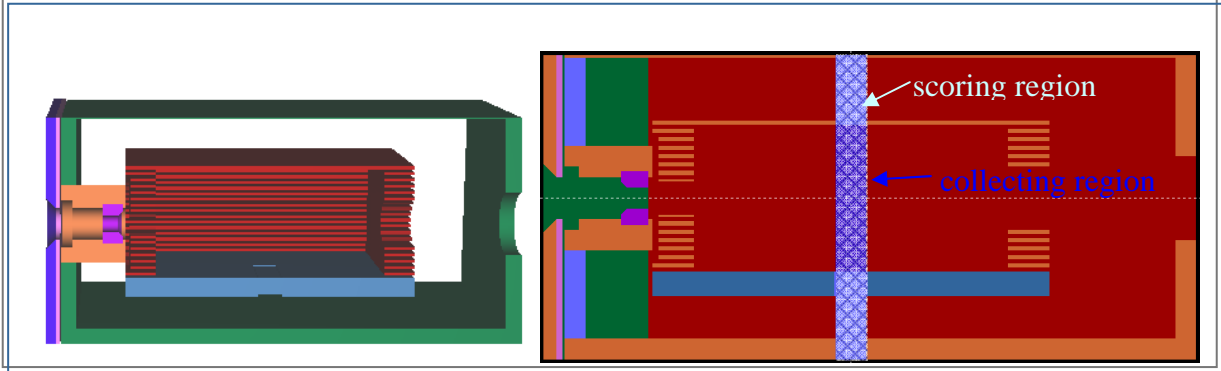


Figure 3.6. A cut-away of the geometry used for Monte Carlo simulations, created using the PENGEOM code of PENELOPE. A 3D representation is shown at the left; the shaded region shown in the 2D representation at the right is identified as the “scoring region” and the blue region at the centre of the air cavity is the “collecting region”, used for the calculation of the correction factors.

A user code was created that calls the subroutine package defined in PENELOPE, follows the particle tracks in the user defined geometry, controls the type of interactions taking place, scores the energy deposited by the particles in the regions and bodies of interest and calculates the correction factors for the standard.

Each particle, its position and the type of interaction taking place are identified by PENELOPE using the parameters KPAR (kind of particle), IBODY (body number defined by the user in the user defined geometry) and ICOL (interaction type), respectively. The parameter ILB is an array of five labels, four of them used by PENELOPE to describe the origin of secondary particles and the interaction mechanism, and the label five can be used by the user to assign flags to the particles to identify them along their tracks.

The simulation is made for mono-energetic photons from 2 keV to 50 keV in steps of 2 keV. A divergent mono-energetic photon beam is defined at 500 mm from the reference plane defined by the aperture; the incident photons crossing the reference plane without interacting in any body of the chamber are identified in the user code as the primary photons. As the primary photons enter in the chamber, appropriate flags are assigned to photons and electrons according the interaction type and the location (body) where the interaction takes place.

The correction factor for electron loss k_e is defined here in terms of the energy deposited by primary electrons and their progeny in the scoring region E_{tot} (energy deposited in the shadow region in Fig 3.6) and the primary energy deposited in the collecting region E_{col} . This can be expressed as

$$k_e = E_{\text{tot}} / E_{\text{col}} \quad (3.8)$$

An appropriate flag is assigned to photons that are scattered within the air volume and the energy deposited in the collecting region by these scattered photons is scored as E_{sc} . Thus, the correction factor for scattered photons k_{sc} is defined in terms of the scattered energy deposited in the collecting region E_{sc} and is expressed as

$$k_{\text{sc}} = E_{\text{col}} / (E_{\text{col}} + E_{\text{sc}}) \quad (3.9)$$

Similarly, the correction factors for fluorescence emission k_{fl} and bremsstrahlung are expressed as

$$k_{\text{fl}} = (E_{\text{col}} + E_{\text{sc}}) / (E_{\text{col}} + E_{\text{sc}} + E_{\text{fl}}) \quad (3.10)$$

$$k_{\text{br}} = (E_{\text{col}} + E_{\text{sc}} + E_{\text{fl}}) / (E_{\text{col}} + E_{\text{sc}} + E_{\text{fl}} + E_{\text{br}}) \quad (3.11)$$

To calculate the diaphragm and the wall transmission correction factors, k_{dia} and k_{wall} , respectively, appropriate flags are assigned to primary photons that interact in the tungsten

aperture and those that are transmitted through the front lead wall of the chamber; scoring the energy deposited by these photons in the collecting region as E_{ap} and E_{wall} , respectively, the correction factors are calculated as

$$k_{\text{ap}} = (E_{\text{col}} + E_{\text{sc}} + E_{\text{fl}} + E_{\text{br}}) / (E_{\text{col}} + E_{\text{sc}} + E_{\text{fl}} + E_{\text{br}} + E_{\text{ap}}) \quad (3.12)$$

$$k_{\text{wall}} = (E_{\text{col}} + E_{\text{sc}} + E_{\text{fl}} + E_{\text{br}} + E_{\text{ap}}) / (E_{\text{col}} + E_{\text{sc}} + E_{\text{fl}} + E_{\text{br}} + E_{\text{ap}} + E_{\text{wall}}) \quad (3.13)$$

Note that equations (3.8)-(3.13) are defined such that their product

$$k_e k_{\text{sc}} k_{\text{fl}} k_{\text{br}} k_{\text{ap}} k_{\text{wall}} = E_{\text{tot}} / (E_{\text{col}} + E_{\text{sc}} + E_{\text{fl}} + E_{\text{br}} + E_{\text{ap}} + E_{\text{wall}}) \quad (3.14)$$

is strictly the desired quantity.

The results for mono-energetic photons were folded with measured and simulated spectra for the BIPM low-energy x-ray reference qualities. The results of these calculations for the various correction factors are in close agreement with similar calculations for the existing standard [18, 19], at the level of 3 parts in 10^4 .

3.6. Comparison with the existing standard

The L-02 chamber was initially mounted with an aluminium collector C1 of 15.464 mm, which defines a collecting volume of 1214.09 mm³. A simple arrangement was designed to fix the collector at the desired height, with no possibility of micrometric adjustment. The coplanarity between the guard plate and the collector was checked with the three dimensional coordinate measuring machine, initially with an accepted tolerance of 50 μm . A thermistor was positioned at one of the lateral sides, between the wall and the guard strips, at the positioned of the eighth guard strip. With this configuration, the new standard was positioned on the calibration bench for the tungsten-anode x-ray tube at the reference distance of 500 mm from the tube centre. The new standard was compared with the existing primary standard L-01, at the five CCRI reference qualities. Measurements were made while applying a polarizing voltage of 1500 V, positive polarity and a pre-measured polarity correction factor k_{pol} was applied to the measured current. The ratios of the currents per unit of volume measured with the standards, corrected by the corresponding k_{pol} , were calculated for each radiation quality. The results of this comparison are shown in Table 3.2.

Table 3.2. Response of the FAC-L-02

Radiation quality	10 kV	30 kV	25 kV	50 kVb	50 kVa
$(I/V)_{L-02} / (I/V)_{L-01}$	1.0045	1.0050	1.0040	1.0035	1.0040

These discrepancies of the order of 4 parts in 10^3 motivated a series of studies that are described in the following paragraphs.

Polarity effect

Measurements with both polarities were made on repeated occasions for all the qualities. The ratios of the currents I_+/I_- were stable at the level of 2 parts in 10^4 ; a correction factor k_{pol} of 1.0004(2) was calculated and applied to the measured current with positive polarity.

Ion recombination

The ion recombination correction of 1.0007(1) for L-01 was applied initially to the new standard L-02 assuming that the same recombination exists for both free air chambers. To determine if the discrepancies observed between the standards could be explained by a different recombination process, this correction was measured for L-02 using the method described previously on two different occasions. The ion recombination correction determined for L-02 was 1.0010 (1).

Temperature

A study of the temperature measurement and its stability inside the chamber was made by adding a second thermistor in the centre of the collecting air volume. The position of the chamber thermistor was chosen in order to minimize the temperature difference measured by each thermistor. Initially, the thermistor was positioned between the right side wall and the eighth guard strip, axially centred. At this position the measured temperature was on average 0.04 °C higher than measured with the thermistor placed in the collecting volume. The thermistor was then placed in different locations inside the chamber; the smallest discrepancy between the measured temperatures was identified when the thermistor was positioned just

above the high-voltage plate, laterally centred, 20 mm behind the front wall; in this new position, the temperatures agreed at the level of 1 part in 10^4 .

Field distortion

Another cause of the discrepancies between the standards could have been distortions in the electric field. Perturbations in the electric field can be caused by the shielding box, the spacers between the guard strips and a difference in the potentials of the collecting electrode and guard plate. Measurements of current were made with the standard L-02 without the side walls and with the top lid of the chamber removed, leaving just the guard strips and high-voltage plate for an otherwise completely open chamber. Another series of measurements was made by adding additional spacers between the guard strips; the measured effects using the chamber in these two configurations with respect to the reference configuration were of the order of the uncertainties associated with the measurements, 2 to 3 parts in 10^4 . The effect of a difference in potentials between the collector and guard plate was studied by applying a few volts to the guard plate while maintaining the collector at ground potential. The result is presented in Table 3.3.

Table 3.3. Effect of contact potentials between collector and guard plate

	I_+ / I_{+ref}	I_- / I_{-ref}	$I_{mean} / I_{mean, ref}$
Ground potential I_{ref}	1	1	1
-0.1 mV	1.0019	0.9981	0.9999
+0.1 mV	0.9981	1.0017	1.0000
-0.1 mV	1.0022	0.9984	1.0003

The measured effect is of the order of 0.2% when 0.1 mV is applied to the guard plate, measured with positive polarity, and it has the opposite effect when the chamber polarity is reversed. Consequently, the effect is eliminated by taking the mean response.

Diaphragm comparison and field size effect

When comparing free air chambers, a cause of discrepancy of the order of up to 3 parts in 10^3 may arise from the different diaphragms of the standards, if no proper correction factor k_{dia} is applied. To evaluate this effect, a diaphragm comparison was made by replacing the L-02

diaphragm (dia-02) by the one used in the L-01 standard (dia-01). The diaphragm dia-01 defines a collecting volume V_1 of 1205.9 mm³ while the volume V_2 defined by the diaphragm dia-02 is 1219.8 mm³ (using a collector of 15.537 mm). As this effect is energy dependent, the comparison was repeated for four different qualities. Table 3.4 summarizes the results of the ratio $(I/V_2)_{\text{dia-02}} / (I/V_1)_{\text{dia-01}}$ measured with L-02 and demonstrates that the diaphragm is not in question.

Table 3.4. Effect of different diaphragms in FAC-L-02

Radiation quality	10 kV	30 kV	25 kV	50 kVb
$(I/V_2)_{\text{dia-02}} / (I/V_1)_{\text{dia-01}}$	1.0007(3)	1.0004(2)	1.0003(2)	1.0001(2)

The response of a free air chamber is expected to be insensitive to different field sizes, or to have a negligible dependence due to different scatter radiation contribution when changing the field size. This was confirmed for both free air chambers when the reference beam of 8.5 cm diameter at the reference plane was reduced to 4.5 cm diameter by placing a lead collimator in the beam axis. Table 3.5 shows the results.

Table 3.5. Effect of field size

Radiation quality	10 kV	30 kV	25 kV	50 kVb	50 kVa
$(I_{\text{large field}} / I_{\text{small field}})_{\text{L-01}}$	1.0009(2)	1.0007(2)	1.0004(2)	1.0003(2)	1.0006(2)
$(I_{\text{large field}} / I_{\text{small field}})_{\text{L-02}}$	1.0010(2)	1.0007(2)	1.0004(2)	1.0007(2)	1.0005(2)

Volume determination

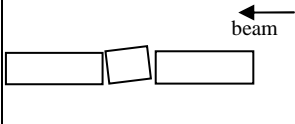
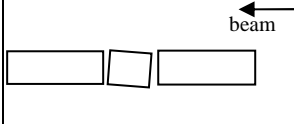
To determine if the discrepancies observed between the two standards were due to the volume determination, the chamber was dismantled and the collector C1 was replaced on several occasions by two aluminium collectors, C2 and C3, of 15.294 mm and 15.705 mm, respectively, over a period of 14 months. The comparison with L-01 was repeated for these two new configurations, accepting each time the same tolerance of 50 µm for the co-planarity between the collector and the guard plate. Table 3.6 summarizes the results for each collector.

Table 3.6. Effect of different collector sizes

$(I/V)_{L-02} / (I/V)_{L-01}$					
collector	10 kV	30 kV	25 kV	50 kVb	50 kVa
C1	1.0045	1.0050	1.0040	1.0035	1.0040
C2	1.0054	1.0052	1.0053	1.0047	1.0055
C3	1.0056	1.0051	1.0048	1.0044	1.0042
C1	1.0085	1.0083	–	–	1.0068
C2	–	1.0097	1.0089	–	–
C1	0.9976	0.9955	0.9983	0.9963	0.9970

All the studies described previously were made in parallel, and on repeated occasions, with this study of volume determination. None of the experiments performed could explain the initial discrepancy, which was unstable and even increased to as much as 1 part in 10^2 . As mentioned before, each time that the chamber was dismantled and reassembled, the planarity of the collector-guard plate was checked using the CMM and a tolerance of 50 μm was accepted, partly because the collector support did not allow a better collector height adjustment. To examine the effect of the mechanical tolerance, the upstream edge of the collector was raised and lowered by around 150 μm and 250 μm , respectively, with respect to the guard plate, as shown in Table 3.7, together with the results.

Table 3.7. Effect of the non co-planarity between collector and guard plate

	$(I/V)_{L-02} / (I/V)_{L-01}$		$(I/V)_{L-02} / (I/V)_{L-01}$
+150 μm	1.0247(5)	-250 μm	0.9809(5)
+160 μm	1.0242(5)	-260 μm	0.9799(5)

This displacement of the collector resulted in discrepancies of up to 2.5 parts in 10^2 , indicating that the tolerance of 50 μm was too high and might explain the fluctuating results. A new collector support was designed that allowed the collector to be adjusted to better than 5 μm with respect to the guard plate. The collector and guard plate, both of aluminium, were cleaned and mounted again with the new support. With this configuration, the discrepancy

between the standards was reduced to 1 part in 10^3 , but it was not stable, increasing to 4 parts in 10^3 three months later with no change in the co-planarity. This change in the response can be explained by oxidation of the aluminium surfaces of the collector and guard plate. Finally, once the collector and guard plate were thinly coated with graphite the discrepancy was reduced again to 1 part in 10^3 and has since remained constant. It is also notable that the polarity effect, previously measured consistently as 1.5 parts in 10^3 , was reduced to below 1 part in 10^4 following the graphite coating.

3.7. Conclusions

A new primary standard, constructed at the BIPM, has been designed for the dosimetry of low-energy x-ray beams operating up to 50 kV. It is now the reference standard accepted by the CCRI for international dosimetry comparisons in mammography radiation beams. The original reference standard for low-energy beams was constructed at the BIPM in 1963 and the experience gained in building and characterizing a new standard now, together with all the studies performed to identify and resolve the initial discrepancies between the two BIPM standards is being used to help some national metrology institutes with their projects to develop similar primary standards.

Chapter 4. Establishment of mammography radiation qualities

4.1. Introduction

Mammography is a method that uses x rays to produce images that provide maximum visualization of breast anatomy and the signs of disease needed for an accurate diagnosis. The most common x-ray tubes used for mammography are those with a molybdenum anode combined with molybdenum filtration, operated in the range from 20 kV to 40 kV. Because of the risk of radiation-induced carcinogenesis associated with an x-ray examination, it is essential to minimize the radiation dose delivered to the breast. Therefore, an accurate calibration of the x-ray beams is needed in order to avoid subjecting the patient to unnecessary radiation. The instruments used in the diagnostic radiology departments to calibrate the radiation beams are commercial ionization chambers; as these detectors are not absolute, they need to be calibrated and characterized at standard reference laboratories for radiation dosimetry; the calibration should be made preferably in the same type of radiation beams as used for diagnosis as these types of detectors are generally energy dependent and may have different responses to different radiation beams. The reference laboratories which provide the calibration service to the diagnostic departments are usually part of the National Metrology Institute (NMI) of each country or at least traceable to the NMI. Those laboratories with primary standards for radiation dosimetry participate in the ongoing comparisons organized by the Bureau International des Poids et Mesures (BIPM) to verify the accuracy of their measurements while those with national secondary standards send their instruments to the BIPM for calibration and thus, they are traceable to the SI units through the BIPM.

The BIPM has carried out low-energy x-ray comparisons and calibrations since 1966 in the range from 10 kV to 50 kV, using a tungsten-anode x-ray tube with Al filters. In 2001, the CCRI requested the BIPM to extend these activities to mammography, to meet the needs of the NMIs for comparisons in this newly regulated domain and to provide SI traceable calibrations. The BIPM began this work by establishing a set of nine radiation qualities using the existing tungsten-anode x-ray tube with molybdenum and rhodium filters to simulate the

radiation beams used in clinical mammography, described in Chapter 2 “Establishment of simulated mammography radiation qualities using a tungsten target x-ray tube with molybdenum and rhodium filters” [10]. In 2009, a molybdenum-anode x-ray tube was installed in the low-energy x-ray laboratory at the BIPM; the existing calibration bench was used to support the new x-ray tube and a high precision translation table. The latter serves to position the new primary standard and the transfer chamber on the beam axis. The new primary standard, described in Chapter 3 “Design and construction of a primary standard for mammography dosimetry”, has now been installed as a permanent facility and it was used to establish a set of four radiation qualities as reference beams for mammography comparisons and calibrations. Five comparisons of primary standards for air kerma have been made in the new set of reference radiation beams with the NMIJ (Japan), NIST (USA), PTB (Germany), VNIIM (Russian Federation) and the IAEA (Vienna), while calibrations of national secondary standards have been made for the NIM (China), HIRCL (Greece), ININ (Mexico) and the CMI (Czech Republic).

4.2. Establishing new radiation beams: determination of the beam quality and the air kerma rate

4.2.1. The BIPM irradiation facility

It was explained in Chapter 2, different x-ray spectra can be generated depending on the target material of the x-ray tube and the filtration added in the beam; for a particular application, the contribution of bremsstrahlung and characteristic radiation to the generated spectrum can be modified significantly by a suitable combination of target material and filter, mammography being a clear example that requires a spectrum with negligible bremsstrahlung contribution. The most appropriate spectra for mammography are thus obtained with target materials of low atomic number like molybdenum or rhodium to reduce bremsstrahlung production and appropriate filtration to attenuate both very low and unwanted high-energy x rays. Reference standard dosimetry laboratories are implementing radiation qualities similar to the beams used in mammography using Mo-anode x-ray tubes to provide calibrations of the radiation instruments for their clinical diagnostic departments; the reference laboratories belonging to the NMIs asked the BIPM also to establish reference mammography radiation qualities and set a new key comparison to validate primary determinations of air kerma and to provide SI traceable calibrations of national standards in this domain.

Following this request, a Mo-anode x-ray tube has been installed in the low-energy x-ray laboratory at the BIPM, sharing the facilities with the W-anode x-ray tube. The existing high-voltage generator, voltage stabilization and anode current measuring system, already described in Chapter 2, are used for both tubes. As the measured anode current is used to normalize for any small deviation from the reference anode current, no transmission ionization chamber is needed to monitor the stability of the radiation output. A new cooling system was installed and also serves both x-ray tubes. The Mo-anode tube is operated in the range from 20 kV to 40 kV; its specification is given in Table 4.1.

Table 4.1. Main characteristics of the Mo-anode x-ray tube

Tube MXR-101 Mo COMET	
Nominal x-ray tube voltage	100 kV
Max. tube current at nominal voltage	10 mA
Power	1 kW
Inherent filtration (window)	0.8 mm Be
Target angle	40°
Focal spot diameter	5.5 mm

The irradiation area is temperature controlled at around 20 °C; two thermistors, calibrated by the BIPM to a few mK, measure the temperature of the ambient air and the air inside the BIPM standard used for the dosimetry of the x-ray qualities. Air pressure is measured by means of a BIPM-calibrated barometer positioned at the height of the beam axis. The relative humidity in the laboratory is controlled within the range 47 % to 53 %.

4.2.2. Mo-anode x-ray tube and calibration bench

The existing calibration bench was used to support the Mo-tube (with the radiation beam projected in the opposite direction to that generated by the W-tube) and also to support a high precision translation table, connected to a motion control device. The tube remains in a fixed position while the translation table enables the alternate positioning on the beam axis of the standard and a transfer instrument. The conditions of the measurements were chosen with the CCRI to be similar to those used at the NMIs: the reference plane at 600 mm from the tube

centre and a circular field of 100 mm diameter at the reference plane. An aluminium housing was placed around the tube with a holder to position the filters; this holder, which also serves to position a laser, fixes the filters parallel to the x-ray tube window. A reference axis was defined mechanically, passing from the centre of the tube window through the filter/laser support and perpendicular to them. A laser beam was aligned to the mechanical axis.

4.2.3. The BIPM standard for mammography qualities

The BIPM standard used for the dosimetry of the Mo-anode radiation qualities is a free-air chamber of the conventional parallel-plate design, identified as L-02. A full description of a free-air chamber is presented in chapter 3 “Design and construction of a primary standard for mammography”. The measuring volume V is defined by the diameter of the chamber aperture and the length of the collecting region. The main dimensions, the measuring volume and the polarizing voltage for the standard are shown in Table 4.2.

Table 4.2. Main characteristics of the standard

Standard	L-02
Aperture diameter / mm	9.998
Air path length / mm	100.2
Collecting length / mm	15.537
Electrode separation / mm	70
Collector width / mm	70
Measuring volume / mm ³	1 219.8
Polarizing voltage / V	1 500

In order to calculate the correction factors to be applied to the standard for the air kerma determination K_{air} , a detailed simulation of the chamber was made using the Monte Carlo code PENELOPE; the correction factors were calculated using the same code for mono-energetic photons from 2 keV to 50 keV, with step of 2 keV; a detailed description of the calculations as well as the chamber simulation is given in Chapter 3.

The standard was positioned on the translation table, with its reference plane defined by the diaphragm at 600 mm from the tube centre. The height and the vertical and horizontal angles

were adjusted so that the laser beam passes through the centre of the entrance and exit apertures of the standard.

4.2.4. Radiation beam

The shape, size and orientation of the radiation field were studied using radiographic films. A set of radiographic films of the focal spot were used to study the direction of the x-ray beam; the images were obtained by placing a lead pinhole collimator on the filter support. The tube was rotated to align the image of the focal spot with the mechanical axis at the reference distance. The field size, defined by the 50 % of the photon fluence rate at the centre of the circular field, was measured ionometrically using a thimble type ionization chamber.

The first set of radiographic films showed an elliptical radiation field of major axis 150 mm and minor axis 110 mm. In order to have a circular radiation field of 100 mm diameter, a system of two collimators was designed and machined; to reduce the radiation field to a circular shape of about 10 cm diameter at the reference distance, a tungsten collimator was placed next to the exit window of the x-ray tube. Horizontal and vertical beam profiles measured with an ionization chamber showed that a second collimator was necessary to have the desired beam size at the reference distance. The diameter and position of the second collimator was defined from the following profile measurements.

Horizontal and vertical beam profiles were measured using a thimble NE2571 ionization chamber, placed at the reference plane of measurements. Chamber displacements of 10 mm were made around the beam axis to measure the photon fluence rate and determine the field size, being defined as the distance from the beam axis at which the fluence rate attenuates to 50 %. The beam profiles are shown in Figure 4.1.

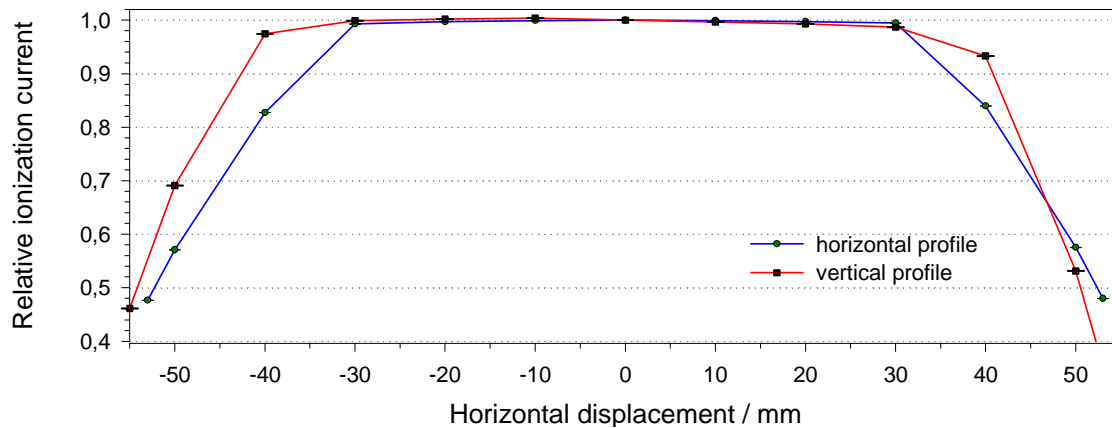


Figure 4.1. Horizontal and vertical beam profiles

4.2.5. New radiation qualities

Following the recommendations made by the CCRI(I) during the 19th meeting in 2009, four radiation qualities, similar to those used in clinical mammography, were set up as reference beams for comparisons and calibrations; the characteristics of the beams are described in Table 4.3.

Table 4.3. Characteristics of the reference radiation beams for mammography

Radiation quality	Mo25	Mo28	Mo30	Mo35
Generating potential / kV	25	28	30	35
Additional filtration	30 μ m Mo			
Al HVL / mm	0.277	0.310	0.329	0.365

Half value layer

The beam quality, expressed in terms of the half-value layer (HVL), was determined for each beam using the new primary standard L-02. The HVL was determined from the air kerma rate measured with no added attenuator in the beam and for 3 different combinations of attenuators placed on the beam axis; the attenuated air-kerma rate values were normalized to the value measured with no attenuator, and they were plotted as a function of the corresponding attenuator thickness as illustrated in Figure 4.2 for the quality corresponding to a generating voltage of 25 kV. The data were fitted using a linear regression and a quadratic fit constrained to unity for zero thickness. The HVL for each radiation quality, derived from

both fits, differs by less than $0.5 \mu\text{m}$. The uncertainty arising from the fitting procedure is taken as the root mean square deviation of the measured values from the fitted line. This is evaluated as 1 part in 10^4 .

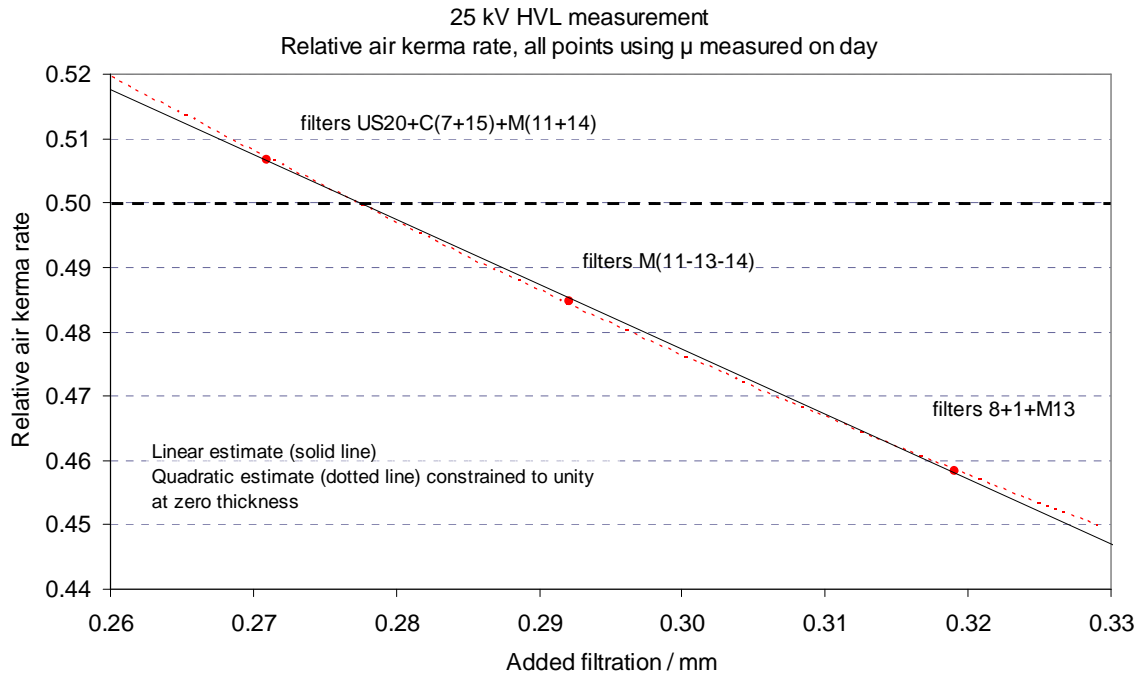


Figure 4.2. Half value layer determination using BIPM coded filters

4.2.6. Measurement and simulation of energy spectra

The photon energy spectra were measured using the Compton scattering method, described in Chapter 2 for the W-Mo beams: a scatterer is placed in the primary beam at the reference distance; the scattered photons are detected at an angle of 90° with a low-energy germanium detector coupled to a multichannel analyser. The primary beam is then reconstructed from the measured pulse height distribution using a commercial software.

The mammography spectra corresponding to the qualities Mo25 and Mo30 were also simulated using the Monte Carlo code PENELOPE. The geometry package PENGEOEM was used for the simulation of the tube target, collimation and filter. Details of the simulation method are described in Chapter 2.

The spectrum corresponding to the quality Mo30 measured with the Compton spectrometer is shown in Figure 4.3, together with that calculated using the PENELOPE code.

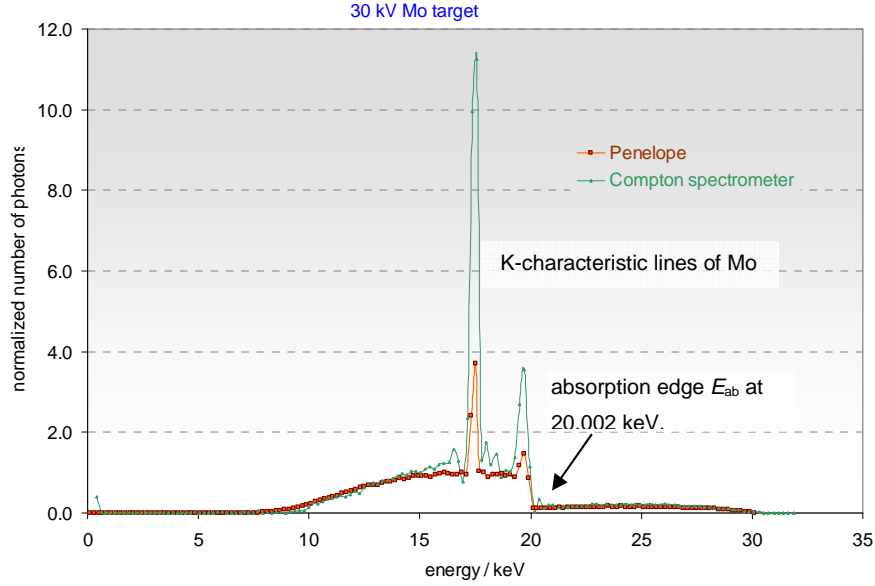


Figure 4.3. Comparison of the simulated and measured spectra for the Mo30 quality

4.2.7. Determination of the air-kerma rate

The air kerma rate was measured using the standard L-02 under the reference conditions described in [16] with the critical positional details reproduced here. The reference plane for the standard was positioned at 600 mm from the radiation source, with a reproducibility of 0.03 mm. The standard was aligned on the beam axis to an estimated uncertainty of 0.1 mm. The beam diameter in the reference plane is 100 mm for all radiation qualities.

For a free-air ionization chamber standard with measuring volume V , the air-kerma rate is determined by the relation

$$\dot{K} = \frac{I}{\rho_{\text{air}} V} \frac{W_{\text{air}}}{e} \frac{1}{1 - g_{\text{air}}} \prod_i k_i \quad (4.1)$$

where ρ_{air} is the density of air under reference conditions, I is the ionization current under the same conditions, W_{air} is the mean energy expended by an electron of charge e to produce an ion pair in air, g_{air} is the fraction of the initial electron energy lost by bremsstrahlung production in air, and $\prod k_i$ is the product of the correction factors to be applied to the standard.

The correction factors for the standard involved in the determination of K_{air} are listed in Table 4.4. The factors for electron loss k_e , photon scatter k_{sc} , fluorescence k_{fl} , the combined

effect of photon transmitted through the diaphragm and scattering and fluorescence photons produced in the diaphragm k_{dia} and front wall transmission k_{wall} were obtained from the calculated factors for mono-energetic photons convoluted with the molybdenum spectra measured with the BIPM Compton spectrometer. These factors were also evaluated using the simulated spectra for the qualities Mo25 and Mo30; despite evident differences in the spectra around the characteristic peaks of Mo (Figure 4.3), the correction factors for the standard were identified as insensitive to these differences. The corrections due to the polarity effect and lack of saturation were obtained from measurements, as described in Chapter 3. No distortion of the electric field near the collecting volume was observed from the simulation made with the software Quick Field; therefore, a unity correction factor was adopted for k_{d} . The air attenuation correction k_{a} was calculated from the measured mass attenuation coefficients $(\mu/\rho)_{\text{air}}$ for each quality using the reduced air pressure pipe method described in Chapter 3.

Table 4.4. Correction factors for the BIPM standard FAC-L-02

Correction factor	Radiation quality			
	Mo25	Mo28	Mo30	Mo35
Scattered radiation k_{sc}	0.9977	0.9977	0.9978	0.9978
Fluorescence k_{fl}	0.9975	0.9976	0.9976	0.9977
Electron loss k_{e}	1.0000	1.0000	1.0000	1.0000
Saturation k_{s}	1.0015	1.0015	1.0015	1.0015
Polarity k_{pol}	1.0000	1.0000	1.0000	1.0000
Air attenuation $k_{\text{a}}^{(1)}$	1.0269	1.0244	1.0233	1.0212
Wall transmission k_{p}	1.0000	1.0000	1.0000	1.0000
Field distortion k_{d}	1.0000	1.0000	1.0000	1.0000
Diaphragm correction k_{dia}	0.9996	0.9995	0.9995	0.9995

⁽¹⁾ Values at 293.15 K and 101.325 kPa for an attenuation length of 10.0 cm.

The anode current for each quality was chosen to give an air-kerma rate of 2 mGy s⁻¹ in the reference plane.

The uncertainties associated with the primary standard L-02 are listed in Table 4.5. The uncertainties for the physical constants are those internationally accepted as advised by the CCRI [22]. The Type B uncertainty values in the second column for the correction factors are based on best estimates derived using different parameters in the MC calculations and different MC codes, while the Type A uncertainty values in the first column are all based on measurement uncertainties.

Table 4.5. Relative standard uncertainties in the BIPM determination of air-kerma rate for mammography x-ray qualities

Symbol	Parameter / unit	Relative standard uncertainty	
		$s_i^{(1)}$	$u_i^{(2)}$
Physical constants			
ρ_a	dry air density (0°C, 101.325 kPa) / (kg m ⁻³)	–	0.01
W/e	mean energy per charge / (J C ⁻¹)	–	0.15
g	fraction of energy lost in radiative processes	–	0.01
Correction factors			
k_{sc}	scattered radiation	–	0.03
k_{fl}	fluorescence	–	0.05
k_e	electron loss	–	0.01
k_s	saturation	0.01	0.01
k_{pol}	polarity	0.01	–
k_a	air attenuation	0.02	0.01
k_d	field distortion	–	0.07
k_{dia}	diaphragm	–	0.03
k_p	wall transmission	0.01	–
k_h	humidity	–	0.03
Measurement of I/v			
I	ionization current (T, P , air compressibility)	0.02	0.02
v	Volume /cm ³	0.03	0.05
	positioning of standard	0.01	0.01
Combined uncertainty of the BIPM determination of air-kerma rate			
	quadratic summation	0.05	0.19
	combined relative standard uncertainty		0.20

⁽¹⁾ s_i represents the relative standard Type A uncertainty, estimated by statistical methods;

⁽²⁾ u_i represents the relative standard Type B uncertainty, estimated by other means.

4.3. Conclusions

Following the recommendations of the CCRI(I), a set of four radiation qualities was set up at the BIPM as reference beams for mammography using a Mo-anode x-ray tube and Mo filtration. These qualities, similar to those established in national standards laboratories, are used to compare their primary standards and to calibrate national secondary standards for other countries, thus providing SI traceability for mammography dosimetry.

Chapter 5. A study of the response of commercial ionization chambers to mammography beams

5.1. Introduction

Mammography is an x-ray examination that requires a good image quality to detect non-palpable, subtle breast cancers while keeping the radiation dose delivered to the breast as low as possible to avoid radiation-induced carcinogenesis. As the glandular tissue of the breast is more radiosensitive than the other tissues of the breast (adipose and fibrous tissues and skin), the estimation of the mean glandular dose (MGD) is the specific dose quantity used in mammography and is the best indicator of the risk to the patient [31, 32]. It is defined as the mean dose to the glandular tissue within the breast and is determined by following a standard two-step protocol [6]:

1. The first step is to determine the beam output (incident air kerma K_{air}) in given reference conditions. This can be determined from measurements made using dosimeters (ionization chambers and electrometer) designed for this application.
2. Then, the MGD is determined by multiplying the incident air kerma value by published dose-conversion factors, calculated using Monte Carlo techniques. The dose factor values are tabulated according to the breast size and composition and the penetrating characteristics of the x-ray beam, i.e. its quality in terms of half-value-layer (HVL), as determined by the anode material, filtration, and generating potential.

The incident air kerma K_{air} is defined as the air kerma from an incident x-ray beam measured on the central beam axis at the position of the patient or phantom⁵ surface (but without the patient or phantom so with no backscatter) and is calculated using the relationship

$$\dot{K}_{\text{air}} = MN_{K,Q_0} \Pi k_i \quad (5.1)$$

where M is the reading of the dosimeter, N_{K,Q_0} is the calibration coefficient of the dosimeter in terms of air kerma obtained from a standard reference laboratory for the radiation quality Q_0 ,

⁵ In diagnostic radiology, a phantom is a block of perspex or water equivalent material to simulate relevant parts of the human body, for the purposes of dosimetry measurements.

and Πk_i is the product of some correction factors to be applied to the reading M . Correction factors may be needed as the calibration coefficient refers only to the reference conditions of calibration whereas a different radiation quality Q , temperature, pressure, polarity, field size, etc., will have an effect.

The dose-conversion factors which relate the incident air kerma to the mean glandular dose have a marked dependence on the x-ray beam quality, expressed in terms of the half-value-layer (HVL). They are tabulated as a function of the compressed breast thickness and the HVL. The HVL is usually calculated from measurements made with an ionization chamber, preferably with a weak energy dependence, to achieve the required accuracy for the beam characterization [5] and so minimize errors in the determination of the MGD; as an example, for a breast thickness of 6 cm, variations of the order of 0.02 mm Al in the HVL determination represent a change of up to 5% in the dose-conversion factor.

The ionization chambers used in diagnostic x-ray departments need to be characterized and calibrated in standard reference dosimetry laboratories. This should be preferably in the same type of beams as used for diagnostic imaging as the chambers can have not only a non-negligible energy dependence, but also a different response to different spectra even in the same energy range.

At present, not all the national reference standard dosimetry laboratories can provide calibrations of ionization chambers in the type of beams used in mammography. For those laboratories not equipped with clinical mammography x-ray tubes, calibration in another type of beam, such as those described in Chapter 2 “Establishment of simulated mammography radiation qualities using a tungsten target x-ray tube with molybdenum and rhodium filters”, is also possible if the chamber response to different spectra and its energy dependence are known and properly considered when the chamber is used to determine the radiation beam output in the diagnostic departments. To take into account the effects of the difference between the reference beam quality Q_0 used for a chamber calibration at the reference laboratory and the actual beam quality Q , a correction factor k_{Q,Q_0} is introduced in (5.1) and an additional uncertainty is included in the evaluation on the dosimetry calibration uncertainty budget.

Various ionization chambers used for mammography can have a marked energy dependence. Bearing in mind that the total expanded uncertainty accepted in mammography dosimetry is

8 % ($k = 2$) [6], it is considered that a variation of 2 % is the acceptable limit for the energy dependence of an ionization chamber used to calibrate the radiation beams [5].

5.2. Calibration of ionization chambers

5.2.1. Ionization chambers

Several commercial ionization chamber types are used in mammography to determine the beam output, mostly being of a plane-parallel chamber design. These chambers use two parallel, flat electrodes, separated by a few millimetres; they vary in composition, volume and geometry and each of these characteristics has an effect on the response of the chambers to different radiation beams.

Four ionization chambers currently used are of the type: Radcal RC6M, Exradin A11TW, Exradin Magna 92650 and PTW 34069. The main characteristic of these chambers, as presented by the manufacturers, is the flat energy response in the energy range used in mammography but the sensitivity and response to different radiation spectra need to be investigated to determine the “flatness” of each chamber’s energy response. Consequently, one instrument of each type has been selected to study their response to both the W/Mo and Mo/Mo beams.

The Radcal and Exradin A11TW chambers belong to the BIPM; the Exradin Magna and the PTW chambers are the reference secondary standards of two National Metrology Institutes and they were sent to the BIPM for characterization and calibration in the reference radiation beams for mammography. The main characteristics of the chambers are listed in Table 5.1.

Table 5.1. Main characteristics of the ionization chambers

Chamber type	Radcal RC6M	Exradin A11TW	Exradin Magna 92650	PTW 34069
Window / mg cm^{-2}	0.7 metalized polyester	3.8 Kapton	3.8 Kapton	38 PMMA ¹ , 0.06 graphite
Collector diameter / mm	29.7	20.0	20.0	30
Cavity height / mm	8.7	3.0	8.0	8.4
Nominal volume / cm^3	6	0.9	3	6
Polarizing potential / V	-300	-300	+200	+200

¹ Polymethyl Methacrylate

The ionization chambers were calibrated in terms of air kerma in the previously characterized W/Mo and Mo/Mo beams at the BIPM.

The air-kerma rate is determined using the BIPM primary air-kerma standards through the measurement equation

$$\dot{K} = \frac{I}{\rho_{\text{air}} V} \frac{W_{\text{air}}}{e} \frac{1}{1 - g_{\text{air}}} \prod_i k_i \quad (5.2)$$

where V is the measuring volume, ρ_{air} is the density of air under reference conditions, I is the ionization current under the same conditions, W_{air} is the mean energy expended by an electron of charge e to produce an ion pair in air, g_{air} is the mean fraction of the initial electron energy lost by bremsstrahlung production in air, and $\prod k_i$ is the product of the correction factors to be applied to the standards. The BIPM standards, identified as L-01 and L-02, are used for the air kerma determination of the W/Mo and Mo/Mo beams, respectively; they are described in [8] and in Chapter 3 “Design and construction of a primary standard for mammography dosimetry”, respectively. The main dimensions, the measuring volume and the polarizing voltage for each standard are shown in Table 5.2.

Table 5.2. Main characteristics of the BIPM primary standards

Standard	FAC-L-01	FAC-L-02
Aperture diameter / mm	9.941	9.998
Air path length / mm	100.0	100.2
Collecting length / mm	15.466	15.537
Electrode separation / mm	70	70
Collector width / mm	71	70
Measuring volume / mm ³	1 200.4	1 219.8
Polarizing voltage / V	1 500	1 500

The calibration coefficient N_K for an ionization chamber is given by the relationship

$$N_K = \frac{\dot{K}}{I_{\text{ch}}} \quad (5.3)$$

where \dot{K} is the air-kerma rate determined by the standard (5.2) and I_{ch} is the ionization current measured by the chamber using the associated current-measuring system. The current I_{ch} is normalized to the standard conditions of air temperature and pressure chosen for the calibrations ($T = 293.15 \text{ K}$, $P = 101\,325 \text{ Pa}$) and is measured in a relative humidity of 50 %.

5.2.2. Irradiation facilities and radiation qualities

The BIPM low-energy x-ray laboratory houses a high voltage generator, a tungsten-anode x-ray tube with an inherent filtration of 1 mm beryllium and a molybdenum-anode x-ray tube with an inherent filtration of 0.8 mm beryllium. A voltage divider is used to measure the generating potential, which is stabilized using an additional feedback system. Rather than use a transmission monitor, the anode current is measured and the ionization chamber currents are normalized for any deviation from the reference anode current. The resulting variation in the BIPM free-air chamber currents over the duration of the calibrations are normally not more than 3×10^{-4} in relative terms.

The irradiation area is temperature controlled at around 20 °C and is stable over the duration of a calibration to better than 0.2 °C. The temperature of the air inside each BIPM standard is measured using their respective thermistors whereas the ambient air temperature is measured with a thermistor positioned on each calibration bench between the standard and the chamber under calibration. All the thermistors are calibrated to a few mK. Air pressure is measured by means of a calibrated barometer positioned at the height of the beam axis. The relative humidity is controlled within the range 47 % to 53 % and consequently no humidity correction is applied to the current measured using transfer instruments.

A combination of the tungsten anode with a molybdenum filter of 0.06 mm thickness and different tube voltages were used to simulate clinical mammography radiation beams. The establishment of the W/Mo radiation qualities is described in Chapter 2 “Establishment of simulated mammography radiation qualities using a tungsten target x-ray tube with molybdenum and rhodium filters”. The molybdenum anode x-ray tube with molybdenum filter of 0.03 mm thickness was used for the mammography radiation qualities, as described in Chapter 4 “Establishment of mammography radiation qualities”.

Information on the measuring conditions used for calibration of ionization chambers at the BIPM is detailed in [16].

The characteristics of the radiation beams used for the calibration of the chambers are listed in Table 5.3 and Table 5.4 for the W/Mo and Mo/Mo qualities, respectively.

Table 5.3. Characteristics of the W/Mo radiation qualities

Radiation quality	M23	M25	M28	M30	M35
Generating potential / kV	23	25	28	30	35
Additional filtration	60 μ m Mo				
HVL / mm Al	0.332	0.342	0.356	0.364	0.388

Table 5.4. Characteristics of the Mo/Mo radiation qualities

Radiation quality	Mo25	Mo28	Mo30	Mo35
Generating potential / kV	25	28	30	35
Additional filtration	30 μ m Mo			
HVL / mm Al	0.277	0.310	0.329	0.365

5.2.3. Positioning of the ionization chambers

The reference planes of measurements are 500 mm from the exit window and 600 mm from the tube centre of the W-anode and Mo-anode x-ray tubes, respectively. The red line around the Radcal chamber, quoted as 8.5 mm behind the front surface of the chamber body, was placed in the reference plane. The reference plane of the Exradin A11TW chamber was taken as 1.5 mm behind the front surface of the chamber body and for the Exradin Magna it was the entrance window itself. The reference plane for the PTW chamber was taken as 4.83 mm behind the window, corresponding to half of the external dimension of the chamber body. The distance was measured to around 0.02 mm. The chamber centre was taken to be at the centre of each circular entrance window. Alignment of each reference plane point on the beam axis was measured to around 0.1 mm.

5.2.4. Charge measurement and leakage

The charge collected by the chambers was measured using the BIPM electrometer, following a pre-irradiation of at least 20 minutes. The measured ionization currents are corrected for

current leakage. This correction varied depending on chamber type but was always less than 5×10^{-4} in relative value. The appropriately related uncertainty is included in each uncertainty budget.

5.2.5. Radial non-uniformity correction

The beam diameter in the reference plane is 84 mm and 100 mm for the W/Mo and Mo/Mo beams respectively. For the Radcal and PTW chambers, with cavity diameter 30 mm, the correction factor $k_{rn} = 1.0022$ is applied for the radial non-uniformity to the measured current in the W/Mo beams; for the Mo/Mo beams, this correction is $k_{rn} = 1.0006$. The radial non-uniformity correction of the W/Mo and Mo/Mo beams for the Exradin chambers, with cavity diameter 23 mm, is $k_{rn} = 1.0012$ and $k_{rn} = 1.0003$, respectively. A relative standard uncertainty of 2×10^{-4} is introduced to account for the uncertainty of these values.

5.2.6. Reproducibility of the ionization chamber measurements

At each radiation quality, two sets of seven measurements were made, each measurement with integration time 30 s for the Radcal and PTW chambers and 60 s for the Exradin chambers (the integration time set for the ionization measurement depends on the volume of the chambers and the choice of the capacitor and is calculated in order to generate a potential around 2 V across the capacitor)

The Radcal and Exradin A11TW ionization chambers have been calibrated periodically for over a year in both beams in order to study their stability. The Exradin Magna and PTW chambers were at the BIPM for a period of one week for calibration. During this period, repeat calibrations were made in some qualities on different days, repositioning the chamber in order to have two independent sets of calibrations. For all the chambers, the relative standard uncertainty of the mean ionization current for each set was less than 3×10^{-4} .

Repeat calibrations of the BIPM chambers made over several months show a standard deviation of 5×10^{-4} . Consequently, an uncertainty component of 5×10^{-4} in relative value is introduced to account for the typical long-term reproducibility of chamber calibration coefficients in low-energy x-rays at the BIPM.

5.2.7. Additional measurements

The ionization chambers were also calibrated in one of the low-energy x-ray reference beams recommended by the CCRI [9]. The characteristics of the quality selected are shown in Table 5.5.

Table 5.5. Characteristics of the CCRI reference quality

Radiation quality	25 kV
Generating potential / kV	25
Additional Al filtration / mm	0.372
Al HVL / mm	0.242

5.3. Uncertainties

The uncertainties associated with the calibration of the ionization chambers are listed in Table 5.6. The uncertainty in the leakage current of each chamber is included in the overall ionization current uncertainty. The uncertainties associated with the primary standards (air-kerma rate) are listed in Table 2.7 of Chapter 2. The combined uncertainty u of the calibration coefficient in terms of air kerma N_K for the ionization chambers is 2.1×10^{-3} .

Table 5.6. Uncertainties associated with the calibration of the ionization chambers at the BIPM

Uncertainty component	$s^a \times 10^2$	$u^b \times 10^2$
air-kerma rate \dot{K}	0.05	0.19
positioning of transfer chamber	0.01	---
ionization current	0.02	0.02
long-term reproducibility	0.05	---
radial non-uniformity	---	0.02
quadratic summation	0.08	0.19
Combined uncertainty of N_K	0.21	

^a s represents the relative standard uncertainty estimated by statistical methods (type A).

^b u represents the relative standard uncertainty estimated by other means (type B).

5.4. Results and discussion

The calibration coefficients measured in each beam for each chamber were normalized to its respective calibration coefficient for the CCRI 25 kV quality. The calibration results are plotted as a function of HVL in Figures 5.1 to 5.4 for the Radcal, Exradin A11TW, Exradin Magna and PTW ionization chambers, respectively. The uncertainty bars shown in the figures represent the combined standard uncertainties, taking into account correlations in the type B uncertainties associated with the physical constants and the humidity correction between both primary standards.

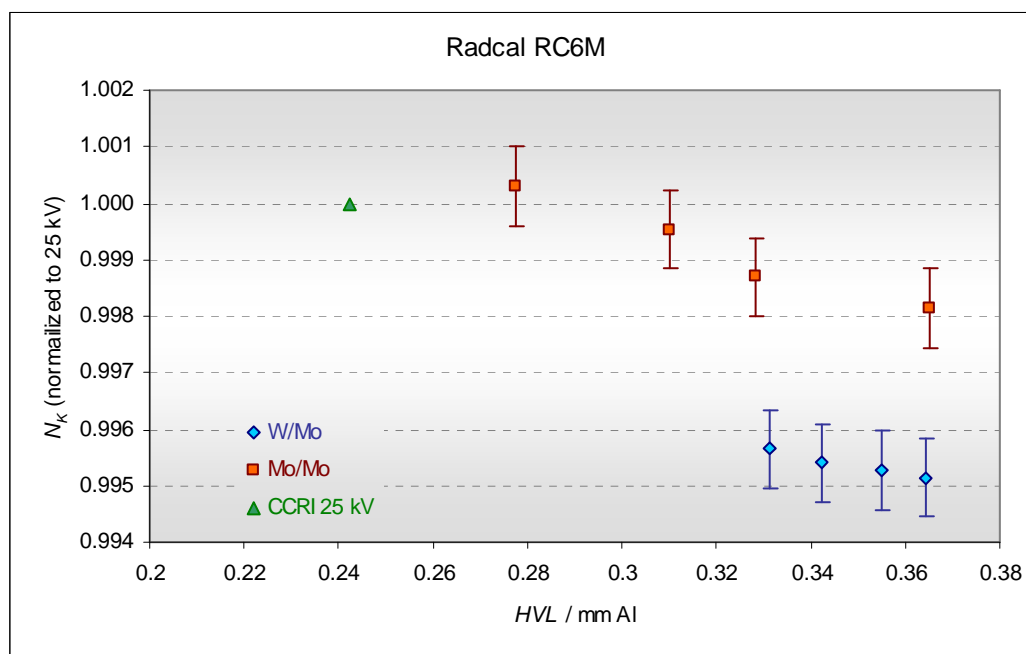


Figure 5.1. Normalized calibration coefficients for the Radcal chamber

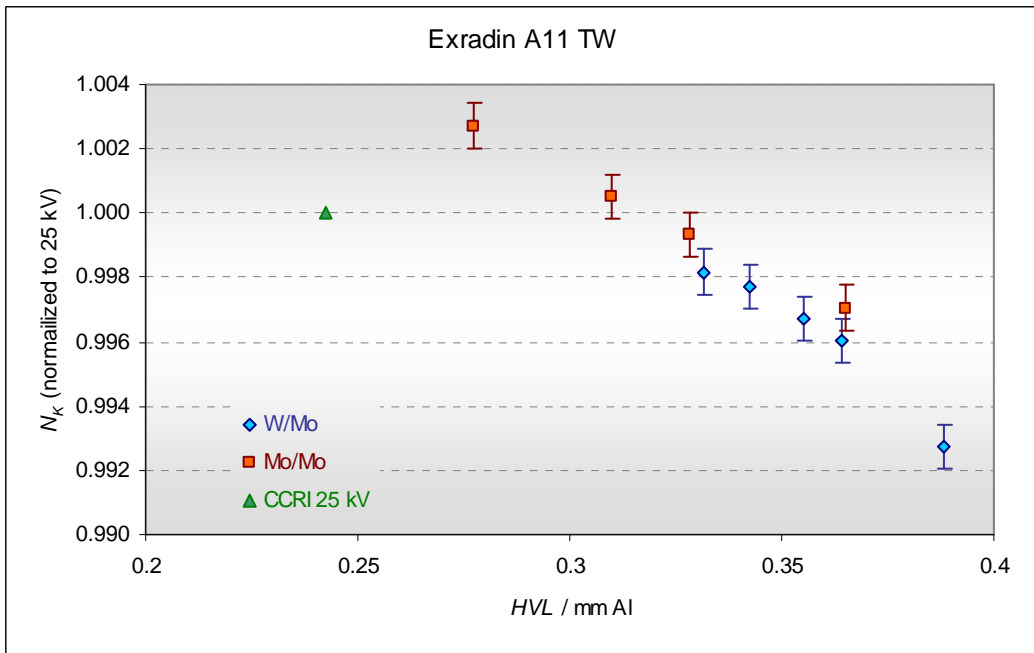


Figure 5.2. Normalized calibration coefficients for the Exradin A11 TW chamber

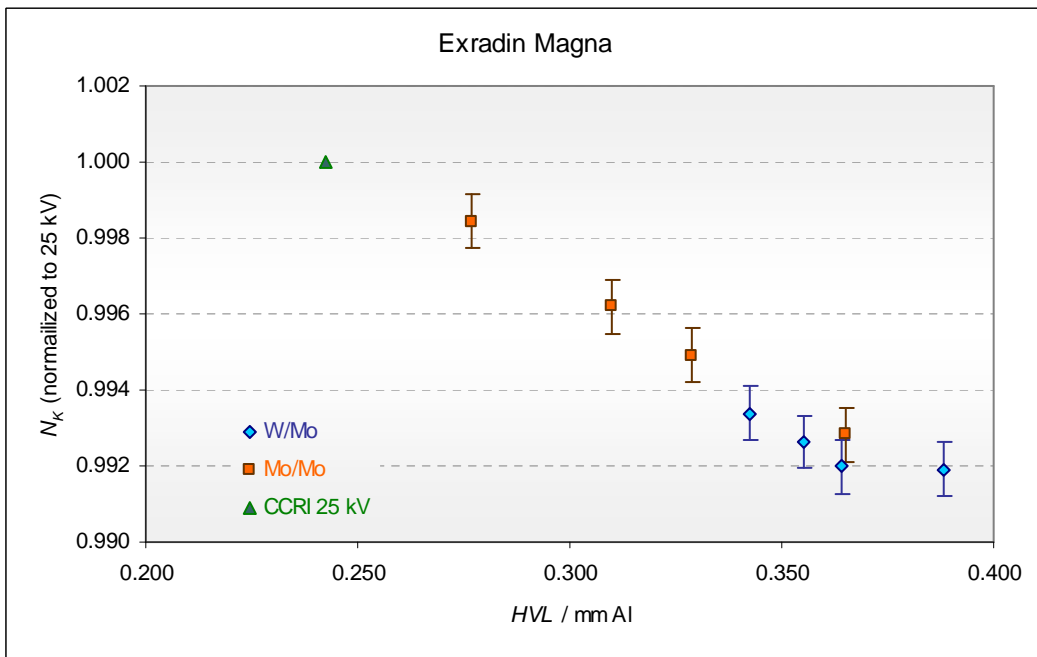


Figure 5.3. Normalized calibration coefficients for the Exradin Magna chamber

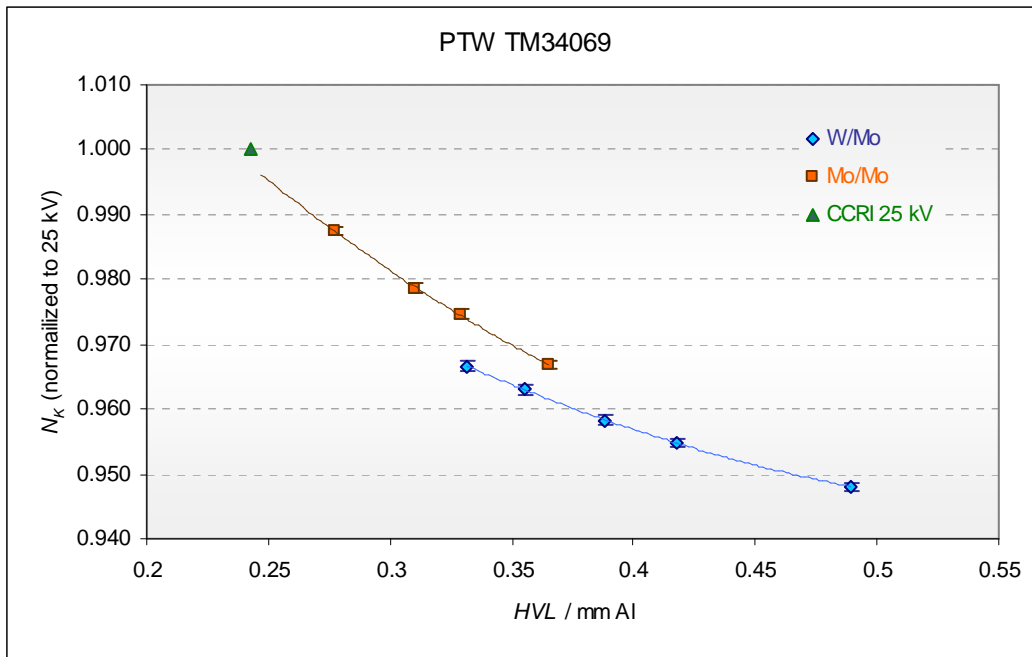


Figure 5.4. Normalized calibration coefficients for the PTW TM34069 chamber

The response of the chambers changes smoothly with energy, showing a similar trend in both types of radiation beams. The relative energy dependence in the range 23 kV to 30 kV for the W/Mo radiation qualities varies from 6×10^{-4} for the Radcal chamber, around 2×10^{-3} for the Exradin chambers and up to 9×10^{-3} for the PTW chamber; in the Mo/Mo beams, the energy dependence is 2×10^{-3} for the Radcal chamber, 6×10^{-3} for the Exradin chambers and 2×10^{-2} for the PTW chamber.

It can be seen from Figure 5.2 and 5.3 that the Exradin chambers show no significant sensitivity to different spectra when their responses are compared in the same HVL range (1×10^{-3}). In the case of the Radcal chamber, the sensitivity is around 3×10^{-3} for an Al HVL value of 0.365 mm corresponding to the qualities Mo/Mo 35 kV and W/Mo 30 kV. The PTW chamber not only shows significant energy dependence but also is the chamber with the largest sensitivity to the spectral differences, up to 8×10^{-3} for an Al HVL value of 0.33 mm.

Table 5.7 summarizes the results for the four chambers with the calibration coefficient ratio for an HVL of 0.365 mm Al also given.

Table 5.7. Response of the ionization chambers to the W/Mo and Mo/Mo beams

Ionization chamber	Normalized N_K^*		$N_{K,Mo/Mo35} / N_{K,W/Mo30}$
	W/Mo qualities Al HVL range / mm 0.33 to 0.43	Mo/Mo qualities Al HVL range / mm 0.27 to 0.37	
Radcal RC6M	0.9957 to 0.9951	1.0003 to 0.9981	1.0030
Exradin A11TW	0.9982 to 0.9960	1.0027 to 0.9971	1.0010
Exradin Magna	0.9934 to 0.9920	0.9984 to 0.9928	1.0009
PTW TM34069	0.9667 to 0.9583	0.9875 to 0.9668	1.0050

* N_K normalized to the N_K for CCRI 25 kV quality

5.5. Conclusion

Four different ionization chamber types have been calibrated in two sets of mammography beams to study their energy dependence and their sensitivity to spectral variations.

The calibration results for the Radcal R6CM ionization chamber in the simulated mammography beams using a W/Mo anode/filtration combination are in agreement with those obtained in the Mo/Mo beams at the level of 3 parts in 10^3 . This sensitivity to both sets of radiation qualities has been observed for other Radcal chambers of the same type. The Exradin chambers responses show a negligible sensitivity to different spectra. The energy dependence of these chambers is well within the recommended limit of 1%. Consequently, it would appear that national standard calibration laboratories can use W/Mo beams in the low HVL range to calibrate Radcal and Exradin chamber types for subsequent use in the dosimetry of Mo/Mo beams, as the combined effect of energy dependence and response to different spectra is less than the 1% expanded uncertainty accepted in mammography for different beams.

The PTW ionization chamber shows a non-negligible energy dependence, which is more important than its sensitivity to different spectra, the combined effect being more than 2% in the mammography energy range considered in the present work. This type of chamber, calibrated in W/Mo beams, can be used for the dosimetry of Mo/Mo beams, if both sets of beams have the same HVL range to avoid extrapolation in the data set of N_{K,Q_0} as a function of HVL determined at the reference laboratory. In the case that the W/Mo beams used for calibration have different HVL values than the Mo/Mo beams, a proper fit to the calibration

coefficients N_{K,Q_0} as a function of the HVL should be made to enable interpolation for the corresponding HVL; or an adequate energy correction factor k_{Q,Q_0} should be introduced in the determination of the incident kerma rate to account for this effect. In this particular case, the uncertainty in the incident air kerma determination should be increased to account for differences in energy spectrum as well as for the chamber's non-negligible energy dependence. An appropriate value for the additional type B relative standard uncertainty may be around 1×10^{-2} .

Chapter 6. Implementation of an international comparison and calibration facility for mammography dosimetry at the BIPM

6.1. Introduction

The Bureau International des Poids et Mesures (BIPM) is an international, intergovernmental organization set up by the Metre Convention in 1875. The Metre Convention is a treaty drawn up in Paris, France, by the representatives of the first seventeen nations and it now has fifty-five Member States. In 1999, under the auspices of the General Conference of Weights and Measures (CGPM), the category of Associate State was introduced and now thirty-three Associate States have also agreed to participate in Metre Convention activities. The Convention also created the Comité International des Poids et Mesures (CIPM) to direct and supervise the work of the BIPM. The BIPM works with and for the National Metrology Institutes (NMIs) (including national designated institutes) of the Member States.

The task of the BIPM is to facilitate worldwide uniformity and equivalence of measurements through direct dissemination of the International System of Units (SI). The BIPM carries out international comparisons to validate the consistency of the primary standards of the NMIs. The participation in these metrological comparisons allows the NMIs to demonstrate their calibration and measurement capabilities (CMCs) and to compare their realizations of the units of the SI with those of other NMIs.

In order to extend and fully document the practice of metrology comparisons, the CIPM established in 1999 a Mutual Recognition Arrangement (CIPM MRA) between NMIs from BIPM's Member States and, more recently, the Associate States. The CIPM MRA establishes a formal system within which NMI signatories and their designated institutes establish the degree of equivalence of their national measurement standards in each metrology domain in which they participate.

The CIPM has set up a number of Consultative Committees, which bring together the world's experts in their specified fields as advisers on the scientific work to be developed in the laboratories of the BIPM and on the international comparison programme to meet the needs of the NMIs. The comparisons conducted by the BIPM and based on the international facilities maintained at the BIPM are designated as key comparisons. The comparison results are published in the BIPM key comparison data base KCDB of the CIPM MRA.

In the field of ionizing radiation, the BIPM has maintained primary standards for dosimetry of x-rays and γ -rays since 1960. As requested by the Consultative Committee for Ionizing Radiation (CCRI), these standards are used in the BIPM key comparisons between the NMIs with primary standards and the BIPM, with reference BIPM.RI(I)- K_n , (n is the number allocated to each key comparison). They are also used to characterize national standards for those countries not holding a primary capability. The BIPM determination of the dosimetric quantity is taken as the key comparison reference value (KCRV) relative to which the degrees of equivalence are established for the NMIs that participate.

International comparisons and characterizations in low-energy x-ray beams started in 1966 in the reference radiation qualities recommended by the CCRI [9]; in 2001, the Consultative Committee for Ionizing Radiation CCRI(I) recommended that the BIPM extend these activities to mammography beams due to the legal requirements in some Member States for traceability. This is to enable them to validate their standards through comparisons in this domain of diagnostic radiology and publish, or validate, their CMCs in this domain. At the same time the BIPM can then characterize and calibrate national secondary standards for other Member States.

In response to the needs of National Metrology Institutes (NMIs) with dosimetry standards for mammography x-ray beams, and following the recommendations made by the CCRI(I) in 2005 and 2009, two sets of radiation qualities were established as reference beams for mammography at the BIPM: one set of seven radiation qualities was established in 2007 using the existing low-energy x-ray tube with its tungsten target and added Mo filtration (see Chapter 2), and a second set of four qualities that was set up in 2009 after the installation of a low-energy x-ray tube with molybdenum target (see Chapter 4). A new key comparison was then included in the BIPM on-going comparison programme of primary standards, identified in the KCDB as BIPM.RI(I)-K7 specifically for mammography beams. The new radiation

beams are also used to provide characterization of national secondary standards traceable to the International System of Units (SI).

The new facility for mammography was included in the quality management system (QMS) of the Ionizing Radiation (IR) Department in 2010; a description of the primary standard and the beam characteristics, including associated uncertainties, were included in the BIPM report of measuring conditions for comparison and calibration of national dosimetric standards [16]. According to the BIPM QMS, a set of four technical instructions were produced together with the corresponding forms and records required for each instruction.

The first international comparison of primary standards for mammography took place at the BIPM in 2007 and, since November 2009, seven international comparisons of primary standards were carried out in the new facility. Four of the seven comparisons were completed: the corresponding reports were published in the *Metrologia Technical Supplement* and the results were entered in the KCDB; one comparison needs to be repeated while the remaining two comparisons will be completed at the beginning of 2013. Five calibrations of secondary standards were carried out with the production of the corresponding certificates.

6.2. An international facility for mammography

6.2.1. International comparisons

The new development made at the BIPM in the domain of mammography, at the request of the CCRI, provides an international facility for comparisons, available for all the NMIs of the Member States holding primary standards for mammography dosimetry. A new ongoing key comparison was established at the BIPM and included in the KCDB as BIPM.RI(I)-K7. Participation in this key comparison enables the NMIs to validate their standards and through the BIPM comparison they can compare their results with all other participants.

The dosimetric quantity that is compared in this field is the air kerma, K_{air} , measured in gray, and calculated from measurements made using a free air chamber.

Comparisons of the standards for air kerma are carried out at the BIPM and can be made directly or indirectly, as described in the “Technical protocol for a BIPM ongoing key comparison in dosimetry” [34].

If the NMI participates in a direct comparison, the BIPM determines the air kerma rate using the NMI standard in the BIPM reference beams by the relation

$$\dot{K}_{\text{NMI}} = \frac{1}{\rho_{\text{air}}} \left(\frac{I}{V} \right)_{\text{NMI}} \frac{W_{\text{air}}}{e} \frac{1}{1 - g_{\text{air}}} \prod_i k_{i,\text{NMI}} \quad (6.1)$$

where ρ_{air} is the density of air under reference conditions, $(I/V)_{\text{NMI}}$ is the ratio of the ionization current I measured using the NMI standard of volume V , W_{air} is the mean energy expended by an electron of charge e to produce an ion pair in air, g_{air} is the fraction of the initial electron energy lost through radiative processes in air, and $\prod k_{i,\text{NMI}}$ is the product of the correction factors to be applied to the standard provided by the NMI.

Similarly, K_{BIPM} is determined using the BIPM standard and the comparison result $R_{K,\text{NMI}}$ is expressed as the ratio $K_{\text{NMI}}/K_{\text{BIPM}}$.

The set of correction factors $k_{i,\text{NMI}}$ are carefully analysed as well as the methods used by the NMI for their determination; additional measurements or calculations are sometimes needed when non-negligible discrepancies exist between the NMI and BIPM determination of these correction factors.

If the comparison is carried out indirectly, the NMI calibrates a transfer ionization chamber in the NMI reference beams, determining the calibration coefficient in terms of air kerma $N_{K,\text{NMI}}$ by the relation

$$N_{K,\text{NMI}} = \frac{\dot{K}_{\text{NMI}}}{I_{\text{tr},\text{NMI}}} \quad (6.2)$$

where \dot{K}_{NMI} is the air kerma rate determined by the NMI primary standard using (6.1) and $I_{\text{tr},\text{NMI}}$ is the ionization current measured by the transfer chamber and the associated current-measuring system. At the BIPM, the transfer chamber is then calibrated against the BIPM primary standard, determining $N_{K,\text{BIPM}}$. The comparison result $R_{K,\text{NMI}}$ is taken as the ratio of the calibration coefficients determined at each laboratory as $N_{K,\text{NMI}}/N_{K,\text{BIPM}}$, where $N_{K,\text{NMI}}$ is taken as the mean of measurements performed at the NMI before and after the measurements at the BIPM.

The current I_{tr} is corrected to the reference conditions of ambient air temperature, pressure and relative humidity chosen by the CCRI for the comparison ($T = 293.15$ K, $P = 101.325$ kPa and $h = 50$ %).

To derive a comparison result from the calibration coefficients $N_{K,BIPM}$ and $N_{K,NMI}$ measured, respectively, at the BIPM and at a national measurement institute (NMI), differences in the radiation qualities and calibration conditions must be taken into account. Appropriate correction factors are derived and applied to the measured current and the corresponding uncertainties are included in the uncertainty budget:

- different air kerma rates: a correction $k_{s,tr}$ can be applied for ion recombination in the transfer ionization chamber to account for the difference in the kerma rates at the two laboratories;
- different radial non-uniformity: a correction $k_{rn,tr}$ can be applied at each laboratory for the radial non-uniformity of the radiation field. However, as this effect is likely to cancel at least to some extent at the two laboratories, no correction is applied and a relative standard uncertainty is introduced for this effect;
- field size: transfer chambers commonly used in mammography are relatively insensitive to field size; no correction is applied but an uncertainty component is included for this effect;
- half-value layer: each quality used for the comparison has the same nominal generating potential and similar filtration at each institute, but the half-value layers (HVLs) can differ. A radiation quality correction factor k_Q can be derived for each comparison quality Q . This corrects the calibration coefficient $N_{K,NMI}$ determined at the NMI into one that applies at the ‘equivalent’ BIPM quality and is derived by interpolation of the $N_{K,NMI}$ values in terms of $\log(\text{HVL})$;
- distance: a correction factor k_{dist} can be determined and applied when the transfer chamber is calibrated at different distances in each laboratory;
- polarity: usually the transfer chamber is used with the same polarity at each institute and so no correction is applied for polarity effects in the transfer chamber. If this is not the case, a correction k_{pol} is calculated from measurements made at the BIPM for both polarities.

As in the case of the direct comparison, the correction factors k_i that the NMI applies to its standard to determine the air kerma rate are carefully analysed. When important discrepancies are observed between the NMI and BIPM correction factors, both laboratories make additional studies after the comparison in order to identify the cause of the discrepancies and make appropriate corrections.

To evaluate the uncertainty of the comparison result, the NMI provides a full uncertainty budget together with the result, at the time of the comparison. The uncertainty budget for the BIPM is taken from [16]. In calculating the combined standard uncertainty of the comparison, correlations in the type B uncertainties, according to the GUM [35], associated with the physical constants ρ_{air} and W_{air} / e , humidity correction k_h , bremsstrahlung correction $(1 - g_{\text{air}})$ and the standard correction factors must be taken into account [36].

The mammography comparisons are often made using transfer chambers, as the primary standards are normally compared directly in the low-energy x-ray beams, the BIPM.RI(I)-K2 key comparison, that covers the mammography energy range. While the use of transfer chambers might introduce more uncertainty in the comparison results than for a direct comparison of the primary standards, useful information is gained on the reproducibility of calibration coefficients and on the behaviour of transfer instruments of the type used in the dissemination chain.

Up to now, seven indirect comparisons have been carried out using transfer chambers with the NRC (Canada), NMIJ (Japan), PTB (Germany), NIST (USA), ENEA (Italy), VNIIM (Russian Federation) and the IAEA (Vienna). The NRC, NMIJ, PTB and NIST comparison results are available in the KCDB and the corresponding reports have been published in the *Metrologia Technical Supplement* series [37, 38, 39, 40].

A brief description of the published comparisons is presented in the following paragraphs and the state of the other comparisons is explained in section 6.2.1.5.

6.2.1.1. Key comparison BIPM.RI(I)-K7 of the air-kerma standards of the NRC, Canada and the BIPM

An indirect comparison has been made between the air-kerma standards of the National Research Council (NRC), Canada and the Bureau International des Poids et Mesures (BIPM) in the x-ray range from 23 kV to 50 kV using mammography beams produced by a tungsten-

anode tube and molybdenum filter combination. Four parallel-plate ionization chambers were used as transfer instruments (two Radcal 10x5-6M and two PTW 23344). The measurements at the BIPM took place in March 2007.

The calibration of the transfer chambers was made at two different distances, as both laboratories have a different reference distance (1 m at the NRC and 0.5 m at the BIPM).

To derive the comparison result from the calibration coefficients $N_{K,BIPM}$ and $N_{K,NRC}$ measured, respectively, at the BIPM and at the NRC, the following considerations were taken into account:

- air kerma rates: the air-kerma rates at the NRC are lower than those at the BIPM for the calibration distance of 0.5 m. No corrections $k_{s,tr}$ were applied for ion recombination and a relative standard uncertainty of 5×10^{-4} was introduced to account for the difference in the kerma rates at this distance;
- field size: the radiation field diameter at 500 mm is significantly different at the two laboratories (84 mm at the BIPM and 47 mm at the NRC). Measurements made at the BIPM over a range of field sizes showed that the effect of this on the calibration coefficients for the PTW chamber in the W/Mo mammography beams is about 3 parts in 10^3 while for the Radcal it is around 1 part in 10^3 . Consequently, the effect of field size on the present comparison was taken into account by applying the correction factors of 0.997 and 0.999 to the comparison results at 500 mm for the PTW and Radcal chambers, respectively. A relative standard uncertainty of 1×10^{-3} was introduced for this effect;
- radial non-uniformity: no correction $k_{rn,tr}$ was applied at either laboratory for the radial non-uniformity of the radiation field. For a chamber with collector radius 15 mm, the correction factor for the BIPM reference field is around 1.002 and this effect is likely to cancel to some extent at the two laboratories. A relative standard uncertainty of 5×10^{-4} was introduced for this effect;
- half-value layer: the radiation qualities at the BIPM and the NRC are not well matched in terms of HVL, despite the use of the same calibrated generating potentials and similar molybdenum filters. To derive a comparison result for the BIPM HVL values, a special analysis was made and is described in the following paragraph;
- distance: as the NRC and the BIPM use different calibration distance, the chambers were calibrated at 0.5 m and at 1 m at both laboratories;

- polarity: the same polarity was applied to the chambers at both laboratories; no correction k_{pol} was applied.

As mentioned before, the radiation qualities at the NRC and the BIPM do not match in terms of the HVL; to derive a comparison result for the BIPM HVL values, a quadratic fit was made to each of the NRC data sets. To avoid the need for extrapolation to the BIPM W/Mo-23 HVL, which has an HVL below the range of the NRC W/Mo qualities, the calibration coefficient for the CCRI 25 kV quality at the NRC was included in each quadratic fit. The calibration coefficients determined at the NRC and at the BIPM at 0.5 m, normalized to the BIPM calibration coefficient for the CCRI 25 kV quality, are plotted in Figures 6.1 and 6.2 for the Radcal RC6M-9646 and the PTW23344-0948, respectively, as a function of the corresponding HVL. Similar behaviour was observed for the other two chambers and also for the calibrations made at 1 m.

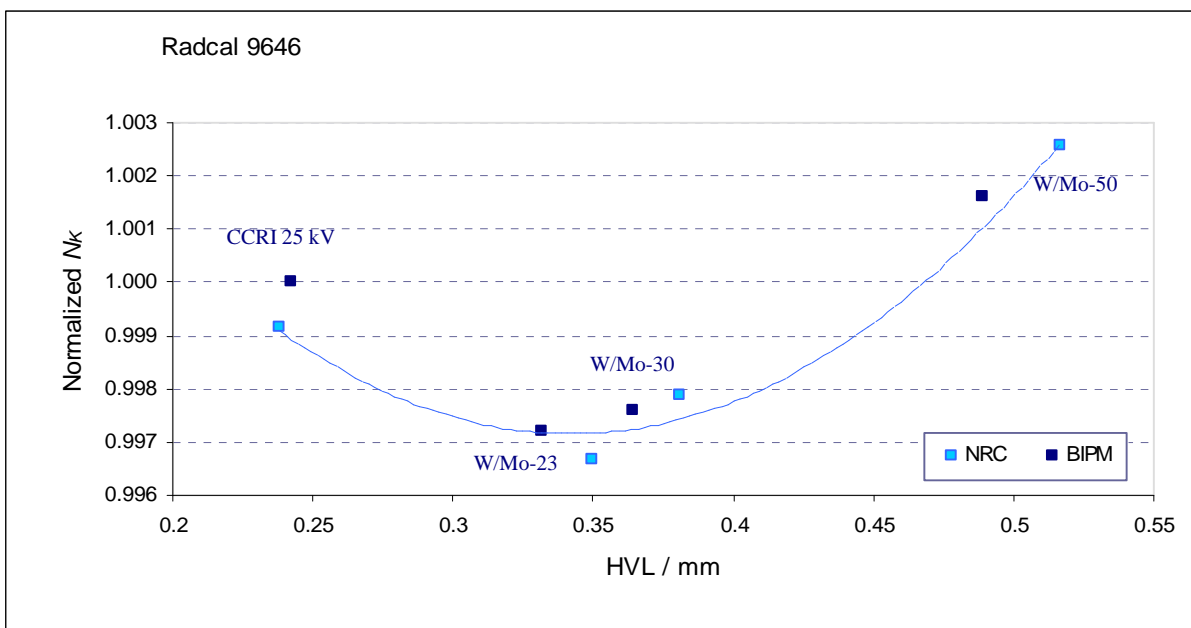


Figure 6.1. Normalized N_K for the Radcal RC6M-9646. The dotted line represents a quadratic fit to the NRC data.

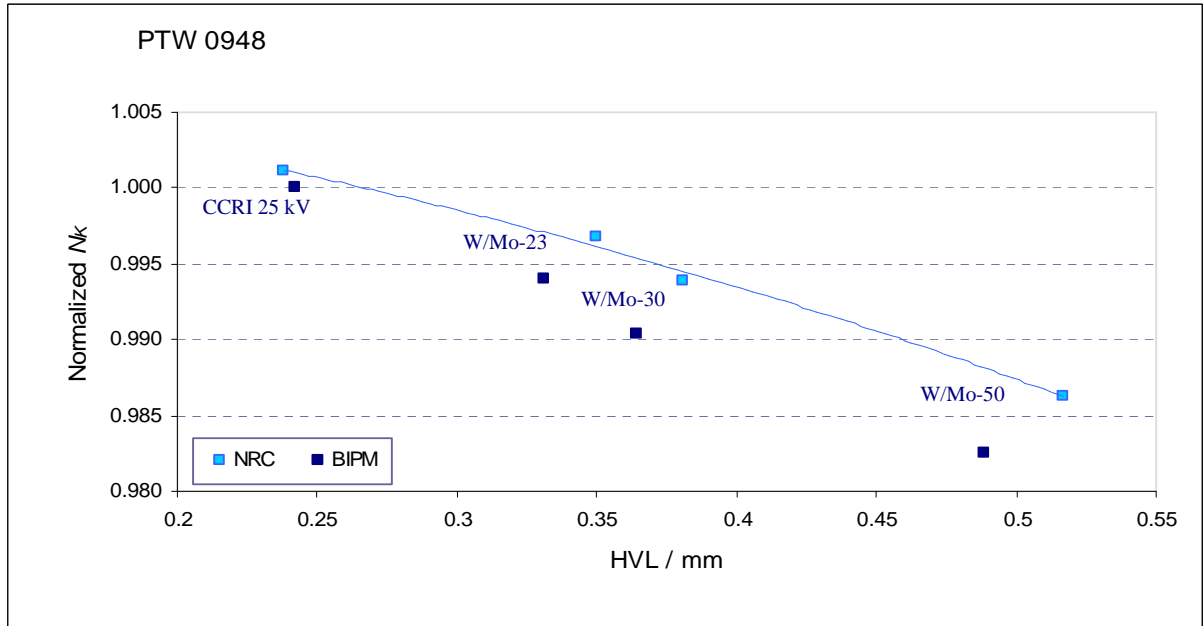


Figure 6.2. Normalized calibration coefficients NK for the PTW23344-0948. The dotted line represents a quadratic fit to the NRC data.

From the data fits, a set of values $N_{K,NRC}(\text{BIPM HVL})$ was derived for each chamber at each distance, leading to seven sets of comparison results (chamber PTW 0949 was measured at 0.5 m only).

$$R_{K,NRC} = \frac{N_{K,NRC}(\text{BIPM HVL})}{N_{K,BIPM}} \quad (6.3)$$

An additional uncertainty of 5 parts in 10^{-4} was included for this fitting procedure.

The seven ratios $N_{K,NRC} / N_{K,BIPM}$ for the four chambers measured at the two distances, showed a significant spread, the relative standard deviation of the distribution for each quality being up to 1.8×10^{-3} . This is significantly greater than the statistical standard uncertainty of each calibration coefficient. However, no clear trends emerge.

Consequently, the best estimate of the comparison result $R_{K,NRC}$ for each radiation quality was considered to be the mean value. These values are given in Table 6.1 along with the standard uncertainty of each mean value, σ_{mean} . The combined standard uncertainty of the air kerma determinations, calibration coefficient and the comparison result (removing correlations) is also presented in Table 6.1.

Table 6.1. Comparison results and combined relative standard uncertainty

Radiation quality	W/Mo23	W/Mo30	W/Mo50	Relative standard uncertainty	BIPM	NRC
$R_{K,NRC}$	0.9984	0.9988	0.9986	\dot{K}	0.0020	0.0026
σ_{mean}	0.0011	0.0013	0.0010	N_K	0.0020	0.0027
u_c	0.0030			$R_{K,NRC}$	0.0030	

The comparison results show general agreement at the level of the combined standard uncertainty of 3.0 parts in 10^3 .

6.2.1.2. Key comparison BIPM.RI(I)-K7 of the air-kerma standards of the NMIJ, Japan and the BIPM

An indirect comparison between the air-kerma standards of the National Metrology Institute of Japan (NMIJ) and the BIPM in the Mo/Mo mammography x-ray beams took place in November 2009. Three parallel-plate ionization chambers were used as transfer instruments (Radcal RC6M, PTW 23344 and Oyogiken C-MA chambers).

The following considerations relating to the transfer chambers were taken into account to derive the comparison result from the calibration coefficients $N_{K,BIPM}$ and $N_{K,NMIJ}$ measured, respectively, at the BIPM and at the NMIJ:

- air kerma rates: no corrections $k_{s,tr}$ were applied for ion recombination in spite of the difference in the kerma rates at the two laboratories; the initial recombination is the same for both beams and volume recombination is negligible for the kerma rates established at the two laboratories; an uncertainty of 5×10^{-4} is introduced to account for this effect;
- field size: both laboratories used the same field size; no correction and no uncertainty is included;
- radial non-uniformity: it was assumed that the effect of radial non-uniformity cancels to some extent at the two laboratories; no k_{rn} was applied but a relative standard uncertainty of 2×10^{-4} was introduced for this effect;

- half-value layer: the radiation qualities at the BIPM and at the NMIJ are very closely matched in terms of HVL and so the correction factor k_Q was taken to be unity for all qualities, with a negligible uncertainty;
- distance: both laboratories used the same calibration distance; no correction k_{dist} was applied to the measured current;
- polarity: the same polarity was applied to the chambers at both laboratories; no correction k_{pol} was applied.

Regarding the air kerma determination using the primary standards, it was observed at the time of the comparison that the correction factors for air attenuation k_a , evaluated using measured air-attenuation coefficients, were significantly higher at the NMIJ than those reported by the BIPM and by other NMIs for similar beams. After the comparison, the NMIJ re-measured the air-attenuation coefficients modifying the configuration used previously; the results were in good agreement with the BIPM values and have been adopted at the NMIJ. No further studies were needed for the remaining correction factors applied to the primary standard.

The best estimate of the comparison result $R_{K,\text{NMIJ}}$ for each radiation quality was taken to be the mean value for the three transfer chambers. The results are given in Table 6.2 along with the standard uncertainty of each mean value, σ_{mean} .

The combined standard uncertainty of the air kerma determinations, calibration coefficient and the comparison result (removing correlations) is also presented in Table 6.2.

Table 6.2. Comparison results and combined relative standard uncertainty

Radiation quality	Mo/Mo25	Mo/Mo28	Mo/Mo30	Mo/Mo35	Relative standard uncertainty	BIPM	NMIJ
$R_{K,\text{NMIJ}}$	0.9984	0.9988	0.9986	0.9988	\dot{K}	0.0020	0.0035
σ_{mean}	0.0011	0.0013	0.0010	0.0013	N_K	0.0021	0.0038
u_c	0.0037				$R_{K,\text{NMIJ}}$	0.0037	

The comparison results show agreement at the level of 1.4 parts in 10^3 , which is within the combined relative standard uncertainty for the comparison of 3.7 parts in 10^3 .

6.2.1.3. Key comparison BIPM.RI(I)-K7 of the air-kerma standards of the NIST, USA and the BIPM

An indirect comparison between the air-kerma standards of the National Institute of Standards and Technology (NIST), USA and the BIPM in the Mo/Mo mammography x-ray beams took place in January 2010. Two thin-window parallel-plate ionization chambers of type Radcal RC6M, belonging to the NIST were sent to the BIPM for the comparison, operating in parallel with the low-energy x-ray BIPM.RI(I)-K2 key comparison, using the same instruments. As one of the instruments exhibited a significant drift during the K2 comparison, only the stable instrument was used in the mammography beams.

- air kerma rates: no corrections $k_{s,tr}$ were applied for ion recombination and a relative standard uncertainty of 5×10^{-4} is introduced to account for the difference in the kerma rates at the two laboratories;
- field size: the radiation field diameter is significantly different at the two laboratories (100 mm at the BIPM and 60 mm at the NIST for the present comparison to match the BIPM calibration distance). While the effect of this on calibration coefficients can be significant for some chamber types, particularly at higher energies, the Radcal is known to be relatively insensitive to field size in the mammography range and no correction was applied; an uncertainty component of 1 part in 10^3 is included for this effect;
- radial non-uniformity: no correction $k_{m,tr}$ is applied at either laboratory for the radial non-uniformity of the radiation field. For a chamber with collector radius 15 mm, the correction factor for the BIPM reference field is around 5×10^{-4} and this effect is likely to cancel at least to some extent at the two laboratories. A relative standard uncertainty of 2×10^{-4} is introduced for this effect;
- half-value layer: the radiation qualities at the BIPM and at the NIST were not well matched in terms of HVL, despite the use of the same calibrated generating potentials and similar molybdenum filters; a special analysis was made to derive the comparison result for each quality, as explained in the following paragraph;
- distance: similar calibration distances were used in the two laboratories; no k_{dist} was applied to the measured current;

- polarity: the transfer chamber was used with the same polarity at each institute and so no corrections are applied for polarity effects in the transfer chamber.

The mean calibration coefficients determined at the NIST and at the BIPM, normalized to the BIPM calibration coefficient for the CCRI 25 kV quality, are plotted in Figure 6.3 as a function of the corresponding HVL. Note that the NIST Mo-23 quality was measured subsequent to and was not part of the original comparison.

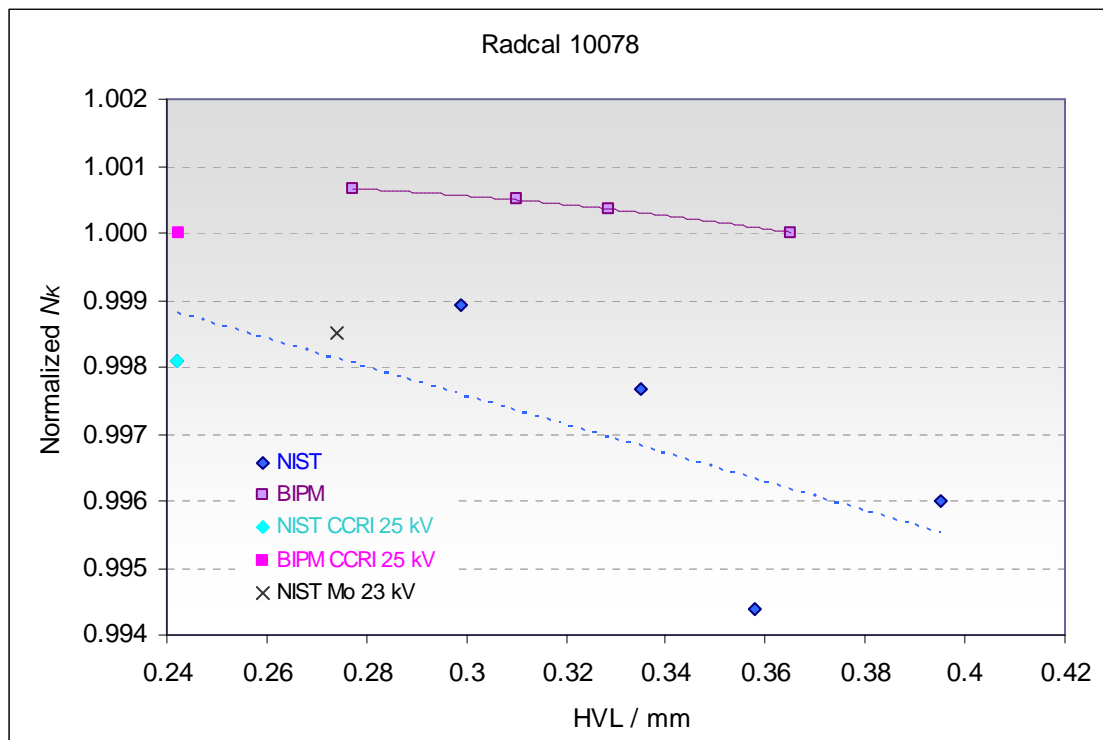


Figure 6.3. Normalized results for the transfer chamber calibration coefficients at the NIST and the BIPM. The dashed blue line through the NIST data represents a linear fit to the NIST data points, including the CCRI 25 kV quality but excluding the Mo-23 quality (see explanation in text).

It can be seen from the BIPM data that the chamber exhibited a smooth and relatively flat energy response, the total variation being less than 7 parts in 10^4 over the energy range considered. In contrast, the NIST results showed significant scatter and a total variation in the chamber response of 4.6 parts in 10^3 .

The scatter of the NIST data, in combination with the disagreement of the HVL values, presented a difficulty in deriving a comparison result for each of the BIPM radiation qualities.

To this end, a linear fit was made to the NIST data. To avoid the need for extrapolation to the BIPM Mo-25 HVL, the calibration coefficient for the CCRI 25 kV quality at the NIST was included in the linear fit (the NIST Mo-23 calibration point shown in Figure 6.3 was not included in the fit for the reason outlined below). From this fit, a set of values $N_{K,NIST}(\text{BIPM HVL})$ was derived, leading to a set of comparison results

$$R_{K,NIST} = \frac{N_{K,NIST}(\text{BIPM HVL})}{N_{K,BIPM}}. \quad (6.4)$$

The uncertainty arising from the fitting procedure, which not only corrects for HVL differences but effectively smoothes the NIST data, was taken as the r.m.s. deviation of the measured values $N_{K,NIST}$ from the fitted line. This was evaluated as 1.5 parts in 10^3 and was included the total uncertainty analysis.

During subsequent discussions of the comparison results, the NIST measured the calibration coefficient for the Mo-23 quality to check the chamber's energy response and the result is included in Figure 3. However, due to the possibility of chamber drift, this new value was not taken into account in the analysis of the results, but it nevertheless served to justify the method used to derive the comparison results.

The final comparison results $R_{K,NIST}$ was derived from the N_K values obtained from the linear fit corresponding to the BIPM HVLs. The results are presented in Table 6.3, together with the combined relative standard uncertainty associated with the primary standards, the transfer chamber calibration and the comparison result.

For a given generating potential, differences in the Al HVL values of between 22 μm and 30 μm are observed for the two laboratories. The NIST uses a Mo filter 32 μm thick while at the BIPM the thickness is 30 μm . Simulations of both sets of radiation qualities using the IPEM software [41] show that the different Mo filter thicknesses can explain around 9 μm of the observed difference in the HVL values.

Another possible source of HVL differences is the calibration of the generating potentials. It can be seen from Figure 6.3 that a change in generating potential of 2 kV to 4 kV would result in better agreement between the NIST and BIPM HVLs. However, such a voltage offset is significantly larger than the calibration uncertainty of the voltage measurement at each laboratory. Furthermore, the systematic progression from 2 kV to 4 kV with increasing HVL is unlikely to be due to a voltage calibration error.

Table 6.3. Comparison results and combined relative standard uncertainty

Radiation quality	Mo/Mo25	Mo/Mo28	Mo/Mo30	Mo/Mo35	Relative standard uncertainty	BIPM	NIST
$R_{K,NIST}$	0.9974	0.9968	0.9966	0.9962	\dot{K}	0.0020	0.0024
u_c	0.0032				N_K	0.0022	0.0026
					$R_{K,NIST}$	0.0032	

The results show the standards to be in agreement at the level of the combined standard uncertainty of 3.2 parts in 10^3 .

6.2.1.4. Key comparison BIPM.RI(I)-K7 of the air-kerma standards of the PTB, Germany and the BIPM

An indirect comparison between the air-kerma standards of the Physikalisch Technische Bundesanstalt (PTB), Germany and the BIPM in the Mo/Mo and W/Mo mammography x-ray beams took place in September 2010. Two thin-window parallel-plate ionization chambers of type Radcal RC6M, belonging to the PTB, were used as transfer instruments for the comparison.

To derive the comparison result $R_{K,PTB}$, the following considerations were taken into account:

- air kerma rates: no corrections $k_{s,tr}$ were applied for ion recombination although the kerma rates at the PTB are lower than those at the BIPM; an uncertainty of 5×10^{-4} is introduced to account for this effect;
- field size: both laboratories used similar field sizes; no correction and no uncertainty is included;
- radial non-uniformity: no correction $k_{m,tr}$ is applied at either laboratory for the radial non-uniformity of the radiation field. For the Radcal chamber, with collector diameter 30 mm, the correction factor for the BIPM reference field is around 1×10^{-3} and this effect is likely to cancel at least to some extent at the two laboratories. A relative standard uncertainty of 5×10^{-4} is introduced for this effect;
- half-value layer: the radiation qualities at the BIPM and the PTB are very closely matched in terms of HVL and so the correction factor k_Q is taken to be unity for all qualities, with a negligible uncertainty;

- distance: both laboratories calibrated the chambers at a distance of 1 m in the W/Mo radiation qualities and no correction k_{dist} was applied to the measured current in these beams; however, in the Mo/Mo beams, the reference distance at the PTB is 1 m whereas at the BIPM, is 0.6 m (it is not possible to measure at another distance in these beams). To estimate the effect on the response of the chambers calibrated at different distances, measurements at 500 mm were also made at the BIPM in the W/Mo beams. The calibration coefficients at both distances measured for three qualities in the HVL range of the Mo/Mo beams differ by 2.1 parts in 10^3 (mean $N_{K, 1000 \text{ mm}} / N_{K, 500 \text{ mm}} = 0.9979(5)$). A similar effect was measured previously at the BIPM for other Radcal chambers, not only in the W/Mo beams but also in the CCRI reference qualities. Assuming that the same effect is present in the Mo/Mo beams, a scaled distance correction factor k_{dist} of 0.9983 has been applied to the N_K values measured at the BIPM at the distance of 600 mm in the Mo/Mo beams to account for the distance difference between the PTB and the BIPM (400 mm). Given the approximate nature of this correction, a relative standard uncertainty of 1.0×10^{-3} is introduced for this effect.
- polarity: no correction k_{pol} was applied as the transfer chambers were used with both polarities at each institute and the mean of the calibration coefficients measured with each polarity was used to evaluate the comparison results.

Both the PTB and the BIPM were satisfied regarding the operation of their primary standards and the corresponding correction factors entering in the air kerma determination to enable the calibration of the transfer instruments.

The best estimate of the comparison result $R_{K, \text{PTB}}$ for each radiation quality is taken to be the mean value for the two transfer chambers. The results are given in Table 6.4 along with the standard uncertainty of each mean value, σ_{mean} . The uncertainties are also included in Table 6.4.

The comparison results show agreement at the level of 7 parts in 10^4 for the Mo/Mo beams, which is within the combined relative standard uncertainty for the comparison of 3.7 parts in 10^3 . For the W/Mo beams, the agreement between the standards is at the level of 1.8 parts in 10^3 , also within the combined relative standard uncertainty for the comparison of 3.5 parts in 10^3 .

Table 6.4. Comparison results and combined relative standard uncertainty

Radiation quality	Mo/Mo25	Mo/Mo28	Mo/Mo30	Mo/Mo35	Relative standard uncertainty	BIPM	PTB
$R_{K,PTB}$	0.9991	0.9994	0.9991	0.9995	\dot{K}	0.0020	0.0030
σ_{mean}	0.0015	0.0012	0.0014	0.0012	N_K	0.0021	0.0035
u_c	0.0037				$R_{K,PTB}$	0.0037	

Radiation quality	W/Mo25	W/Mo28	W/Mo30	W/Mo35	Relative standard uncertainty	BIPM	PTB
$R_{K,PTB}$	1.0018	1.0019	1.0019	1.0014	\dot{K}	0.0020	0.0030
σ_{mean}	0.0015	0.0015	0.0010	0.0010	N_K	0.0021	0.0034
u_c	0.0035				$R_{K,PTB}$	0.0035	

The results presented in Tables 6.1 to 6.4 show the standards of the NRC, NMIJ, NIST, PTB and the BIPM to be in agreement at the level of the combined standard uncertainty for the comparison.

6.2.1.5. Other comparisons

A direct and indirect comparison was carried out with the ENEA (Italy) in the simulated mammography beams (W/Mo qualities) as the ENEA disseminates the calibration coefficients in these beams. Measurements with the ENEA primary standard and one transfer ionization chamber were made at the BIPM during February 2011. Important discrepancies were identified at the time of the comparison (the results were kept blind). Subsequent discussions with the ENEA about their measuring conditions enabled them to identify some irregularities in their calibration process, and they requested to repeat the comparison in the near future.

The International Atomic Energy Agency establishes a link to the international measurement system by providing dosimetry calibration services to their Member States through the network of Secondary Standards Dosimetry Laboratories (SSDLs). In the mammography domain, the IAEA is traceable to the PTB. In 2007 they declared their dosimetry calibration and measurement capabilities (CMCs), published in the Appendix C of the CIPM MRA key

comparison database. To maintain the validity of the CMCs, the IAEA asked the BIPM to run a bilateral comparison in the Mo/Mo beams. The measurements were performed in 2012 and the comparison report has been sent to the CCRI(I) for approval and future publication. The comparison report will be published in the *Metrologia Technical Supplement*, but the comparison results will not be included in the BIPM.RI(I)-K7 as the IAEA doesn't hold a primary standard.

A recent comparison with the VNIIM (Russia) has been carried out in the Mo/Mo beams using a transfer chamber; repeat calibrations of the transfer chamber are still being carried out at the VNIIM, after the measurements made at the BIPM.

6.2.1.6. Degrees of equivalence

The analysis of the results of BIPM comparisons in low-energy x-rays in terms of degrees of equivalence is described in [35] and a similar analysis is adopted for comparisons in mammography x-ray beams. Following a decision of the CCRI, the BIPM determination of the air-kerma rate is taken as the key comparison reference value, for each of the CCRI radiation qualities. It follows that for each laboratory i having a BIPM comparison result x_i with combined standard uncertainty u_i , the degree of equivalence with respect to the reference value is the relative difference $D_i = (K_i - K_{\text{BIPM},i}) / K_{\text{BIPM},i} = x_i - 1$ and its expanded uncertainty $U_i = 2 u_i$. In the case when an NMI participates in the K7 key comparison for the two sets of radiation beams, the Mo/Mo results are those considered to evaluate the degree of equivalence. The results for D_i and U_i expressed in mGy/Gy, are shown in Table 6.5.

Table 6.5. Degrees of equivalence

	Mo/Mo25		Mo/Mo28		Mo/Mo30		Mo/Mo35	
	D_i	U_i	D_i	U_i	D_i	U_i	D_i	U_i
	/(mGy/Gy)		/(mGy/Gy)		/(mGy/Gy)		/(mGy/Gy)	
NMIJ	-1.6	7.4	-1.2	7.4	-1.4	7.4	-1.2	7.4
NIST	-2.6	6.4	-3.2	6.4	-3.4	6.4	-3.8	6.4
PTB	-0.9	7.4	-0.6	7.4	-0.9	7.4	-0.5	7.4

	W/Mo23		W/Mo30		W/Mo50	
	D_i	U_i	D_i	U_i	D_i	U_i
	/(mGy/Gy)		/(mGy/Gy)		/(mGy/Gy)	
NRC	0.9	6.0	1.5	6.0	1.0	6.0

6.2.2. Calibration of national secondary standards in mammography beams

For those dosimetry laboratories of the Member States of the BIPM, being either part of their National Metrology Institute or a designated institute in their own right, that do not hold primary standards, the BIPM is able to characterize their national standards and provide calibration certificates in terms of air kerma in the mammography beams. In this way, the NMIs then disseminate the SI unit for air kerma by calibrating the ionization chambers used in the diagnostic radiology departments of their countries health-care system.

The calibration process is made following the steps described in four technical instructions (written by C. Kessler) of the BIPM Quality Management System (QMS) and using a set of forms, pro-forma spreadsheets (modified or produced by C. Kessler), the output calibration records and a BIPM-designed data acquisition software. The six steps are outlined in the following paragraphs:

- a. Reception of the chamber: a form is used for this purpose, the corresponding fields being filled with the identification of the chamber, NMI, date of reception and data provided by the NMI needed for the calibration (reference plane of measurement, voltage and polarity); the instrument is inspected and the general conditions are recorded on the form; electrical measurements are made to verify that there is no short-circuit between the electrodes. Dimensional measurements are also made: external diameter, height and entrance surface-reference measurement plane dimensions are needed to set up the chamber correctly in the beam centre at the reference distance.
- b. Set-up of the chamber: the technical instructions “Setting up an ionization chamber in mammography” and “Setting up an ionization chamber in low-energy x-rays” are followed to position the chamber in the reference measurement conditions, either on the Mo/Mo or W/Mo calibration bench, respectively, using the corresponding positioning record form. The

reference point for the chamber is positioned in the reference plane with a reproducibility of 0.03 mm. The distance is measured to around 0.02 mm. The chamber is aligned on the beam axis to an estimated uncertainty of 0.1 mm.

c. Beam quality: the x-ray generator is operated according the technical instruction “Source operation” which describes also the steps that must be followed to set a particular radiation quality.

d. Measurements: The normal calibration procedure is to measure twice using the NMI chamber and between these measurements to determine the air-kerma rate using the BIPM standard. The chamber and the standard are pre-irradiated at least 30 min before any measurement is made; this period of time is also needed to warm-up and stabilize the x-ray system. A data acquisition program is used to register the ionization current measured using the chamber and the standard, as well as all the parameters needed for the calibration (temperature measured by three thermistors, pressure, humidity); the program also communicates and registers data from the voltage and anode current measuring system. The data are transferred to a proforma Excel file which calculates automatically the air-kerma rate and the calibration coefficient with the uncertainty associated with the calibration measurements. The calibration procedure is described in the technical instructions “Calibration measurements in mammography x-rays” for the Mo/Mo beams and “Calibration measurements in low-energy x-rays” for the W/Mo radiation qualities.

e. Data analysis: the data are analysed according to the instruction “Data analysis in low-energy and mammography x-rays”. The calibration data are entered in the corresponding fields of the spreadsheet created for this purpose. This spreadsheet produces the final calibration results (calibration coefficients for each quality and uncertainties) that will appear in the calibration certificate. Once the data analysis is made, it must be verified and approved by another authorized person.

f. Calibration certificate: a standard pro-forma certificate is modified as necessary incorporating the data recorded in the form produced during the reception of the chamber and the data from the analysis spreadsheet. The calibration certificate is checked and approved by the Department Director and signed by the BIPM Director in accordance with the BIPM QMS policy.

During the calibration procedure, the chamber is removed and set up again, and the calibration is repeated; the choice of the radiation qualities to repeat the calibration depends on the results and the stability of the chamber. This ensures the robustness of the calibration.

To date, five NMIs have asked for calibration of their national standards in the BIPM mammography radiation beams: the standards of the National Institute of Metrology (NIM), China, and the Czech Metrology Institute (CMI), Czech Republic were calibrated in the Mo/Mo radiation beams; the Instituto Tecnológico e Nuclear (ITN), Portugal, requested the BIPM to calibrate its standard in the W/Mo radiation qualities; whereas the Hellenic Ionizing Radiation Calibration Laboratory (HIRCL), Greece, and the Instituto Nacional de Investigaciones Nucleares (ININ), Mexico requested calibration in both sets of radiation qualities.

These standards were calibrated, as requested, in the reference conditions described in [16] and the corresponding calibration certificates were issued.

It is likely that two or three NMIs will make such requests each year.

6.2.3. Technical cooperation

Two NMIs, in the process of installing a mammography facility in their laboratories and developing an air-kerma standard for the beam dosimetry, have requested and received BIPM technical cooperation to advise and help them in the establishment of reference radiation qualities in this domain. Once they have completed their projects, each will need a comparison with the BIPM to validate their standards and thus be able to disseminate the SI unit for air kerma for mammography to their radiological departments.

6.3. Quality system

The new international facility for mammography comparisons of primary standards and calibrations of national standards has been included in the quality management system of the Ionizing Radiation (IR) Department of the BIPM.

The overall procedure of the Department entitled “Dosimetry comparisons and calibrations” describes in a systematic way the steps that must be followed to calibrate a national standard or conduct a comparison with a NMI in the reference radiation beams at the BIPM. It lists all

the technical instructions and forms needed to make the measurements, the software used for this purpose and all the relevant documents involved; it describes how to record the results and the way that certificates and comparison reports are produced.

Four technical instructions describe the steps to follow to make the measurements for a calibration of a national standard or a comparison of primary standards in each set of mammography beams:

- Setting up an ionization chamber in mammography or Setting up an ionization chamber in low-energy x-rays (for the Mo/Mo or W/Mo radiation beams, respectively);
- Source operation and security: mammography or Source operation and security: low-energy x-rays (for the Mo/Mo or W/Mo radiation beams, respectively);
- Calibration and comparison measurements in mammography x-rays or Calibration and comparison measurements in low-energy x-rays (for the Mo/Mo or W/Mo radiation beams, respectively);
- Data analysis for low-energy x-rays and mammography

These instructions make reference to the pro-forma spreadsheets needed for the measurements, which collectively form, after completion, the positioning, calibration and data analysis records.

Regarding radiation protection and source security, all the activities are carried out according to the instruction “Local rules for the ionizing radiation department – dosimetry”, to comply with the Basic Safety Standards Directive 96/29 Euratom.

The measurement chain is formed by some fifteen elements, such as the electrometer, capacitors, thermometers, etc., each of which is calibrated periodically according to a fixed planning schedule. All the elements are registered in the BIPM equipment data base, with a record of the history and state of each element, the calibration period, results of acceptance tests and calibration results. All the elements of the measurement chain are calibrated at the BIPM, most of them within the IR Department with reference to the other scientific departments as appropriate.

The stability of the air kerma rate determination, calculated from the ionization current measured using the primary standard, serves as a check of the whole system. As an example, Figure 6.4 shows the air kerma normalized to the mean for the radiation qualities

corresponding to 25 kV and 30 kV, measured since the establishment of the Mo/Mo facility in 2009; the relative standard uncertainty of the mean is 2×10^{-4} .

In accordance with the BIPM QMS, the IR Department is audited internally once per year, except when an external audit is planned, every third year. So far, the mammography facility has been audited internally in 2010 and in 2011 and an external audit took place in 2012; no non-conformity was identified.

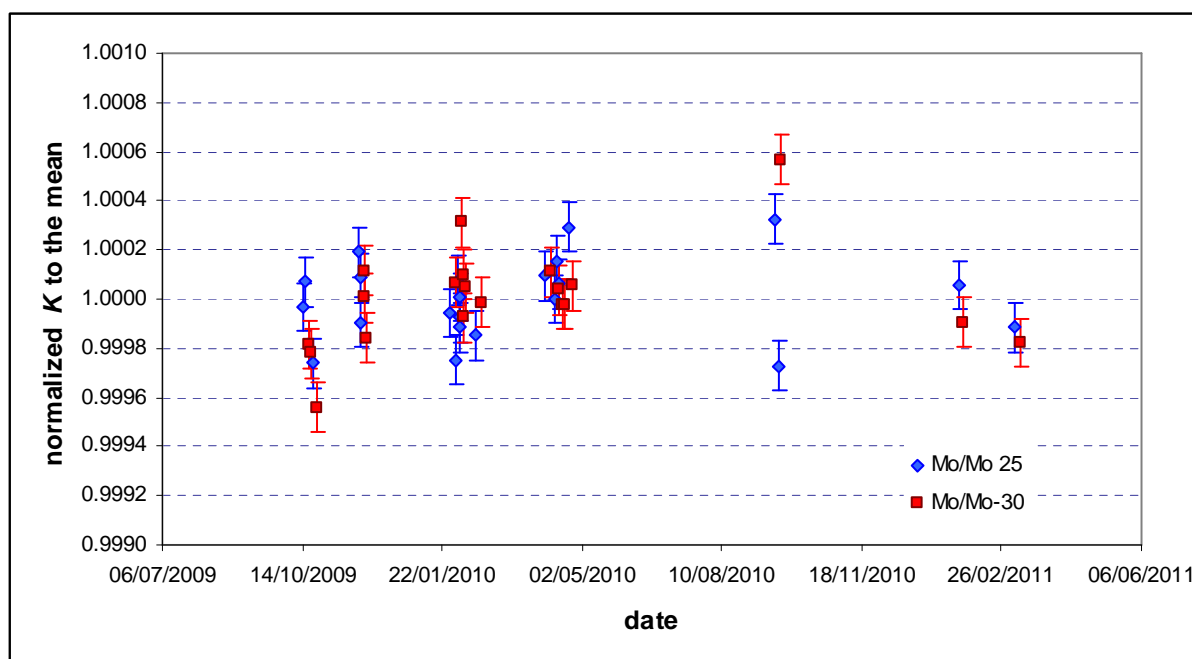


Figure 6.4. Normalized air kerma rate at the BIPM corresponding to the Mo/Mo 25 and Mo/Mo 30 radiation qualities

6.4. Conclusions

Six NMIs have participated in the on-going mammography key comparison BIPM.RI(I)-K7; among them, the standards of the NRC, NMIJ, NIST, PTB and the BIPM are in agreement at the level of the combined standard uncertainty for the comparison. The comparison results are published in the BIPM key comparison data base KCDB and in the *Metrologia Technical Supplement*. The ENEA (Italy) has requested to repeat their comparison in the near future. A comparison with the VNIIM (Russia) is in progress.

Chapter 7. Final conclusions

General conclusions

Over the last five years, I have established a full mammography dosimetry facility at the Bureau International des Poids et Mesures (BIPM) comprising:

- a set of seven reference radiation beams using the existing tungsten-anode x-ray tube and molybdenum filtration (W/Mo beams),
- a set of four reference radiation beams, after the installation of a molybdenum-anode x-ray tube, and molybdenum filtration (Mo/Mo beams),
- a new primary standard free-air chamber designed to be used up to 50 kV, for the dosimetry of the Mo/Mo beams,
- an ongoing air-kerma comparison in the new reference mammography beams, registered in the BIPM key comparison database KCDB as BIPM.RI(I)-K7, already with six participants
- a programme for the calibration of national secondary standards by including the new facility in the quality management system of the Ionizing Radiation (IR) Department of the BIPM

This work was requested by the Committee Consultative for Ionizing Radiation CCRI(I) to meet the needs of the National Metrology Institutes (NMIs):

- to have a reference facility to verify the accuracy of their primary measurements by taking part in a dosimetry comparison,
- to be traceable to the international system of units SI by having their national standards characterized and calibrated in well defined reference radiation beams,
- to comply with legal requirements imposed in their countries

The BIPM now maintains a demonstrated stable reference standard for mammography offering the NMIs the benefits summarized as follows:

- an international facility that has been approved and endorsed by the CCRI, and is used for comparisons of primary standards whose results are registered in the key comparison database KCDB; these results are used to support the calibration and measurement capabilities (CMCs) of the NMI participants,
- well-defined reference radiation beams to provide calibrations and characterizations of the national secondary standards of the NMIs,
- the experience obtained during the development of the new primary standard is now being transferred to the NMIs that are in the process of constructing a standard for the dosimetry of x-ray beams; several NMIs have requested visits to discuss details of a technical cooperation and to receive advice for the development and improvement of their facilities,
- the two sets of mammography beams established, that is, the beams produced using the combination target/filter W/Mo and Mo/Mo, serve to study the response of commercial ionization chambers as these instruments can have not only a non-negligible energy dependence, but also a different response to different spectra even with the same mean energy.

REFERENCES

- [1] International Agency for Research on Cancer, World Health Organization WHO, Globocan 2008, <http://globocan.iarc.fr>.
- [2] Witzani, J., et al., Calibration of dosimeters used in mammography with difference x-ray qualities: Euromet Project No. 526. *Radiation Protection Dosimetry* (2004) Vol **108**, No 1, p.33
- [3] ISO/IEC. International Organization of Standardization/International Electrotechnical Commission, General Requirements for the Competence of Testing and Calibration Laboratories, ISO/IEC 17025 (International Organization of Standardization, Geneva)
- [4] Medical diagnostic x-ray equipment-Radiation conditions for use in the determination of characteristics, (2005), IEC 61267
- [5] Mammography – Assessment of Image Quality, *ICRU Report 82* (2009), Vol **9**, No 2
- [6] Dosimetry in Diagnostic Radiology: An International Code of Practice, IAEA (2007) *Technical Reports Series* No 457
- [7] The BIPM key comparison database (KCDB) <http://kcdb.bipm.org/>
- [8] Boutillon, M., Henry, W.H., Lamperti, P.J., Comparison of exposure standards in the 10–50 kV x-ray region, 1969, *Metrologia* **5**, 1–11.
- [9] BIPM, Qualités de rayonnement, CCEMRI(I), 1972, R15.
- [10] Kessler, C. Establishment of simulated mammography radiation qualities at the BIPM, [Rapport BIPM-2006/08](#).
- [11] Kessler, C., Roger, P., Burns, D.T., 2010, Establishment of reference radiation qualities for mammography, [Rapport BIPM-2010/01](#).
- [12] De Almeida CE, Niattel MT, 1986, Comparison between IRD and BIPM exposure and air kerma standards for cobalt gamma rays. [Rapport BIPM-1986/12](#) (Sèvres: Bureau International des Poids et Mesures).
- [13] Boutillon M. Volume recombination parameter in ionization chambers, *Phys.Med.Biol.* 1998, **43**, 2061-2072.
- [14] Salvat, F., Fernandez-Varea, J.M., Acosta, E., Sempau, J., PENELOPE – A Code System for Monte Carlo Simulation of Electron and Photon Transport, NEA/NSC/DOC(2001)19 (ISBN 92-64-18475-9).
- [15] Matscheko, G., Ribberfors, R., A generalised algorithm for spectral reconstruction in Compton spectroscopy with corrections for coherent scattering, *Phys. Med. Biol.* **34** (1989) 835-841.
- [16] Allisy P.J., Burns D.T., Kessler C., 2011, Measuring conditions and uncertainties for the comparison and calibration of national dosimetric standards at the BIPM, [Rapport BIPM-2011/04](#).
- [17] Roger, P., High-voltage measurement for the BIPM x-ray generators, *Rapport BIPM-2012/04*
- [18] Burns, D.T., New correction factors for the BIPM free-air chamber standards. [CCRI\(I\)/03-28](#) .

- [19] Burns, D.T, Kessler, C., Allisy, P., Re-evaluation of the BIPM international standards for air kerma in x-rays, *Metrologia*, 2009, 46(5), L21-L23.
- [20] Burns D.T., Kessler C., Diaphragm correction factors for free-air chamber standards for air kerma in x-rays, *Phys. Med. Biol.*, 2009, **54**, 2737-2745
- [21] Burns D.T, Büermann L., Free-air ionization chambers, *Metrologia*, 2009, **46**, S9-S23
- [22] BIPM, Constantes physiques pour les étalons de mesure de rayonnement, in *Com. Cons. Etalons Mes. Ray. Ionisants* (Section I), 1985, 11, R45 (Offilib, F-75240 Paris Cedex 05)
- [23] Genie 2000, Logiciel de spectrométrie, Canberra.
- [24] Radionucléides, DAMRI Département des Applications et de la Métrologie des rayonnements ionisants.
- [25] Fundamental Quantities and Units for Ionizing Radiation, *ICRU Report 60* (1998)
- [26] Attix F. H., Introduction to radiological physics and radiation dosimetry, A Wiley-Interscience Publication.
- [27] Stopping Powers for Electrons and Positrons, *ICRU Report 37*(1984)
- [28] Wyckoff, H.O. and Attix, F.H., Design of free-air chambers, National Bureau of Standards Handbook 64
- [29] Ritz V.H., Design of free-air chambers for the soft x-ray region (20-100 kV), *Radiology*, 1959, **73** 911-22
- [30] Allisy A., Roux A.M., Contribution à la mesure des rayons roentgen dans le domaine de 5 à 50 kV, *Acta Radiol.*, 1961, **55** 57-74
- [31] Uotila I.K., Field distortion in guarded-wall free-air ionization chambers, *Metrologia*, 1980, 16 15-9
- [32] International Commission on Radiological Protection, radiological Protection and Safety in Medicine, Publication 73, Pergamon Press, Oxford and New York (1997)
- [33] National Council on Radiation Protection and Measurements (NCRP), 1986, Mammography – a user’s guide. NCRP Report 85, National Council on Radiation Protection and Measurements, Bethesda, MD, pp. 40-56
- [34] Technical protocol for a BIPM ongoing key comparison in dosimetry, [http://kcdb.bipm.org/appendixB/appbresults/BIPM.RI\(I\)-dosimetry/BIPM-dosimetry_Technical_Protocol.pdf](http://kcdb.bipm.org/appendixB/appbresults/BIPM.RI(I)-dosimetry/BIPM-dosimetry_Technical_Protocol.pdf)
- [35] Guide pour l’expression de l’incertitude de mesure GUM, 2008.
- [36] Burns D.T., 2003, Degrees of equivalence for the key comparison BIPM.RI(I)-K2 between national primary standards for low-energy x-rays, *Metrologia*, 2003, **40** Technical Supplement, 06031
- [37] Kessler C., Burns D.T., McCaffrey J.P., Key comparison BIPM.RI(I)-K7 of the air-kerma standards of the NRC, Canada and the BIPM in mammography x-rays, *Metrologia*, 2011, **48**, *Tech. Suppl.*, 06022
- [38] Kessler C., Burns D.T., Tanaka T., Kurosawa T., Saito N., Key comparison BIPM.RI(I)-K7 of the air-kerma standards of the NMIJ, Japan and the BIPM in mammography x-rays, *Metrologia*, 2010, **47**, *Tech. Suppl.*, 06024

- [39] Kessler C., Burns D.T., Büermann L., Key comparison BIPM.RI(I)-K7 of the air-kerma standards of the PTB, Germany and the BIPM in mammography x-rays, [*Metrologia*, 2011, 48, Tech. Suppl., 06011](#)
- [40] Kessler C., Burns D.T., O'Brien M., Key comparison BIPM.RI(I)-K7 of the air-kerma standards of the NIST, USA and the BIPM in mammography x-rays, [*Metrologia*, 2011, 48, Tech. Suppl., 06014](#)
- [41] Catalogue of diagnostic x-ray spectra and other data, Report No 78, 1997 The Institute of Physics and Engineering in Medicine, York, UK

DEVELOPPEMENT ET MISE EN PLACE AU BIPM D'UN SYSTEME INTERNATIONAL DE COMPARAISON ET D'ETALONNAGE POUR LA DOSIMETRIE EN MAMMOGRAPHIE

Résumé

Un système international pour la comparaison des étalons primaires et la caractérisation des étalons nationaux secondaires pour la dosimétrie en mammographie a été mis en place au Bureau international des poids et mesures (BIPM). Ce développement a été demandé au BIPM par les Instituts nationaux de métrologie (INM) afin de répondre aux besoins des laboratoires de référence pour la dosimétrie dans le domaine de la mammographie. Une nouvelle comparaison clé a été créée et enregistrée dans la base de données du BIPM sur les comparaisons clés.

Ces comparaisons internationales bilatérales organisées par le BIPM permettent aux laboratoires nationaux de métrologie de vérifier l'exactitude de leurs mesures et de démontrer leurs aptitudes en matière de mesures et d'étalonnages, tel que cela est défini dans l'Arrangement de reconnaissance mutuelle.

La caractérisation des étalons nationaux secondaires assure la traçabilité de ces derniers au Système international d'unités.

Summary

An international facility for comparisons of primary standards and characterizations of national secondary standards for mammography dosimetry has been established at the Bureau International des Poids et Mesures (BIPM). This development was demanded to the BIPM by the National Metrology Institutes (NMIs) to meet the needs of the reference dosimetry laboratories in the field of mammography. A new key comparison was created and registered in the Key Comparison Database of the BIPM.

These international bilateral comparisons organized by the BIPM enable the national metrology laboratories to verify the accuracy of their measurements and demonstrate their calibration and measurement capabilities as presented in the Mutual Recognition Arrangement.

The characterization of national secondary standards ensures their traceability to the International System of Units.